Structure-function relationships, tertiary interactions and thermostabilty of RNase P

Dissertation

zur

Erlangung des Doktorgrades

der Naturwissenschaften

(Dr. rer. nat.)

dem Fachbereich

Pharmazeutische Chemie

der Philipps-Universität Marburg

vorgelegt von

Michal Marszalkowski

Marburg/Lahn 2007

Vom Fachbereich Pharmazeutische Chemie
der Philipps-Universität Marburg als Dissertation am 14 November 2007
angenommen.

Erstgutachter: Prof. Dr. Roland K. Hartmann
Zweitgutachter: PD Dr. Klaus Reuter

Tag der mündlichen Prüfung am: 14 November 2007

Table of Contents

1. Introduction

1.1. Ribozymes

A ribozyme (from **ribo**nucleic acid en**zyme,** also called RNA enzyme or catalytic RNA) is a RNA molecule that catalyses a chemical reaction. Most natural ribozymes catalyse cleavage of the molecule they are part of (cleavage in *cis*) but also the aminotransferase activity of the ribosome was found to be essentially RNA-catalysed (activity in *trans*).

Before the discovery of ribozymes, protein enzymes were the only known biological catalysts. The first ribozymes were discovered in the 1980s by Thomas R.Cech, who was studying RNA splicing in the ciliated protozoan *Tetrahymena thermophila*, and by Sidney Altman, who was working on bacterial ribonuclease P (RNase P) complexes. In 1989 T.R.Cech and S.Altman won the Nobel Prize in chemistry for their "discovery of catalytic properties of RNA." The term *ribozyme* was first introduced by Kelly Kruger *et al*. in their 1982 Cell publication.

Nowadays, ribozymes are classified in terms of their diverse size and function. Naturally existing catalytic RNAs include small ribozymes like the hammerhead, hairpin, hepatitis delta virus and Varkud satellite ribozymes (Symons, 1992; Carola & Eckstein, 1999), and large ribozymes like group I and II introns (Kruger *at al*., 1982) and the RNA subunit of RNase P called P RNA (Guerrier-Takada *et al*., 1983). Further, among the ribozymes there exist two major ribonucleoprotein machines, the ribosome (Nissen *et al.*, 2000; Muth *et al*., 2000, Steitz & Moore, 2003) and the spliceosome (Collins & Guthrie, 2000; Valadkhan & Manley, 2001).

All known ribozymes are metalloenzymes: for their catalytic activity and proper tertiary folding they require divalent cations (Mg^{2+} or Mn^{2+}, Sun & Harris, 2007). The reaction catalysed by ribozymes is an endonucleolytic transesterification of a phosphodiester bond with an activated nucleophile. In contrast to all known ribozymes that act in *cis*, there is a single naturally occurring one that cleaves RNAs in *trans:* RNase P (Tanner, 1999).

1.2. RNase P

Ribonuclease P (RNase P) is a ribonucleoprotein that is responsible for the 5'-maturation of precursor tRNAs (pre-tRNAs). It is an essential ubiquitous endonuclease that is found in cells from all three domains of life: the Bacteria , Eukarya and Archaea (Kazantsev & Pace, 2006; Hartmann & Hartmann, 2003; Lee *et al.*, 1991; Jarrous & Altman, 2001). RNase P carries out a simple enzymatic reaction: the hydrolysis of a specific phosphodiester in pre-tRNAs to release the 5'- flank and thereby generate tRNAs with mature 5'ends. *E. coli* RNase P also

cleaves other substrates, such as some viral RNAs (Mans *et al.*, 1990; Hartmann *et al.*, 1995), p4.5S RNA (Peck-Miller & Altman, 1991), ptmRNA (Komine *et al.*, 1994), a few mRNAs (Li & Altman, 2003; Alifano *et al.*, 1994) and some riboswitches (Altman *et al.*, 2005).

RNase P is required for cell viability (Schedl & Primakoff, 1973, Gößringer *et al.*, 2006). So far, all known RNase P enzymes consist of one RNA subunit and at least one protein subunit (Fig. 1.1) encoded by the *rnpB* and *rnpA* genes n bacteria. Both the RNA and protein components are essential *in vivo*. An exception might be protein-only enzymes acting like RNase P in spinach chloroplasts (Wang *et al.*, 1988, Thomas *et al.*, 1995) and mitochondria of *Trypanosoma brucei* (Salavati *et al.*, 2001).

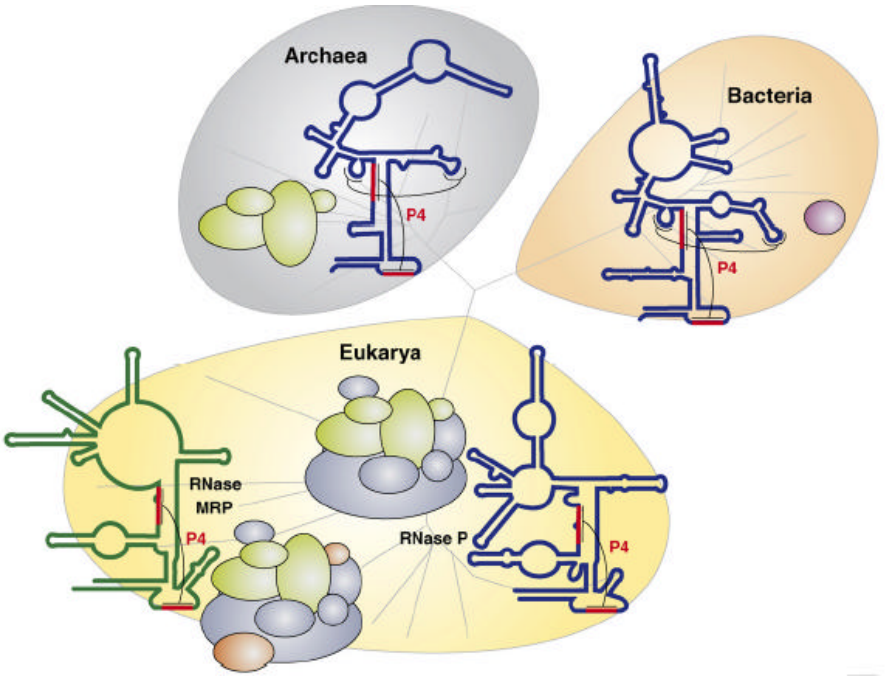

Fig. 1.1: RNase P holoenzymes from Bacteria, Archaea and Eukarya. The RNA subunit is marked in blue. The single protein subunit from bacteria is indicated by a purple oval. Archaeal proteins are shown in green and eukaryal ones in green (homologs of archaeal P proteins) and gray. All RNAs share conserved nucleotides in helix P4 (indicated in red). In Eukarya there is a sibling of RNase P, RNase MRP (dark green), which is involved in processing of precursor rRNAs and shares the majority of its protein subunits with eukaryal RNase P. In addition, the core of its RNA subunit is structurally related to eukaryal P RNA. (Figure from Willkomm & Hartmann, 2007).

Catalytic activity in general seems to reside in the RNA subunit of RNase P (Guerrier-Takada *et al.*, 1983). Thus at high concentrations of divalent metal ions all bacterial RNase P RNAs analysed so far display catalytic activity in the absence of the protein when tested *in vitro*. RNA alone activity *in vitro* has also been demonstrated under very high ion concentrations for some Archaea (Hall & Brown, 2002), and recently also residual activity for eukaryal RNase P RNAs has been shown (Kikovska *at al.*, 2007).

The RNA subunits of RNase P from all the kingdoms of life share a conserved core, pointing to a common evolutionary origin. In contrast, the protein composition of RNase P holoenzymes differs markedly between the bacterial (one small basic protein), archaeal (four to five different protein subunits, Andrews *et al.*, 2001; Hartmann & Hartmann, 2003; Fukuhara *et al.*, 2006) and eukaryal (nine or ten different protein subunits) versions of the enzyme (Hartmann & Hartmann, 2003, Chamberlain *et al.*, 1998; Jarrous & Altman, 2001; Van Eenenaam *et al.*, 1999 & 2001). The archaeal RNase P protein subunits have been identified as homologues of yeast and human RNase P proteins (Evans *et al.*, 2006; Hall & Brown, 2002).

1.3. The RNA subunit of bacterial RNase P

The RNA component of RNase P (P RNA) from bacteria varies in length between 350-450 nucleotides (Brown & Pace, 1992).

There are two main structural types of bacterial P RNA: the A type (ancestral type), represented e.g. by *E. coli*, and the B (*Bacillus*) type (see Fig 1.2, Haas *et al*., 1996). Despite some significant structural differences between type A and B, RNAs fold into globally similar three-dimensional structures (Chen *et al.*, 1998; Massire *et al.*,1998). Differences between both types of RNAs are mainly caused by the variable number of helical elements and their distribution in the overall stucture (Kazantsev & Pace, 2006; Torres-Larios *et al*., 2005).

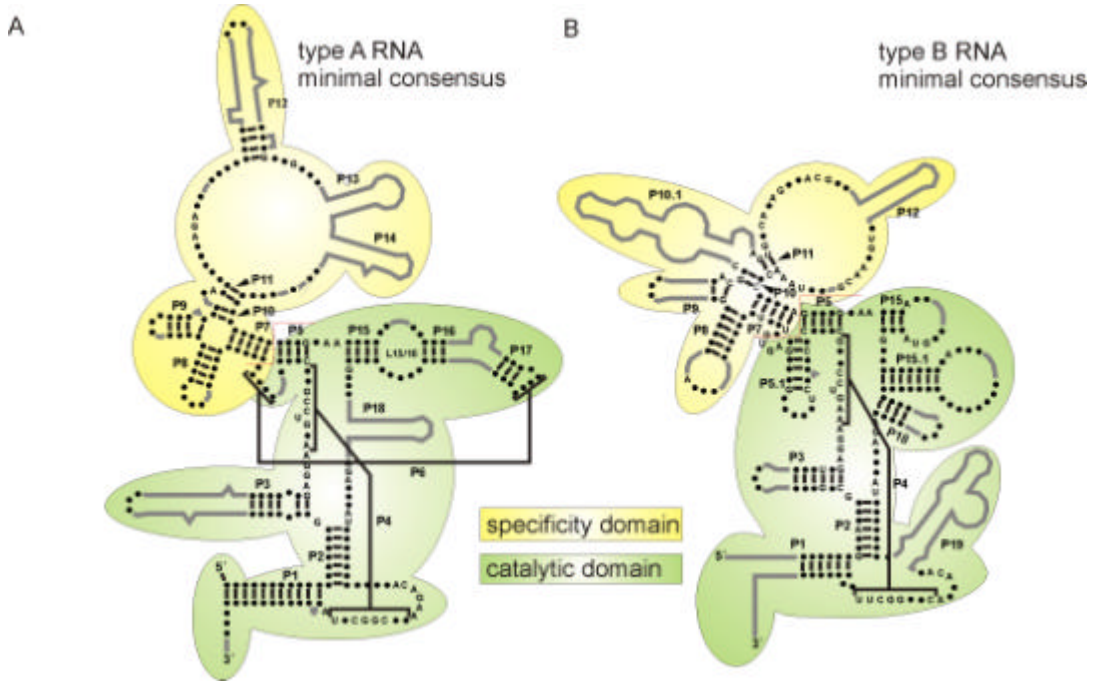

Fig. 1.2: Bacterial Type A (A) and B (B) secondary structures. Consensus nucleotides are indicated by capital letters (A, G, C or U), variable nucleotides are marked as dots (?). Elements marked in grey are absent in some of the RNAs of each type (modified figure from Haas *et al*., 1996).

All P RNAs consist of two independently folded domains (Pan, 1995; Loria & Pan, 1996): the specificity domain (S-domain) including helices P7-P14 (responsible mainly for substrate binding; Pan *et al.*, 1995; Loria & Pan, 1998; Nolan *et al.*, 1993; Chen *et al.*, 1998) and the catalytic domain (C-domain) composed of helices P1–6 and P15–18. The C-domain contains residues conserved among all known P RNAs, and is further responsible for recognition of the acceptor-stem and 3'CCA motif of tRNA.

Comparison of all known bacterial P RNA structures shows that despite many differences in their peripheral elements, all of them share a set of highly conserved structural elements (phylogenetic minimal structure, see Fig.1.3.). Among these, helix P4 and adjacent sequences, which represent an essential part of the catalytic centre of the bacterial enzyme (Christian *et al.*, 2000, 2002; Crary *et al.*, 2002), seem to be the regions of highest conservation (Frank *et al.*, 2000). A synthetic minimal P RNA structure consisting of the conserved core is catalytically active *in vitro* (Siegel *et al.*, 1996; Waugh *et al.*, 1989; see also bacterial minimal consensus Fig 1.3.). It has been suggested that conserved residues are mainly distributed in the vicinity of the ptRNA binding interface (Haas & Brown 1998).

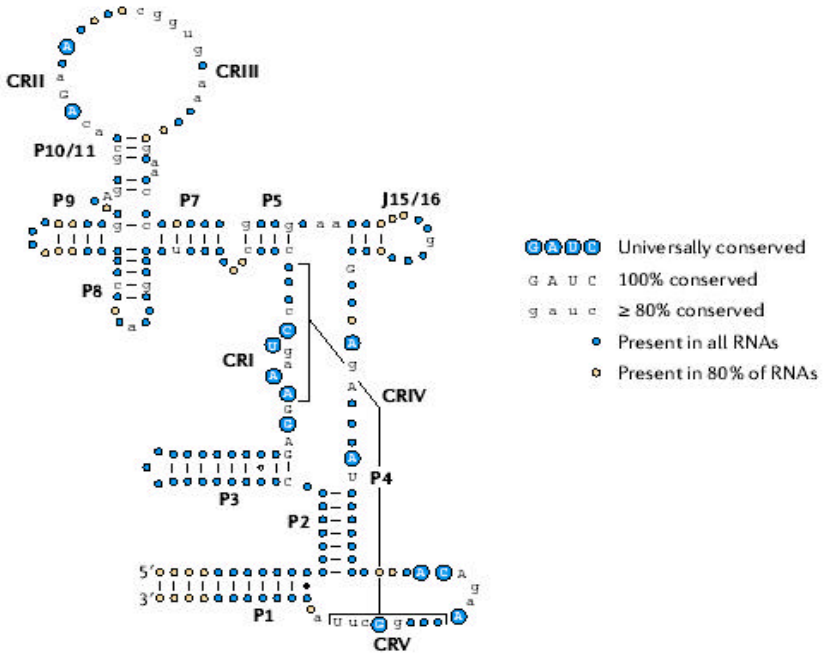

Fig.1.3: The phylogenetic minimal structurally conserved core of bacterial P RNAs. CRI-V indicate the regions of highest conservation (from Kazantsev & Pace, 2006).

Recently, the three dimensional structures of P RNA from *Thermotoga maritima* (type A; Torres–Larios *et al.*, 2005) and *Bacillus stearothermophilus* (type B; Kazantsev *et al.*, 2005)

were solved by *X-ray* crystallography. These studies proved the existence of interactions between the two domains predicted ealier by phylogenetic comparison and a variety of biochemical approaches, and agree with models of secondary and tertiary structure proposed earlier (Harris *et al*., 1994; Chen *et al*., 1998; Massire *et al*., 1998; Tsai *et al*., 2003). Crystal structures are discussed in detail in section 1.7.

1.4. Substrate recognition by RNase P

The major function of RNase P is maturation of pre-tRNA; therefore, efficient and specific recognition of substrates is required. The T-stem loop and the acceptor helix of the pre-tRNA are recognition elements for RNase P (McClain *et al*., 1987; Thurlow *et al.*, 1991; Schlegl *et al.*,1992). The interaction between acceptorstem and RNase P is mainly mediated by the C-domain of the P RNA subunit. In particular the CCA motiv located at the 3' end of the pre-tRNA acceptor stem can form two specific G-C Watson-Crick base pairs with the C-domain of the RNase P RNA subunit (in the P15/16 loop; Kirsebom & Svärd, 1994). However, although the 3' -CCA tail is found in all tRNAs, it was shown that it is not essential for RNase P processing *in vitro*. Disruption of the CCA-L15 interaction by mutation of G292/293 residues (*E. coli*) or G259/258 (*B. subtilis*) caused severe growth defects in respective complementation strains (Wegscheid & Hartmann 2006, 2007). The 3' -CCA tail substantially influences cleavage rate and cleavage site positioning (Guerrier-Takada *et al*., 1984; Kirsebom & Svärd, 1994; Krupp *et al*., 1991; Oh & Pace, 1994; Hardt *et al.*, 1995) and plays a role in the recruitment of catalytically important metal ions (Wegscheid & Hartmann 2006, 2007).

Recent modelling of tRNA into the crystal structure of *T. maritima* (Torres-Larios *et al*., 2005) showed that the T-stem loop of the pre-tRNA lies in the S-domain of RNase P RNA and that the 5' end of pre-tRNA is very close to the P4/P5 region. The acceptor stem is sandwiched into the shallow groove of the C-domain parallel to P1/P4/P5 very close to universally conserved residues. According to this model, the cleavage site sits exactly on A49 (*E. coli* A66) of helix P4 and A 314 (*E. coli* A 352) in J2/4.

1.5. The catalytic mechanism of cleavage

RNase P catalyses the hydrolysis of a phosphodiester bond to generate a monophosphate at the 5'end of the mature tRNA (Altman *et al.*, 1971) and to release the 5' flank of the precursor with a terminal 2',3'-cis-glycol (Fig.1.4). For catalysis, the labile phosphodiester bond is encaged by two or more Mg^{2+} ions to form a trigonal bipyramidal transition state, and

the 2'OH at nt –1 of the 5' flank of the precursor facilitates protonation of the leaving 3'-oxygen (S_N2-like nucleophilic substitution mechanism, Persson *et al.*, 2003). Under single-turnover conditions the rate of the chemical step of catalysis increases with pH and is approximately first-order in the pH range of 6 to 8. Mg^{2+} ion concentration dependency indicates stabilization of the transition state by up to three cooperatively bound Mg^{2+} ions. The metalloenzyme nature of RNase P is supported by studies of the cleavage of pre-tRNA that contain R_p-phosphorothioate substitutions at the substrate phosphodiester bond.

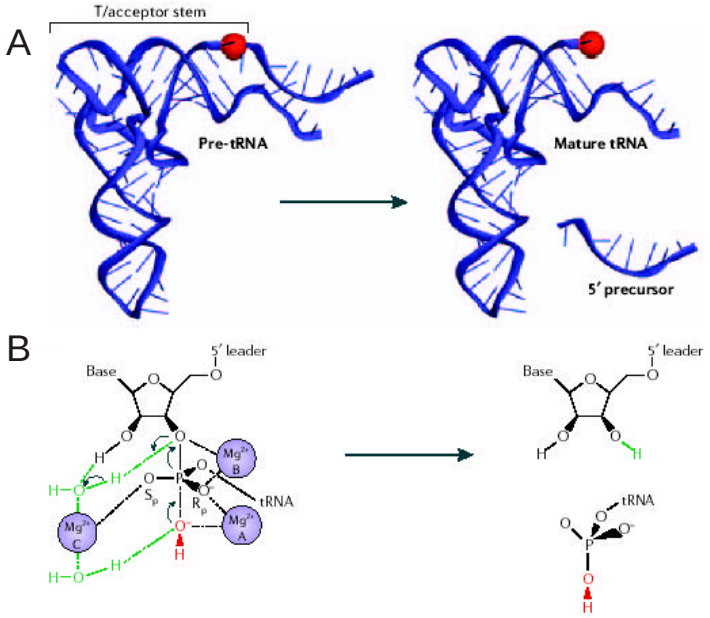

Fig.1.4: RNase P catalyses maturation of the 5'end of tRNA. **(A)** pre-tRNA and the products of the reaction, mature tRNA and the released 5' flank. The substrate phosphate is indicated by a red sphere. **(B)** One proposed mechanism of the reaction including three metal ions. On the left is a putative structure of the transition state of the reaction. The electron flow is indicated by arrows. The pro-R_p oxygen of the scissile phosphate coordinates two Mg^{2+} ions A and B. Ion A activates and positions the nucleophile (the hydroxide ion, red) and ion B stabilizes the transition state and activates the 3'-oxygen leaving group by neutralizing the developing negative charge. Ion C is has been proposed to coordinate the 2'-OH of the preceding nucleotide (N_{-1}). The reaction products (on the right) possess a terminal 2',3'-cis-glycol and a 5' phosphate, respectively. (Figure from Kazantsev & Pace, 2006).

Such substitution switches the metal-ion specificity of the chemically active site to thiophilic metal ions (Cd^{2+} or Mn^{2+}, Warnecke *et al.*, 1996, 1999, 2000). Substitution of the pro-R_p non bridging phosphate oxygen with sulphur results in a significant (~10^4) reduction in the catalytic activity of the Mg^{2+}-supported reaction (Kazantsev & Pace, 2006).

1.6. The protein subunit of bacterial RNase P

Bacterial RNase P holoenzymes contain only one small basic protein subunit that contributes one-tenth to the mass of the holoenzyme. The precise role of the protein subunit is not yet fully understood. Under physiological salt concentrations and *in vivo*, the protein component is essential for cleavage by RNase P (Schedl *et al.*, 1974; Guerrier-Takada *et al.*, 1983; Reich *et al.*, 1988; Kirsebom *et al.*, 1998; Gößringer *et al.*, 2006). The protein subunit is not directly involved in the cleavage mechanism, but influences binding affinity of pre-tRNA and affects structural rearrangements to obtain the optimal conformation of the holoenzyme (Christian *et al.*, 2002; Buck *et al.*, 2005b). Other studies have shown that the protein subunit increases the affinity of metal ions in the active site of P RNA and enhances the catalysis step (Sun & Harris, 2007).

The sequences of bacterial RNase P proteins are poorly conserved; similarity is rather confined to their three dimensional structures (Kirsebom & Vioque, 1995). Crystal structures of RNase P proteins from *Bacillus subtilis* (Stams *et al.*, 1998) and *Thermotoga maritima* (Kazantsev *et al.*, 2003) are available; furthermore, the structure of the RNase P protein from *Staphylococcus aureus* (Spitzfaden *et al.*, 2000) was determined by NMR.

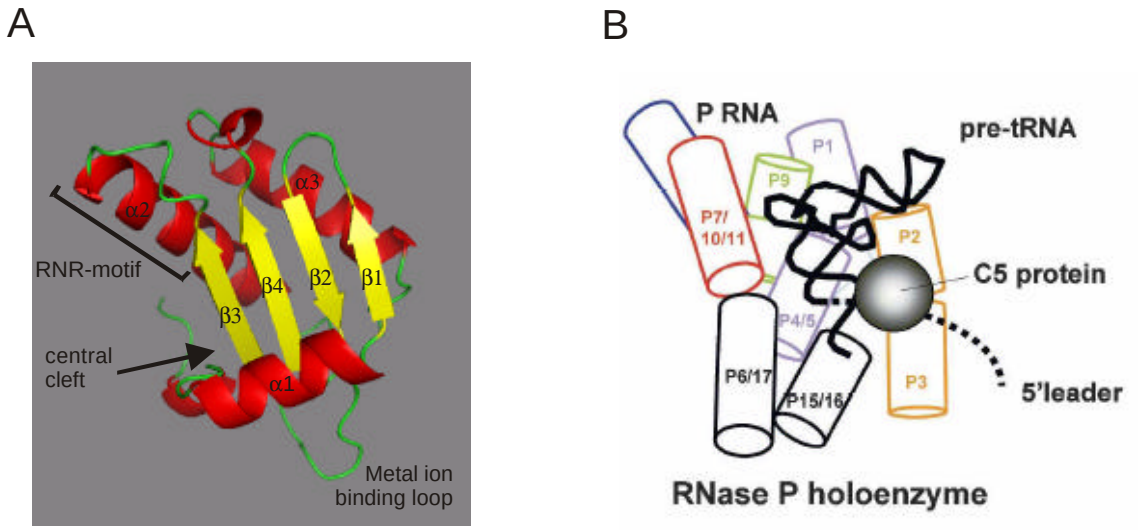

Fig. 1.5: (A) *B. subtilis* RNase P protein. α-helices (red) and the β-sheet (yellow). The RNR-motif, the metal ion binding loop and the central cleft formed by α1 and the β-sheet are potential RNA-binding sites (Niranjanakumari *et al.*, 2007). **(B)** Schematic representation of the three-dimensional structure of type A RNase P holoenzyme with pre-tRNA bound. Individual helices are shown as cylinders, pre-tRNA is indicated as a black ribbon and the P protein as a sphere (Sun & Harris, 2007).

Analysis of these structures combined with phylogenetic comparative and biochemical data revealed three potential RNA binding motifs: an RNR-motif with 11 conserved amino acids (Altman, 1989; Pace and Brown, 1995), a metal binding loop and a central cleft motif formed by four β-sheets and helix α1 (Fig. 1.5 A). The RNase P protein binds to residues of the RNase P RNA subunit located in helices P2, P3 and at the periphery of P4 (see Fig. 1.5 B) as was shown by phosphorothioate-iodine protection assays (Buck *et al.*, 2005b). Assembly of the holoenzyme itself and binding of pre-tRNA seems to be a very complex process with many transition states. Induced fit, the theory suggesting that binding of the protein to the RNA subunit changes the structure of both, may explain this process. The specific interactions between the holoenzyme components induce global rearrangements that at the end result in assembly of an active complex (Buck *et al.*, 2005b; Guo *et al.*, 2006). The roles assigned to bacterial P protein include electrostatic neutralization effects on P RNA and 5'-precursor tRNA backbone phosphates (Reich *et al.*, 1988), conformational stabilization and fine-tuning of the active site structure (Guerrier-Takada et al., 1983; Westhof *et al.*, 1996; Kim *et al.*, 1997; Buck *et al.*, 2005a) and increases in the binding affinity for pre-tRNA (Kurz *et al.*, 1998; Rueda *et al.*, 2005, Buck *et al.*, 2005b). The P protein also increases the affinity for essential metal ions involved in pre-tRNA binding and catalysis (Kurz and Fierke, 2002), likely by stabilization of conserved local structure in the catalytic core of P RNA. The protein subunit further mediates RNase P dimer formation in *B. subtilis* system (Fang *et al.*, 2001). Recently it was also shown that the bacterial P protein is involved in offseting differences in pre-tRNA structure, such that binding and catalysis are uniform for all pre-tRNAs (Sun *et al.*, 2006).

1.7. Crystal structure, long range tertiary interactions and thermostability of bacterial RNase P RNA

Understanding bacterial RNase P RNA structure has been significantly advanced by several *X-ray* structures. Low resolution X-ray crystal structures of full-size RNase P RNAs from *Thermotoga maritima* (type A, 3.85 Å) and *Bacillus stearothermophilus* (type B, 3.3 Å) have been solved, as well as the structures of S-domains from *T. thermophilus* (type A) and *B. subtilis* (type B). Comparison of the S-domains of the two types of bacterial P RNAs reveals a common arrangement of regions involved in pre-tRNA recognition, namely stems P9, P10 and P11 and the joining regions J11/12-J12/11. In particular the assumed binding interface of

pre-tRNA in type A and B RNase P RNAs is very similar, whereas the stabilisation of the core is achieved by different overall folds (Krasilnikov *et al.*, 2004, Torres-Larios *et al.*, 2006).

Comparison of the entire structures from *T. maritima* and *B. stearothermophilus* reveals a remarkably flat architecture formed by helical subdomains connected by a variety of long-range interactions (Fig. 1.6). The RNase P RNA from *T. maritima* (Torres-Larios *et al.*, 2005) is composed of two layers of stacked helices. The first includes paired regions P1-P12 and P15-P17, with junctions J5/15 and J11/12-J12/11. In this layer the most universally conserved regions are located, the areas responsible for contact to the pre-tRNA substrate and the putative active site. The second layer is composed of helical stems P13, P14 and P18 that interact with the first layer through P8 and P9 in the specificity domain. P4 is the region of highest conservation, is located proximal to the catalytic site, is a potential metal binding site and important for catalysis.

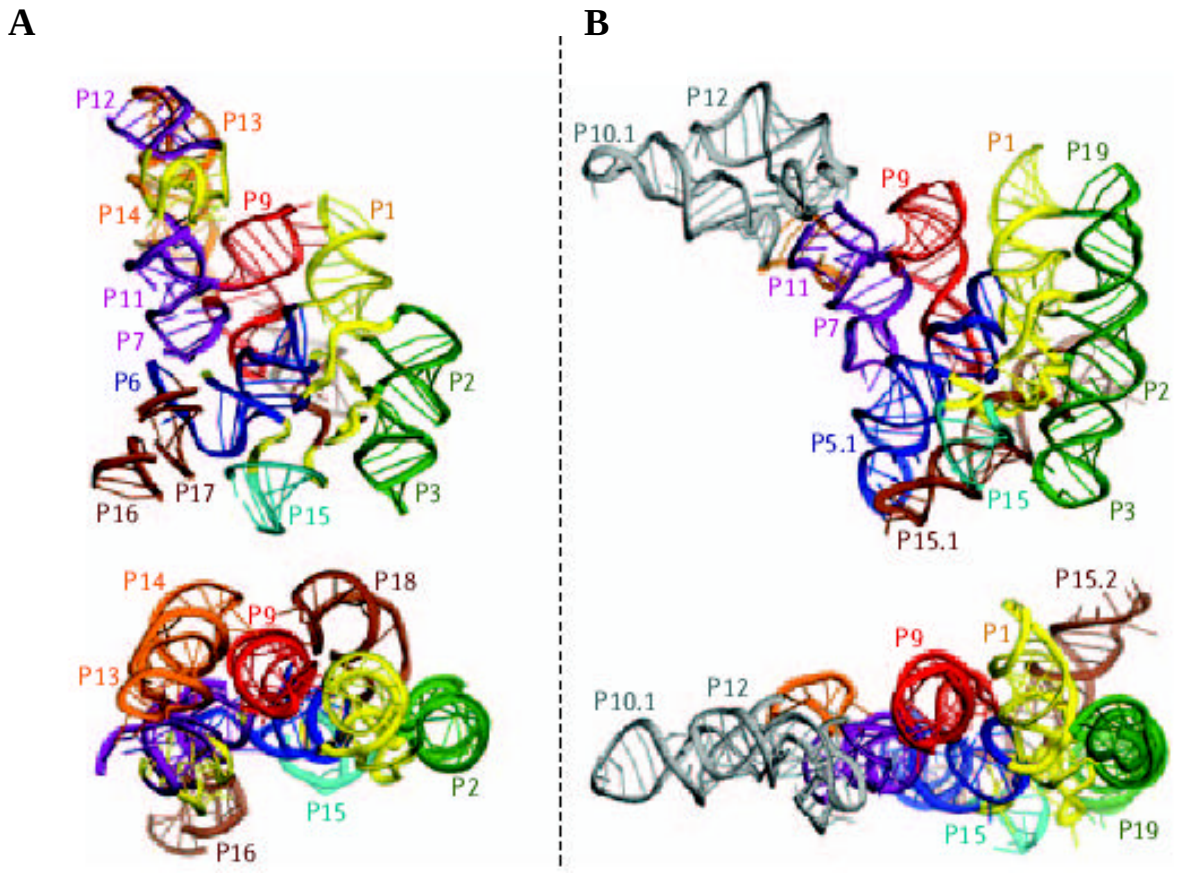

Fig. 1.6: Crystal structure of the RNA component of **(A)** *T. maritima* RNase P (Torres-Larios *et al*., 2005) **(B)** *B. stearothermophilus* (Kazantsev *et al*., 2005). A stereo ribbon diagram of two orthogonal views of the structure is shown for each structure (Kazantsev & Pace, 2006).

The crystal structure suggests mainly a structural function for P4, and its sequence conservation could be due to constraints imposed by its proximity to and interaction with the connectors in the C-domain. Similar to the type A structure, also the structure of *B. stearothermophilus* type B RNase P RNA consists of coaxially stacked helical elements held together by three long-range interactions (Kazantsev *et al.*, 2005). The overall structure is remarkably flat (like in type A), and reveals a characteristic interaction between L5.1 and L15.1, a hallmark of type B RNase P RNAs.

A key feature becoming evident from the crystal structures and the previous structural predictions is that the RNA's architecture is built up from a hierarchical assembly of helical elements, formed by Watson-Crick base pairs, which are connected and interlinked by RNA modules mainly involving non-Watson-Crick interactions (Fig. 1.7).

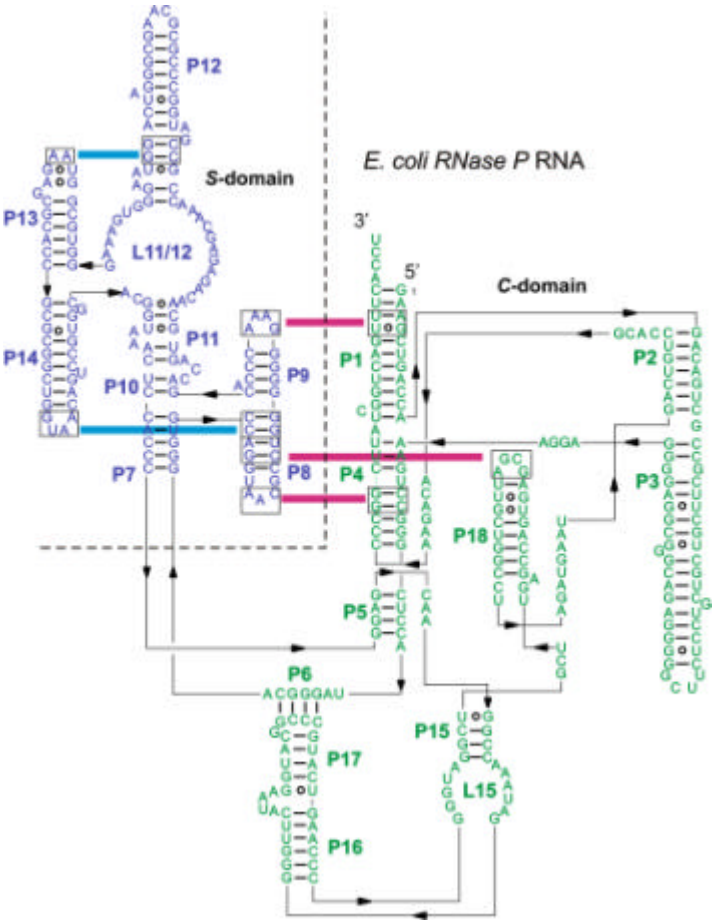

Fig. 1.7: Secondary structure of *E. coli* P RNA as a typical representative of type A RNase P RNAs. Specificity and catalytic domains are indicated in blue and green respectively. Major long range tertiary interactions are marked by red bars and the interdomain tetraloop-helix interacion are indicated in light blue.

These bridging, long range interactions are represented mainly by GNRA tetraloops (where N is any nucleotide, and R is A or G) bringing together very distant regions of the RNA chain

by specific interaction with a receptor stem. Thus, in type A RNase P RNAs typically tetraloop-acceptor stem long-range interactions occur between P8 and L14, P8 and L18, and L9 and P1 (Massire *et al*., 1997) and bridge the S- and C-domains (see Fig. 1.7).

These interactions ensure that the two domains are positioned correctly and oriented in the manner appropriate for accomodation and processing of pre-tRNA. Other loop-helix interactions are found within the domains: P8/L14 and P12/L13 contribute substantially to stabilization of the S-domain (see Fig. 1.7). Such loop-receptor stem contacts have been identified in a number of structured RNAs where they were found to be essential for proper folding of the RNA and to also serve as basic building blocks of RNA and as recognition elements for proteins (Wool *et al*., 1992) and RNAs (Dohethy *et al*., 2001; Nissen *et al*., 2001). Recently solved crystal structures (1.4 Å) of GUAA tetraloops of the mutant *E. coli* SRL RNA shed more light on structural details of this specific type of interaction (Correll & Swinger, 2003). GNRA sequences share a common backbone geometry that was revealed by NMR spectroscopy (Heus & Pardi, 1991) and later by X-ray crystallography (Cate *et al*., 1996; Correll *et al*., 1999). The last two purines of a GNRA loop can form a contact with two consecutive base pairs in the minor groove of an RNA helix (receptor stem). The last three bases in tetraloops are exposed and remain stacked nearly paralleling the basis of the closing Watson-Crick pair (see Fig 1.8 A).

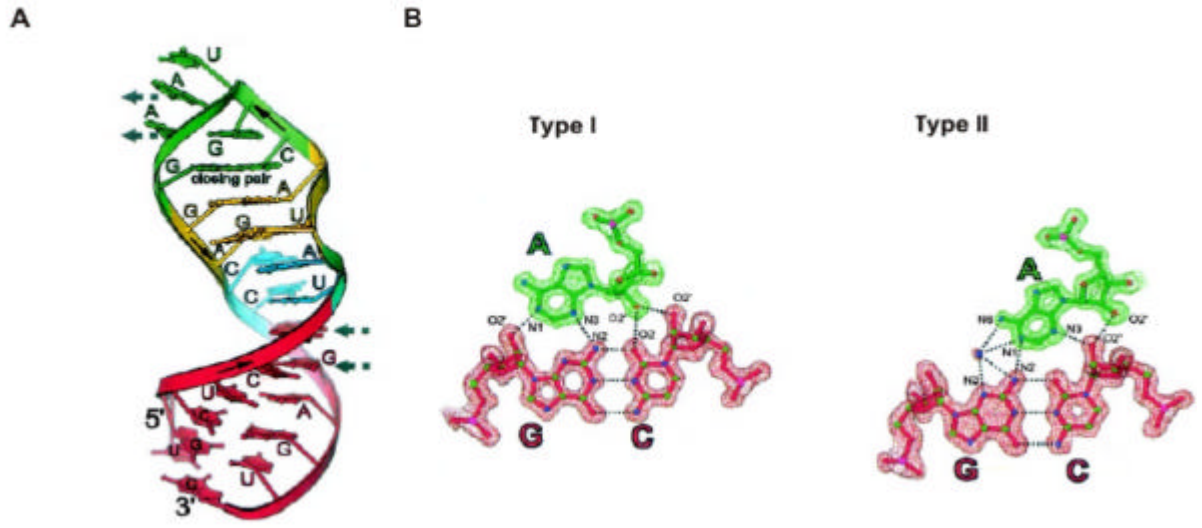

Fig. 1.8: (A) Crystal structure of a hairpin RNA that combines a GNRA tetraloop and a tetraloop receptor site. The GUAA tetraloop shown in green, the bulged G motif in yellow, the flexible region in blue and the stem region in red. Gray arrows indicate the two adenosines and Watson-Crick base pairs involved in lattice contacts that mimic A-minor like interactions. **(B)** Models of type I and type II A-minor contacts (Correll & Swinger, 2003).

GNRA tetraloops are involved in the most common type of specific tertiary interaction: A-minor motifs (Doherty *et al*., 2001; Nissen *et al*., 2001). These were first observed in the crystal structure of the hammerhead ribozyme (Pley *at al*., 1994a); the structure of the P4-P6 domain of group I introns was the first to illustrate this motif as a tertiary contact (Cate *at al*., 1996). The most abundant types of A-minor motifs are type I and type II, both characterized by interaction of two consecutive adenines in the tetraloop with two consecutive Watson-Crick pairs in the shallow/minor groove of a helix receptor. In type I, the adenosine makes four favourable hydrogen bonds to the receptor C/G base pairs, spanning across the minor groove. In the type II A-minor interaction, the adenosine makes direct and solvent-mediated contacts to the receptor C/G base pairs that span only part of the way across the minor groove (Fig. 1.8 B).

An extremely interesting aspect of RNase P RNA structure is if and how this RNA has adapted to the different growth temperatures of its hosts, which range from psychrophiles (low temperature of growth close to 0°C) to mesophiles (optimum at 37°C) and thermophiles (up to 90°C).

RNA tertiary structures from thermophilic bacteria generally are more stable than their mesophilic homologues (Baird *at al*., 2006). Several features have been observed in thermophilic RNAs that may contribute to thermal stability: first of all the number of hydrogen bonds in helices is increased by raising the G/C content. P RNAs from thermophilic bacteria usually have a much higher G/C content, exceeding even 80% for *T. maritima* and *T. neapolitana,* in comparison with e.g. 37% average G/C content of P RNAs from proteobacteria (Brown *at al*., 1992). In line with this observation, it was recently shown that strategic mutation of base pairs to G-C pairs in the C-domain of *B. subtilis* RNase P RNA results in free energy increase, reaching stabilities characteristic for the G-domain of the thermophile *B. stearothermophilus* (Fang *at al*., 2003). However, it was not shown in this study whether increased stability was indeed related to higher activity at elevated temperature. Thermodynamic calculations have shown that thermophilic P RNAs have fewer alternative structures near the free energy minimum (Haas *et al*., 1991).

Minimization of irregularities in helices and decreasing the number of bulges is another way towards higher thermostability. Many of the bases which flank helices, at either the proximal or distal end, clearly have the potential to form base-pairs in thermophilic P RNAs, in contrast to mesophiles where the homologous bases form non-canonical pairs or are solely stacked onto the end of the helices. Another means leading to thermostability is reduction of the number of connecting nucleotides between helices, thus causing a decreased flexibility of the

global tertiary structure. Also the length of the helices themselves seems to be important for thermostability. Comparison of P RNAs from *Thermotoga* and *E. coli* shows that in the thermophile some helices are shortened (mainly P12 and P3). Also minimization of alternative foldings may be a key for achieving thermostability. This can be the result of decreasing pairing possibilities or minimization of the sequence length.

All these features are characteristic of thermostable P RNAs (with a bias for increased GC content or reduction of bulged bases), nonetheless each RNA seems to have 'selected' its own way of gaining thermostability. For example, thermostability of *Thermus* seems to rely mostly on strengthening the secondary structure by addition of base-pairs to the ends of helices, while *Thermotoga* seems to have minimized alternative foldings and the length of the sequence. Apparently, each RNA has developed an individual, unique strategy to achive thermostability often gained by combination of more then one feature outlined above.

1.8. References

Alifano, P., Rivellini, F., Piscitelli, C., Arraiano, C.M., Bruni, C.B. and Carlomagno, M.S.1994. Ribonuclease E provides substrates for ribonuclease P-dependent processing of a polycistronic mRNA. *Genes Dev*. **8:** 3021-3031.

Altman, S. and Smith, J.D. 1971. Tyrosine tRNA precursor molecule polynucleotide sequence. *Nat. New Biol*. **62:** 1-36.

Altman, S. 1989. Ribonuclease P: an enzyme with a catalytic RNA subunit. *Adv. Enzymol. Relat. Areas. Mol. Biol*. **62:** 1-36.

Altman, S., Wesolowski, D., Guerrier-Takada, C. and Li, Y. 2005. RNase P cleaves transient structures in some riboswitches. *Proc. Natl. Acad. Sci. USA* **102:** 11284-11289.

Andrews, A.J., Hall, T.A. and Brown, J.W. 2001. Characterization of RNase P holoenzymes from *Methanococcus jannaschii* and *Methanothermobacter thermoautotrophicus*. *Biol Chem.* **382:** 1171-7.

Baird, N.J., Srividya, N., Krasilnikov, A.S., Mondragon, A., Sosnic T.R., Pan, T. 2006. Structural basis for altering the stability of homologous RNAs from mesophilic and a thermophilic bacterium. *RNA* **12:** 598-606.

Brown, J. W., & Pace, N. R. 1992. Ribonuclease P RNA and protein subunits from bacteria. *Nucleic Acids Res*, **20(7):** 1451-1456.

Brown, J. W., Haas, E.S., Pace, N.R. 1992. Characterization of ribonuclease P RNAs from thermophilic bacteria. *Nucleic Acids Res.* **21(3):** 671-679.

Buck, A.H., Kazantsev, A.V., Dalby, A.B. and Pace, N.R. 2005a. Structural perspective on the activation of RNAse P RNA by protein. *Nat. Struct. Mol. Biol.* **12(11):** 958-64.

Buck, A.H., Dalby, A.B., Poole, A.W., Kazantsev, A.V., and Pace, N.R. 2005b. Protein activation of a ribozyme: the role of bacterial RNase P protein. *EMBO J.* **24:** 3360-3368.

Carola, C., and Eckstein, F. 1999. Nucleic acid enzymes. *Curr Opin Chem Biol*, 3: 274-283.

Cate, J.H., Gooding, A.R., Podell, E., Zhou, K., Golden, B.L., Kundrot C.E., Cech, T.R., and Dounda, J.A. 1996. Crystal structure of a group I ribozyme domain: Principles of RNA packing. *Science* **273:** 1678-1685.

Chamberlain, J.R., Lee, Y., Lane, W.S. and Engelke, D.R. 1998. Purification and characterization of the nuclear RNase P holoenzyme complex reveals extensive subunit overlap with RNase MRP. *Genes Dev*. **12(11):** 1678-1690.

Chen, J., Nolan, J.M., Harris, M.E. and Pace, N. 1998. Comparative photo-cross-linking analysis of the tertiary structures of *Escherichia coli* and *Bacillus subtilis* RNase P RNAs. *EMBO J.* **17(5):** 1515-1525.

Collins, C. A., & Guthrie, C. 2000. The question remains: is the spliceosome a ribozyme. *Nat Struct Biol,* **10:** 850-854.

Correl C.C, Wool, I.G., and Munishkin, A. 1999. The two faces of the *Escherichia coli* 23 S rRNA sarcin/ricin domain. The structure at 1.11 ? resolution. *J. Mol. Biol.* **292:** 275-287.

Correl C.C, Swinger K.,2003. Common and distinctive features of GNRA tetraloops based on a GUAA tetraloop structure at 1.4? resolution. *RNA,* **9:** 355-363.

Crary, S. M., Niranjanakumari, S., & Fierke, C. A. 1998. The protein component of *Bacillus subtilis* ribonuclease P increases catalytic efficiency by enhancing interactions with the 5' leader sequence of pre-tRNAAsp. *Biochemistry,* **37(26):** 9409-9416.

Doherty, E.A., Batey, R.T., Masquida, B., and Doudna, J.A. 2001. A universal mode of helix packing in RNA. *Nat. Struct. Biol.* **8:** 339-343.

Christian, E.L., Zahler, N.H., Kaye, N.M. and Harris, M.E. 2002. Analysis of substrate recognition by the ribonucleoprotein endonuclease RNase P. *Methods* **28:** 307-322.

Evans, D., Marquez, S.M.and Pace, N.R. 2006. RNase P: interface of the RNA and protein worlds. *TRENDS in biochemical Science* **31(6):** 333-41

Fang, X.W, Srividya, N., Golden, B.L., Sosnick, T.R. and Pan, T. 2003. Stepwise conversion of a mesophilic to a thermophilic ribozyme. *JMB* **330(2):** 177-83.

Fang, X.W., Yang, X.J., Littrell, K, Niranjanakumari, S., Thiyagarajan, P., Fierke, C.A., Sosnick, T.R. and Pan, T. 2001. The *Bacillus subtilis* RNase P holoenzyme contains two RNase P RNA and two RNase P protein subunits. *RNA* **7:** 233-241.

Frank, D.N., Adamidi, C., Ehringer, M.A., Pitulle, C. and Pace, N.R. 2000. Phylogenetic-comparative analysis of the eukaryal ribonuclease P RNA. *RNA* **6(12):** 1895-1904.

Fukuhara, H., Kifusa, M., Watanabe, M., Terada, A., Honda, T., Numata, T., Kakuta, Y. and Kimura M. 2006. A fifth protein subunit Ph1496p elevates the optimum temperature for the ribonuclease P activity from *Pyrococcus horikoshii* OT3. *Biochem. Biophys. Res. Commun.* **343(3):** 956-64.

Gößringer, M., Kretschmar-Kazemir Far, R. and Hartmann, R.K. 2006. Analysis of RNase P protein (*rnpA*) expression in *Bacillus subtilis* utilizing strains with suppressible *rnpA* expression. *J. Bacteriol.* **188(19):** 6816-23.

Guerrier-Takada, C., Gardiner, K., Marsh, T., Pace, N. and Altman, S. 1983. The RNA moiety of ribonuclease P is the catalytic subunit of the enzyme. *Cell* **35(3 Pt 2):** 849-57.

Guo, X., Campbell, F.E., Sun, L., Christian, E.L., Anderson, V.E. and Harris, M.E. 2006. RNA-dependent Folding and Stabilization of C5 Protein During Assembly of the *E. coli* RNase P Holoenzyme. *J. Mol. Biol.* **360(1):** 190-203.

Haas, E.S., Banta, A.B., Harris, J.K., Pace, N.R. and Brown, J.W. 1996. Structure and evolution of ribonuclease P RNA in Gram-positive bacteria. *Nucleic Acids Res.* **24:** 4775–4782.

Haas, E.S. and Brown, J.W. 1998. Evolutionary variation in bacterial RNase P RNAs. *Nucleic Acids Res.* **26(18):** 4093-4099

Haas, E.S., Morse, D.P., Brown, J.W., Schmidt, F.J. and Pace, N.R. 1991. Long-range structure in ribonuclease P RNA. *Science,* **254:** 853–856.

Hall, T.A. and Brown, J.W. 2002. Archaeal RNase P has multiple protein subunits homologous to eukaryotic nuclear RNase P proteins. *RNA* **8(3):** 296-306.

Harris, M.E., Nolan, J.M., Malhotra, A., Brown, J.W., Harvey, S.C. and Pace, N.R. 1994. Use of photoaffinity crosslinking and molecular modeling to analyze the global architecture of ribonuclease P RNA. *EMBO J.* **13:** 3953-63.

Hardt, W.D., Schlegl, J., Erdmann, V.A. and Hartmann, R.K. 1995. Kinetics and thermodynamics of the RNase P RNA cleavage reaction: analysis of tRNA 3'-end variants. *J. Mol. Biol.* **247:**161-72

Hartmann, R.K., Heinrich, J., Schlegl, J., Schuster, H. 1995. Precursor of C4 antisense RNA of bacteriophages P1 and P7 is a substrate for RNase P of *Escherichia coli. Proc. Natl. Acad. Sci. USA* **92:** 5822-5826.

Heus, H.A., and Pardi, A., 1991. Strucural features that give rise to the unusual stability of RNA hairpins containing GNRA loops. *Science* **253:** 191-194.

Jarrous, N. and Altman, S. 2001. Human ribonuclease P. *Methods Enzymol.* **342:** 93-100.

Kazantsev, A.V., Krivenko, A.A., Harrington, D.J., Carter, R.J., Holbrook, S.R., Adams, P.D. and Pace, N.R. 2003. High-resolution structure of RNase P protein from *Thermotoga maritima*. *Proc. Natl. Acad. Sci. U S A.* **100(13):** 7497-502.

Kazantsev, A.V. and Pace, N.R. 2006. Bacterial RNase P: a new view of an ancient enzyme. *Nat Rev Microbiol.* **4(10):**729-40.

Kazantsev, A.V., Krivenko, A.A., Harrington, D.J., Holbrook, S.R., Adams, P.D. and Pace, N.R. 2005. Crystal structure of a bacterial ribonuclease P RNA. *Proc. Natl. Acad. Sci. U S A,* **102(38):** 13392-13397

Kikovska, E.; Svard, S.G.; Kierebom, L.A. 2007. Eukaryotic RNase P RNA mediates cleavage in the absence of protein. *PNAS* **104:** 2062-2067.

Kim, J.J, Kilani A.F., Zahn, X., Altman, S. and Liu, F. 1997. The protein cofactorallows the sequence of an RNase P ribozyme to diversify by maintaining the catalytically active structure of the enzyme. *RNA* **3:** 613-623.

Kirsebom, L.A, Baer, M.F., and Altman, S. 1988. Differential effects of mutatations in the protein and RNA moieties of RNAse P on the efficiency of suppression by various tRNA suppressors. *J. Mol. Biol.* **204:** 879-888.

Kirsebom, L.A. and Svärd, S.G. 1994. Base pairing between *Escherichia coli* RNase P and its substrate. *EMBO J*. **13(20):** 4870-4876.

Kirsebom, L.A. and Vioque, A. 1995. RNase P from bacteria. Substrate recognition and function of the protein subunit. *Mol. Biol. Rep.* **22:** 99-109.

Komine, Y., Kitabatake, M., Yokogawa, T., Nishikawa, K. and Inokuchi, H. 1994. A tRNA-like structure is present in 10Sa RNA, a small stable RNA from *Escherichia coli. Proc. Natl. Acad. Sci. USA* **91:** 9223-9227.

Krasilnikov, A.S., Xiao, Y., Pan, T. and Mondragon A. 2004. Basis for structural diversity in homologous RNAs. *Science* **306(5693):**104-7.

Kruger, K., Grabowski, P., Zaug, A., Sands, J., Gottschling, D., & Cech, T. 1982. Self-splicing RNA: autoexcision and autocyclisation of the ribosomal RNA intervening sequence of *Tetrahymena*. *Cell*, **31:** 147–157.

Krupp, G., Kahle, D., Vogt, T., & Char, S. 1991. Sequence changes in both flanking sequences of a pre-tRNA influence the cleavage specificity of RNase P. *J Mol Biol*, **217(4):** 637-648.

Kurz, J.C., Niranjanakumari, S. and Kierke, C.A. 1998. Protein component of *Bacillus subtilis* RNase P specifically enhances the affinity for precursor-tRNAAsp. *Biochemistry* **37(8):** 2393-400.

Lee, J.Y., Rohlman, C.E., Molony, L.A. and Engelke, D.R. 1991. Characterization of RPR1, an essential gene encoding the RNA component of *Saccharomyces cerevisiae* nuclear RNase P. *Mol. Cell Biol*. **11(2):** 721-730.

Li, Y. and Altman, S. 2003. A specific endoribonuclease, RNase P, affects gene expression of polycistronic operon mRNAs. *Proc. Natl. Acad. Sci. USA* **100:** 13213-13218.

Loria, A. and Pan, T. 1996. Domain structure of the ribozyme from eubacterial ribonuclease P. *RNA* **2(6):** 551-563.

Loria, A. and Pan, T. 1998. Recognition of the 5'-leader and the acceptor-stem of a pre-tRNA substrate by the ribozyme from *Bacillus subtilis* RNase P. *Biochemistry* **37(6):** 10126-10133.

Mans, R.M., Guerrier-Takada, C., Altman, S. and Pleij, C.W. 1990. Interaction of RNase P from *Escherichia coli* with pseudoknotted structures in viral RNAs. *Nucleic Acids Res.* **18:** 3479-3487.

Massire, C., Jaeger, L., & Westhof, E. 1997. Phylogenetic evidence for a new tertiary interaction in bacterial RNase P RNAs. *RNA,* **3(6):** 553-556.

Massire, C., Jaeger, L., & Westhof, E. 1998. Derivation of the three-dimensional architectureof bacterial ribonuclease P RNAs from comparative sequence analysis. *J Mol Biol,* **279(4):** 773-793.

McClain, W. H., Guerrier-Takada, C., & Altman, S. 1987. Model substrates for an RNA enzyme. *Science,* **238:** 527-530.

Muth, G. W., Ortoleva-Donnelly, L., & Strobel, S. A. 2000. A single adenosine with a neutral pKa in the ribosomal peptidyl transferase centre. *Science,* **289:** 947-950

Nissen, P., Hansen, J., Ban, N., Moore, B., & Steitz, T. A. 2000. The structural basis of ribosome activity in peptide bond synthesis. *Science,* **5481:** 920–930.

Niessen, P., Ippolito, J.A., Ban N., Moore, P.B., and Steitz, T.A. 2001. RNA tertiary interactions in the large ribosomal subunit: The A-minor motif. *Proc. Natl. Acad. Sci.* **98**: 4899-4903.

Niranjanakumari, S., Day-Storms, J.J., Ahmed, M., Msieh, J., Zahler, N.H., Venters, R.A. and Fierke, C.A. 2007. Probing the architecture of *Bacillus subtilis* RNase P holoenzyme active site by cross-linking and affinity cleavage. *RNA* **13:** 521-535.

Nolan, J.M., Burke, D.H. and Pace, N.R. 1993. Circularly permuted tRNAs as specific photoaffinity probes of ribonuclease P RNA structure. *Science* **261(5122):** 762-765.

Oh, B.K., Frank, D.N. and Pace, N.R. 1998. Participation of the 3'- CCA of tRNA in the binding of catalytic Mg^{2+} ions by ribonuclease P. *Biochemistry* **37:** 7277–7283.

Pace, N.R. and Brown, J.W. 1995. Evolutionary perspective on the structure and function of ribonuclease P, a ribozyme. *J. Bacteriol.* **177(8):** 1919-28.

Pan, T. 1995. Higher order folding and domain analysis of the ribozyme from *Bacillus subtilis* ribonuclease P. *Biochemistry* **34(3):** 902-909.

Pan, T., Loria, A. and Zhong, K. 1995. Probing of tertiary interactions in RNA: 2'-hydroxyl-base contacts between the RNase P RNA and pre-tRNA. *Proc. Natl. Acad. Sci. U S A* **92:** 12510-12514.

Peck-Miller, K.A. and Altman, S. 1991. Kinetics of the processing of the precursor to 4.5S RNA, a naturally occurring substrate for RNase P from *Escherichia coli*. *J. Mol. Biol.* **221:** 1-5.

Persson, T., Cuzic, S., Hartmann, R.K. 2003. Catalysis by RNase P RNA: unique features and unprecedented active site plasticity. *J Biol Chem*. **278(44):** 43394-401.

Play, H.W., Flaherty, K.M., and McKay, D.B., 1994a. Model for RNA tertiary interaction from the structure of intermolecular complex between a GAAA tetraloop and RNA helix. *Nature* **372:** 111-113.

Reich, C., Olsen, G.J., Pace, B. and Pace, N.R. 1988. Role of the protein moiety of ribonuclease P, a ribonucleoprotein enzyme. *Science* **239(4836):** 178-81.

Rueda, D., Hsieh, J., Day-Storms, J.J., Fierke, C.A and Walter, N.G. 2005. The 5' leader of precursor tRNAAsp bound to the Bacillus subtiolis RNase P holoenzyme has an extended conformation. *Biochemistry* **44:** 16130-16139.

Salavati, R., Panigrahi, A. K. and Stuart, K.D. 2001. Mitochondrial ribonuclease P activity of *Trypanosoma brucei*. *Mol. Biochem. Parasitol.* **115(1):** 109-117..

Schedl, P. and Primakoff, P. 1973. Mutants of *Escherichia coli* thermosensitive for the synthesis of transfer RNA. *Proc. Natl. Acad. Sci. U S A* **70(7):** 2091-2095.

Schedl, P., Primakoff, P., and Roberts, J. 1974. Processing of *E.coli* t RNA precursors. *Brookhaven Symp Biol*. **26:** 53-76.

Schlegl, J., Furste, J.P., Erdmann, V.A., Hartmann R.K. 1992. Cleavage efficiencies of model substrates for ribonuclease P from *Escherichia coli* and *Thermus thermophilus*. *Nucleic Acids Res.* **20(22):** 5963-70.

Siegel, R.W., Banta, A.B., Haas, E.S., Brown, J.W. and Pace, N.R. 1996. *Mycoplasma fermentans* simplifies our view of the catalytic core of ribonuclease P RNA. *RNA* **2(5):** 452–462.

Spitzfaden, C., Nicholson, N., Jones, J.J., Guth, S., Lehr, R., Prescott, C.D., Hegg, L.A. and Eggleston, D.S. 2000. The structure of ribonuclease P protein from *Staphylococcus aureus* reveals a unique binding site for single-stranded RNA. *J. Mol. Biol.* **295(1):**105-15.

Steitz, T. A., & Moore, P. B. 2003. RNA, the first macromolecular catalyst: the ribosome is a ribozyme. *Trends Biochem Sci,* **28(8):** 411-418.

Sun, L.; Harris, M.E. 2007. Evidence that binding of C5 protein to P RNA enhances ribozyme catalysis by influencing active site metal ion affinity. *RNA* **13**: 1505-1515.

Sun, L.; Campbell, F.E., Zahler, N.H. and Harris, M.E. 2006. Evidence that substrate-specific effects of C5 protein lead to uniformity in binding and catalysis by RNase P. *EMBO J.* **25:** 3998-4007.

Svärd, S.G. and Kirsebom, L.A. 1992. Several regions of a tRNA precursor determine the *Escherichia coli* RNase P cleavage site. *J. Mol. Biol.* **227(4):** 1019-31.

Svärd, S.G. and Kirsebom, L.A. 1993. Determinants of *Escherichia coli* RNase P cleavage site selection: a detailed *in vitro* and *in vivo* analysis. *Nucleic Acids Res*. **21(3):** 427-434.

Symons, R. H. 1992. Small catalytic RNAs. *Annu Rev Biochem*, **61:** 641-661.

Tanner K.N., 1999. Ribozymes: the characteristics and properties of catalytic RNAs. *FEMS Microbiol. Rev*. **23:** 257-275.

Thomas, B.C., Gao, L., Stomp, D., Li, X. and Gegenheimer, P.A. 1995. Spinach chloroplast RNase P: a putative protein enzyme. *Nucleic Acids Symp. Ser*. **33:** 95-98.

Thurlow, D.L., Shilowski, D. and Marsh, T.L. 1991. Nucleotides in precursor tRNAs that are required intact for catalysis by RNase P RNAs. *Nucleic Acids Res.* **19(4):** 885-891.

Torres-Larios, A., Swinger, K.K., Krasilnikov, A.S., Pan, T. and Mondragon, A. 2005. Crystal structure of the RNA component of bacterial ribonuclease P. *Nature*, **437(7058):** 584-587.

Torres-Larios, A., Swinger, K.K., Pan, T. and Mondrago, A. 2006. Structure of ribonuclease P-a universal ribozymes. *Curr. Opin. Struct. Biol.* **16:** 327–335

Tsai, H.Y., Masuida, B., Biswas, R., Westhof, E. and Gopalan, V. 2003. Molecular modeling of the three-dimensional structure of the bacterial RNase P holoenzyme. *J. Mol. Biol.* **325(4):** 661-75.

Valadkhan, S., & Manley, J. L. 2001. Splicing-related catalysis by protein-free snRNAs. *Nature*, **413:** 701 - 707.

Van Eenenaam, H., Pruijn, G.J. and van Venrooij, W.J. 1999. hPop4: A new protein subunit of the human RNase MRP and RNase P ribonucleoprotein complexes. *Nucleic Acids Res*. **27:** 2465-2472.

Van Eenenaam, H., Jarrous, N., van Venrooij, W.J. and Pruijn, G.J. 2000. Architecture and function of the human endonucleases RNase P and RNase MRP. *IUBMB Life* **49:** 265-272.

Walker, S.C. and Engelke, D.R. 2006. Ribonuclease P: the evolution of an ancient RNA enzyme. *Crit. Rev. Biochem. Mol. Biol.* **41(2):** 77-102.

Wang, M.Y., Chien, L.F. and Pan, R. L. 1988. Radiation inactivation analysis of chloroplast CF0-CF1 ATPase. *J Biol Chem*, **263(18):** 8838-8843.

Warnecke, J.M., Furste, J.P., Erdmann, V.A., Hartmann, R.K. 1996. Ribonuclease P (RNase P) RNA is converted to a Cd(2+)-ribozyme by a single Rp-phosphorothioate modification in the precursor tRNA at the RNase P cleavage site. *Proc Natl Acad Sci* **93(17):** 8924-8.

Warnecke, J.M., Held, R. Busch, S. Hartmann, R.K. 1999. Role of metal ions in the hydrolysis reaction catalyzed by RNase P RNA from *Bacillus subtilis*. *J Mol Biol.* **290(2):** 433-45.

Warnecke, J.M., Sontheimer, E.J. Piccirilli, J.A. Hartmann, R.K. 2000. Active site constraints in the hydrolysis reaction catalyzed by bacterial RNase P: analysis of precursor tRNAs with a single 3'-S-phosphorothiolate internucleotide linkage. *Nucleic Acids Res*. **28(3):** 720-7.

Waugh, D.S., Green, C.J. and Pace, N.R. 1989. The design and catalytic properties of a simplified ribonuclease P RNA. *Science* **244:** 1569–1570.

Wegscheid, B., Condon, C., Hartmann, R.K. 2006. Type A and B RNase P RNAs are interchangeable in vivo despite substantial biophysical differences. *EMBO* **7(4):** 411-7.

Wegscheid, B., Hartmann, R.K. 2006. The precursor tRNA 3'-CCA interaction with *Escherichia coli* RNase P RNA is essential for catalysis by RNase P *in vivo*. *RNA* **12(12):** 2135-48.

Wegscheid, B., Hartmann, R.K. 2007. *In vivo* and *in vitro* investigation of bacterial type B RNase P interaction with tRNA 3'-CCA. *Nucleic Acids Res*. **35(6):** 2060-73.

Westhof, E., Wesolowski, D. and Altman S. 1996. Mapping in the three dimensions of regions in a catalytic RNA protected from attac by an Fe(II)-EDTA reagent. *J. Mol. Biol.* **258:** 600-613.

Willkomm D.K.and Hartmann R.K.,2007. An important piece of the RNase P jigsaw solved. *TRENDS in biochemical science* **32(6):** 247-50.

Wool, I.G., Gluck, A., and Endo, Y. 1992. Ribotoxin recognition of ribosomal RNA and Proposal for the mechanism of translocation. *Trends. Biochem. Sci*. **17:** 266-269.

2. Goal of the project

1. Identification of *rnpB* and *rnpA* from *Aquificales*

The ubiquitous ribonucleoprotein enzyme ribonuclease P (RNase P) is essential for maturation of pre-tRNAs throughout the three kingdoms of life. Surprisingly, in the sequenced genome of the hyperthermophilic bacterium *Aquifex aeolicus*, considered to represent the deepest branching of the bacterial 16S rRNA-based phylogenetic tree, neither a gene for RNase P RNA nor for the RNase P protein component has been identified.
In this project we wanted to clarify whether other representatives of the *Aquificales* possess an RNase P RNA. For this approach we selected close relatives of *Aquifex aeolicus*: *Aquifex pyrophilus* VF5, *Hydrogenobacter thermophilus* TK6 and *Thermocrinis ruber, Sulfurihydrogenibium azorense* and *Persephonella marina.* We tested extracts from these bacteria for precursor tRNA processing *in vitro*; and by bioinformatic studies we tried to identify *rnpB* and *rnpA* genes in their genomes if available. RNase P RNA candidates were then characterized by kinetic studies, and potential secondary structures were defined.

2. Interdomain interactions in RNase P RNA

The overall conformation of structured RNAs is stabilized by long range interactions. In P RNAs of type A architecture the two independently folded domains, the specificity and the catalytic domain, are connected and oriented towards each other by three interdomain tetraloop-helix contacts L18-P8, L8-P4 and L9-P1. The precise role of each of the three is so far largely unclear and was addressed in two different projects:

2a. Structural basis of a ribozyme's thermostability: L9-P1 interdomain interaction in RNase P RNA

The starting point for this project was our observation that the L9 tetraloop from thermophiles is a characteristic 5' GYAA contacting two consecutive G-C pairs in the minor groove of P1. We therefore suspected this very strong interaction to be a key to activity at higher temperatures. To test that hypothesis, we exchanged the P1P9 module from a mesophile, *E. coli*, for its thermophilic homologue from *T. thermophilus* (or the very stable pseudoknot P1P9 homologue from *Mycoplasma*). Indeed, by these exchanges *E. coli* P RNA gained markedly in activity at increased temperature. Disruption of the P1L9 interaction in *T.*

thermophilus resulted in the opposite effect: substantial loss of activity at higher temperatures. We also tested these engineered P RNAs *in vivo* for complementation of the RNase RNA knockdown *E. coli* strain BW.

2b. *In vitro* and *in vivo* role of interdomain contacts in P RNAs from a psychrophilic, a mesophilic and a thermophilic bacterium

The goal of this second project was to investigate the role of the interdomain interactions in selected RNase P RNAs from bacteria growing at different temperatures (a psychrophile, a mesophile and a thermophile). Towards that aim L9, L8 or L18 were mutated and the respective interactions disrupted in these RNase P RNAs, and processing activity was tested under *single* and *multiple turnover* conditions at different temperatures. This approach was intended to reveal if and how RNase P RNAs are specifically adapted to growth temperature. Further, *in vivo* complementation tests were performed to analyse which interactions are required for viability. Finally, probing and native gels were employed to study how structure and folding of *T. thermophilus* P RNAs changes upon shifting temperature.

3. Methods

3.1. Bacterial cell culture

Equipment, all media and buffers used for bacterial cell culture were autoclaved for 20 min at 121°C and 1 bar. Heat labile solutions were sterilized by filtration.

LB (Luria Bertani) Medium	
Peptone	10 g / l
Yeast extract	5 g / l
NaCl	10 g / l
adjust pH to 7.5 (with NaOH)	

E. coli cells were grown in LB medium at 37°C. For selection of clones with antibiotic resistance genes, growth media were supplemented with the appropriate antibiotic (see below). For *E. coli* BW strain with an inducible pBAD promoter 10 mM L(+)-arabinose for induction and 0,5 % (w/v) glucose for repression of the promoter was used. For sufficient overexpression of P proteins from *E. coli* or *B. subtilis*, strains carying derivatives of plasmid pQE30 were grown in the presence of 1 mM IPTG.

Antibiotic	Bacteria	Concentration [µg/ml]	used for strain/plasmid
ampicillin	*E. coli*	100	pACYC177, pSP64, pSBpt3'HH, pUC19 derivatives
chloramphenicol	*E. coli*	25	BW

For liquid bacterial cultures 3, 50, 100 or 500 ml of LB medium were inoculated directly from a glycerol stock or with a single colony from an agar plate, and incubated under shaking (180-220 rpm, GFL 3033 shaking incubator) at 37°C. Glycerol stocks were prepared by mixing 500 µl sterile glycerol (99 %) and 500 µl fresh bacterial liquid culture, then shock frozen in liquid nitrogen and stored at –80°C.

3.1.1. Cell growth on agar plates

To prepare LB-agar plates 1l of LB medium was supplemented with 12 g/l agar-agar before autoclaving. Antibiotics were added after the medium was cooled down to 50°C. Aliquots (~20 ml) were poured into sterile Petri dishes. After the agar medium had become solid, the plates were transferred to 4°C and stored upside down until use.

3.1.2. Preparation of competent cells

Treatment of bacterial cells with $CaCl_2$ or cold causes the cellular walls to become permeable. Cells thus become competent for the uptake of exogenous DNA during transformation.

3.1.2.1. Preparation of chemically competent *E. coli* cells, RbCl method

TFB1-buffer	
MOPS*	10 mM
RbCl	10 mM
pH 7.0 with NaOH	

TFB3-buffer	
MOPS	100 mM
$CaCl_2$	50 mM
KCl	10 mM
Glycerol	15 % (w/v)
pH 6.5 with NaOH	

*-MOPS should be sterylized by filtration

100 ml of an *E. coli* culture was grown at 37°C until the OD_{578} reached 0.5-0.6 under shaking at 180 rpm. The flask with the cells was transferred to ice for 10 min followed by 5 min centrifugation at 4°C and 4000 rpm (Eppendorf 5810R). The cell pellet was suspended in 30 ml TFB1 buffer for 5 min on ice and then centrifuged again. The cell pellet was resuspended in 4 ml TFB3 buffer, and 100-200 µl aliquots were frozen in liquid nitrogen and stored at –80°C.

3.1.2.2. Preparation of electrocompetent *E. coli* cells

Flasks with 500 ml of LB medium with *E. coli* cells grown at 37°C to an OD_{578} ~0.6 were incubated on ice for 20 min and then centrifuged for 15 min at 4°C, 4000 rpm (Eppendorf 5810R). The cell pellet was resuspended in 500 ml ice-cold 10 % (v/v) glycerol, after another centrifugation in 250 ml and after a third time with 50 ml 10 % (v/v) glycerol. After a final centrifugation step, the cell pellet was resuspended in 2 ml 10 % (v/v) glycerol, and 100-200 µl aliquots were frozen in liquid nitrogen and stored at –80°C.

3.1.3. Transformation

The uptake of exogenous DNA by cells that alters the phenotype or genetic trait of a cell is called transformation. It can be achieved by thermal shock (chemical transformation) or by electric pulse (electroporation).

SOC Medium(1l)	
Peptone	20 g
Yeast extract	5 g
NaCl	0.6 g
KCl	0.17 g
adjust to pH 7.5 with NaOH and autoclave	
Glucose (autoclave separately)	20 mM
$MgCl_2$	10 mM
$MgSO_4$	10 mM
Magnesium salts (sterile filtered stock solutions) are added prior to use	

3.1.3.1. Transformation of chemically competent *E. coli* cells

10 ng DNA (alternatively up to 10 µl of a ligation reaction) were mixed with 50 µl of competent cells (3.1.2.1.). Cells were incubated on ice for 30 min, then heat-shocked for 45 s at 42°C followed by another 2 min incubation on ice. 800 µl of SOC medium prewarmed to 37°C were added and cells were incubated for another hour at 37°C while shaking. After this time cells were sedimented by centrifugation (30 s, 6000 rpm Eppendorf Minispin). 700 µl of the supernatant were discarded, and after resuspension in the residual supernatant the cells were plated on appropriate agar plates.

3.1.3.2. Transformation of electrocompetent *E. coli* cells (electroporation)

10 ng plasmid DNA mixed with 30 µl of electrocompetent cells (3.1.2.2.) were introduced into a precooled Biorad cuvette (1 mm gap) and incubated on ice for ~3 min. After the pulse (1.8 kV; 5 ms, 50 µF, 100 Ω, Biorad GenePulser) 800 µl SOC medium (supplemented with 10 mM arabinose for strain BW) was added and cells were shaken at 37°C for 1 h. Then different volumes of culture (5-50 µl) were plated directly on LB agar plates with appropriate antibiotics.

3.1.4. *In vivo* complementation of *E.coli* strain BW

For complementation tests, BW cells were tranformed with complementation plasmids by electroporation as described (3.1.3.2.), with the modification that the inductor (10 mM arabinose) added after transformation was removed after 1 h of incubation at 37°C by two washing steps (centrifugation for 1 min, 6000 rpm, Eppendorf Minispin followed by

resuspension in 1 ml LB medium). Cells were then plated on agar plates containing arabinose 10 mM (inductor) or glucose 0.5% (v/v) (repressor) followed by incubation at 37°C or 43°C for up to 24 h. For complementation analyses it was important that the number of colonies that grew under permissive and non-permissive conditions was comparable.

3.2. General nucleic acids techniques

3.2.1. Nucleic acid gel electrophoresis

Nucleic acid gel electrophoresis is used to separate DNA or RNA (anionic polymers) through an electric field. Separation efficiency correlates with differences in size and net charge of the molecule.

3.2.1.1. Agarose gel electrophoresis

5 x TBE buffer	**final concentration**
Tris	445 mM
Boric acid	445 mM
EDTA	10 mM

5 x DNA sample buffer	
Bromophenol blue (BPB)	0.25 % (w/v)
Xylene cyanol blue (XCB)	0.25 % (w/v)
Glycerol	25 % (w/v)
In 5 x TBE buffer; pH 8.0	

For separation of DNA fragments mainly agarose gels were used. Agarose is a polysaccharide (composed of galactose and galactose derivatives) and different pore sizes of the gel matrix are adjusted by varying the concentration of agarose. The pores in agarose gels are larger than in polyacrylamide gels, and these gels are used to resolve large double-stranded DNA fragments (table 3.1). For gel preparation agarose was dissolved in 1 x TBE buffer by heating, then the gel solution was cooled down to about 50-60°C and ethidium bromide was added to a final concentration of 40 µg / 100 ml. The solution was poured into a prepared gel tray with a comb. The solid gel was placed in an electrophoresis chamber containing 1x TBE buffer, and DNA samples mixed with 5 x loading buffer (to 1 x final concentration) were loaded into the gel pockets. Gels were run at 70-100 volts (7.5 mA / cm^2).

% agarose (w/v)	DNA fragment size (kbp)
0.5	1.0 - 30
0.7	0.8 - 12
1.0	0.5 - 7
1.2	0.4 – 6.0
1.5	0.2 – 3.0
2.0	0.1 – 2.0

Table 3.1. Resolution of DNA fragments in agarose gels of different concentration.

3.2.1.2. Crystal violet gels

Crystal violet gels were run for preparation of high quality DNA to avoid staining with ethidium bromide (that has some mutagenic properties and inhibits several enzymes acting on nucleic acids) and UV detection. The agarose solution was prepared as described in 3.2.1.1 and in addition 10 µg / ml of crystal violet (stock solution 10 mg / ml in 1x TBE) was added to the agarose gel solution after cooling to 50-60°C as well as to the running buffer. DNA was visible under normal light as a dark violet band. Since sensitivity of this staining is low, it was important to load sufficient amounts of DNA. For cloning purposes combined pockets were used to obtain preparative amounts of DNA (usually the plasmid vector).

3.2.1.3. Polyacrylamide gel electrophoresis (PAGE)

Polyacrylamide (PAA) gels are generated by crosslinking polymers of acrylamide with the co-monomer bis-acrylamide. Polymerisation of polyacrylamide is initiated by addition of APS (ammonium persulfate) and TEMED. The solution of APS forms radicals, which react with PAA, TEMED in this reaction serves as a catalyst. Different concentrations of acrylamide used for gel preparation correlate with different pore sizes.

3.2.1.3.1. Denaturing PAGE

denaturing sample buffer (PPF buffer)	
2 x concentrated	
Urea	2.6 M
TBE	2 x concentrated
Bromophenol blue (BPB)	0.02 % (w/v)
Xylene cyanol blue (XCB)	0.02 % (w/v)
Formamide	66 % (v/v)

PAA gel solution	Final concentration	20 %
5 x TBE	1 x TBE	200 ml
Acrylamide (48 %)/ Bisacrylamide (2 %)	in desired concentration	400 ml
Urea	8 M	480 g
H_2O		ad 1000 ml

8 M urea is denaturing agent that disrupts the secondary structure ofnucleic acid; therefore migration in denaturing PAA gels is a function of the molecular size of the molecule.
Table 3.2 presents relation of migration of single-stranded DNA to BPB and XCB dyes of the sample buffer in denaturing polyacrylamide gels of different percentage.

% Polyacrylamide	Bromophenol blue	Xylene cyanol
5	35	130
6	26	106
8	19	70-80
10	12	55
20	8	25

Table 3.2. Comigration of single-stranded DNA fragments (given in nucleotides) with the dyes of the sample buffer in denaturing polyacrylamide gels.

A 20 % PAA solution was prepared as a stock that was diluted with 8 M urea (dissolved in 1xTBE) to desired PAA concentrations (the usually used range of concentration was 5-20 %). For gel preparation, two glass plates were cleaned with 70 % ethanol and assembled with appropriate spacers.Then a PAA solution of desired concentration was prepared, 1/100 volume 10 % (w/v) APS and 1/1000 volume TEMED was added, all mixed and poured between the clamped glass plates. At the top of the gel a comb was inserted, to create pockets for later sample loading (the size of the pockets varied from 0.4 cm for kinetics analyses to 20 cm for preparative RNA preparation). The comb was removed after approximately 30 min, and pockets were immediately rinsed with 1 x TBE buffer to remove diffused urea (that tends to accumulate in the pockets), and rests of unpolymerised acrylamide. The gel thus prepared was fixed in the electrophoresis equipment to bridge the buffer reservoirs filled with 1 x TBE buffer and electrophoresis was performed at 5–30 mA (depending on gel size and PAA concentration).

3.2.1.3.2. Native polyacrylamide gels

Native gels do not contain any denaturing agent and therefore are commonly used for the separation of double-stranded DNA or folded RNAs. In such a gels the migration mobility depends not only on the size but also on the secondary/tertiary structure of the nucleic acid. This method provides the possibility to separate molecules with the same molecular size but different structure. Table 3.3 presents the sizes of DNA fragments (in base pairs) that comigrate with the two dyes of the sample buffer in non-denaturing polyacrylamide gels of different concentration.

% polyacrylamide	Bromophenol blue	Xylene cyanol
3.5	100	460
5	65	260
8	45	160
12	20	70
20	12	45

Table 3.3. Comigration of double-stranded DNA fragments (given in base pairs) with the dyes of the sample buffer in non-denaturing polyacrylamide gels.

The solution of PAA for native gels was prepared in the same way as for denaturing PAA gels, except that no urea was added. Also assembly and preparation of the gels was identical to the procedure described for denaturing gels. Samples were loaded onto the gel in the presence of 1 x DNA sample buffer (3.2.1.1.).

3.2.1.3.2.1. Non-denaturing polyacrylamide gel electrophoresis for RNA folding analysis

2 x native loading buffer	
Glycerol	10 % (v/v)
$MgCl_2$	4.5 or 10 mM
Bromophenol blue	0.025 % (w/v)
Xylene cyanol	0.025 % (w/v)

10 x THE buffer (pH 1 x buffer 7.4)	Final concentration
Tris	660 mM
Hepes	330 mM
EDTA	1 mM
For folding experiments 1 x THE buffer was supplemented with 100 mM NH_4OAc and 4.5-10 mM $MgCl_2$.	

PAA gel solution	Final concentration	11.25 %
10 x THE buffer	1 x THE	10 ml
2 M NH_4OAc	100 mM	5 ml
2 M $MgCl_2$	4.5 - 10 mM	x µl
Acrylamide (48 %) bisacrylamide (2 %)	4.5-20 %	x ml
H_2O		ad 100 ml

The system for resolution of native RNA conformers was adopted from Buck *et al.*, 2005a. In this procedure magnesium and ammonium ions stabilize RNA tertiary structures. After folding (see 3.4.6.), samples were supplemented with an equal amount of 2 x native loading buffer and loaded on thin (< 1 mm) polyacrylamide gels. To prevent any structural RNA rearrangement during electrophoresis, gels were run in a 4°C cold room to not exceed 15°C of internal gel temperature at 180-240 V.

3.2.2. Detection of nucleic acids in gels

Different methods were applied to DNA/RNA depending on the experimental context and downstream application.

3.2.2.1. Ethidium bromide staining

Ethidium bromide is the best known nucleic acid intercalator that visualizes nucleic acids after exposition to UV light (between 254-366 nm) due to emission of fluorescent light at 590 nm (orange). In case of agarose gels already containing ethidium bromide it is possible to visualize DNA fragments directly after or even during electrophoresis using an UV transilluminator. For detection of DNA/RNA in PAA, gels were sealed into plastic bags together with ethidium bromide staining solution (0.5 µg / ml in 1 x TBE) after electrophoresis. Subsequent to 10 min incubation under gentle shaking, the staining solution was removed and the gel exposed to UV light on a transilluminator.

3.2.2.2. UV-shadowing

UV-shadowing (254 nm) is the method that permits to visualize DNA or RNA in PAA gels and avoids ethidium bromide staining. It is especially important for preparative purposes. Gels after electrophoresis were wrapped in transparent foil and placed on a fluorescent chromatography plate with fluorescence indicator (254 nm). By focussing a hand-held UV light source (254 nm) on the surface of the gel it was possible to visualize nucleic acids appearing as dark bands.

3.2.2.3. Visualization using crystal violet

Crystal violet agarose gels (3.2.1.2.) were supplemented with 1/1000 of a 10 mg / ml aqueous crystal violet solution. DNA was seen under normal light and appeared as a dark violet band.

3.2.2.4. Radioluminography

Radioactively (^{32}P) labelled RNA or DNA could be detected using a phosphoimager. The gel was wrapped in transparent foil, and then an image plate was exposed to it. The time of exposition varied and depended on the amount of radioactivity loaded onto the gel. The imaging plate was scanned using a BIO-imaging analyser BAS 1000 (Raytest, Fujifilm) and the PC-BAS software. Gels were evaluated and bands were quantified using the AIDA version 3.42 software (Raytest Isotopenmessgeräte GmbH).

3.2.3. Gel elution of nucleic acids

Selection of the elution method depended on the gel matrix, molecular weight and the type of nucleic acid.

3.2.3.1. Elution by diffusion

Elution by diffusion was applied to elute RNA molecules from denaturing polyacrylamide gels. The RNA band of interest, detected by UV-shadowing or using a phosphoimager (radiolabelled RNA), was excised using a sterile scalpel and incubated overnight in 5-8 volumes of elution buffer at 4°C while shaking. The eluate was precipitated with ethanol (3.2.6.) and the RNA pellet dissolved in sterile RNase free water. Different elution buffers were used depending on the application:

RNA elution buffer 1:

200 mM Tris / HCl, pH 7.0; 1 mM EDTA; 0.1% SDS. This buffer was efficient for elution of P RNA constructs.

RNA elution buffer 2:

1 M NH_4OAc, pH 7.0. This buffer was preferentially used for elution of RNAs randomly modified with nucleotide analogues.

RNA elution buffer 3:

1 M NaOAc, pH 5.0. This buffer was preferentially used for elution of radiolabelled pre-tRNA substrates. This buffer limits RNase induced degradation due to the low pH.

3.2.4. Isolation of DNA from agarose gels

Isolation of double-stranded DNA from agarose gels was performed using the Qiagen QIAquick Gel Extraction Kit according to the protocol of the manufacturer.

3.2.5. Photometric concentration determination of nucleic acids

Measuring the absorbance of nucleic acids at 260 nm permits to calculate the concentration using the Lambert Beer law:

$$\mathbf{A} = \varepsilon \cdot \mathbf{c} \cdot \mathbf{d}$$

where :

A: Absorbance; c: molar concentration of DNA/RNA [mol / l]; ε: molar extinction coefficient [1 / (M·cm)]; d: path length of the cuvette [cm])

Samples of DNA/RNA were usually diluted 1:70 in water, and absorbance at 260 nm against water was measured using a UV spectrophotometer.

The concentration was calculated using the known values c(1 A_{260}) that represent the concentration corresponding to one absorbance unit at 260 nm (1 A_{260}):

1 A_{260} **double-stranded DNA**	corresponds to a c(1 A_{260}) of ~ 50 µg / ml
1 A_{260} **single-stranded DNA**	corresponds to a c(1 A_{260}) of ~ 33 µg / ml
1 A_{260} **RNA**	corresponds to a c(1 A_{260}) of ~ 40 µg / ml

The general formula for RNA/DNA concentration calculation:

$$c[mg/ml] = \frac{A_{260} \cdot c(1A_{260}) \cdot D_f}{1000}$$

(c is concentration in µg/µl, D_f is the dilution factor)

3.2.6. Ethanol precipitation

For concentration or desalting of DNA/RNA samples ethanol precipitation was applied. 1/10 volume of 3 M NaOAc pH 4.7 was added to one volume of DNA/RNA sample, mixed with 2.5 volumes of 99.6% ethanol and kept for 60 min at –20°C. After 1 hour of centrifugation at 4°C, 13,000 rpm (Biofuge fresco) the pellet was washed with 70 % (v/v) ethanol and centrifuged for another 15 min at 13,000 rpm. The pellet after this step was dried at 50°C for ~2-5 min and dissolved in an appropriate volume of double-distilled water.

3.2.7. Phenol/chloroform extraction

To increase the quality of a DNA/RNA sample phenol/chloroform extraction was performed. This method allows removal of any protein-based contaminations. The procedure is based on using two different organic solvents. TE-saturated (10 mM Tris-HCl, 1 mM EDTA, pH 7.5-8.0) phenol is added to an equal volume of DNA/RNA sample, vortexed (30 s) and then centrifuged (5 min, 13,000 rpm at room temperature) to achieve phase separation. The upper aqueous phase is carefully collected and transferred into a new tube. The procedure is repeated twice with chloroform instead of phenol and followed by ethanol precipitation (3.2.6.).

3.3. DNA techniques

3.3.1. Preparation of genomic DNA

Isolation of genomic DNA from *Aquificales* cells was performed using Nucleobond AX-G columns according to protocol of the manufacturer Macherey-Nagel. Usually 0.1 g of cells were used.

3.3.2. Preparation of plasmid DNA

The procedure of plasmidal DNA isolation is based on a modified alkaline lysis method (Birnboim and Doly, 1979; Birnboim, 1983).

3.3.2.1. Preparative plasmid DNA isolation from *E. coli* cells

For Midi or Maxi preparation of plasmid DNA a 50 or 500 ml culture of bacteria was prepared. Cells were harvested and resuspended in a buffer containing RNase A (cell resuspension buffer). SDS/alkaline lysis with lysis buffer was the next step, and then the solution was neutralised with neutralisation buffer and applied to a respective anion exchange resin column equilibrated with column equilibration buffer. Removal of contaminations like proteins, RNA, dyes and soluble macromolecular components was achieved using a buffer with intermediate ionic strength (washing buffer). Pure plasmid DNA was finally eluted in a high salt buffer (elution buffer) and concentrated by isopropanol precipitation followed by centrifugation (4°C, 10400 rpm). The DNA pellet was washed with 70 % ethanol, dryed and suspended in DNAse free water. The procedure was performed precisely as described by the manufacturer (Macherey-Nagel, Qiagen Nucleobond AX-G).

Buffers used for preparative plasmid preparation

Cell resuspension buffer	50 mM Tris / HCl, pH 8.0 10 mM EDTA 100 µg / ml RNase A
Lysis buffer	200 mM NaOH 1 % (w/v) SDS
Neutralisation buffer	3 M KOAc, pH 5.5
Column equilibration buffer	750 mM NaCl 50 mM MOPS pH 7.0 15 % (v/v) isopropanol 0.15 % (v/v) Triton X-100
Washing buffer	1 M NaCl 50 mM MOPS pH 7.0 15 % (v/v) isopropanol
Elution buffer	1.25 M NaCl 50 mM Tris / HCl pH 8.5 15 % (v/v) isopropanol

3.3.2.2. Analytical scale preparation of plasmid DNA (Mini prep)

The isolation of plasmid DNA for analytical purposes (Mini prep) was performed using Nucleospin Plasmid Kit (Macherey-Nagel) according to the supplied protocol. Normally 3 ml

(for cells containing high-copy plasmids like pUC19 derivatives) or 5-10 ml (for cells containing low-copy plasmids such as pACYC177 derivatives) of bacterial culture were used.

3.3.3. Restriction digest of DNA

Cleavage by restriction endonucleases is a relatively simple method to quickly analyse DNA. Type II restriction endonucleases are very specific and cleave double-stranded DNA at defined positions known as recognition sequences (mostly palindromic). They generate DNA fragments with either 5' or 3'overhangs (sticky ends) or blunt ends and 3'-hydroxyl and 5'-phosphate termini enabling religation.

Restriction digest	
DNA (0.1–20 µg)	x µl
10 x buffer	2 µl
Restriction enzyme	0.2 - 2 µl
H_2O	ad 20 µl
	Σ 20 µl

Each enzyme has different requirements for optimal activity (indicated by the manufacturer). Incubation time varies from 1 h for analytical digestion to overnight for the preparative scale. Usually digestion of DNA was analysed on agarose gels (3.2.1.1.). If the DNA was subjected to additional reactions, it was purified by phenol/chloroform extraction or (for cloning experiments) gel extraction was performed to remove primers or small cleavage fragments (see 3.2.5.).

3.3.4. 5'- Phosphorylation of DNA

T4 Polynucleotide Kinase (T4 PNK) catalyses the transfer of the ?-phosphate from ATP to the 5'-OH group of single- and double-stranded DNA and RNA (forward reaction). This reaction is necessary for obtaining phosphorylated primers for PCR, the products of which can to be blunt-ligated with T4 DNA ligase. An example phosphorylation reaction is shown below.

Phosphorylation reaction		
DNA primer 100 pmol / µl	5 µl	
10 mM ATP	2.5 µl	
10 x T4 PNK buffer (forward)	2.5 µl	
T4 PNK (NEB, 10 U / µl)	1 µl	
H_2O	14 µl	
	S 25 µl	1 h 37°C

The phosphorylated primers were used directly in the PCR reaction (2.5 µl in a 50 µl PCR reaction).

3.3.5. Ligation

DNA ligation is used for linking one end of a DNA fragment to another end using either complementary overhangs ('sticky' ends) or blunt ends. This method was mostly used to insert DNA fragment into a vector (plasmid). The ligation reaction (generation of a phosphodiester bond between a 3'-hydroxy and a 5'-phosphate group) is catalysed by T4 DNA ligase from *E. coli* phage T4. The DNA fragment to be inserted and the vector were gel purified and their concentration was determined. A standard ligation reaction is shown below. A very important control reaction was ligation without any insert to check for traces of uncut vector. Also molar ratios of vector to insert were varied (usually 1:3 or 1:9). The ligation reaction after appropriate incubation was directly used for transformation of *E. coli* cells (3.1.3.).

Ligation reaction	**control**	**1:3**	**1:9**	
Vector	2 µl	2 µl	2 µl	30-100 ng
Insert	-	1 µl	3 µl	
5 x T4 DNA ligase buffer	2 µl	2 µl	2 µl	
H_2O	5 µl	4 µl	2 µl	
T4 DNA ligase (Invitrogen, 1U/µl)	1 µl	1 µl	1 µl	
	Σ 10 µl	Σ 10 µl	Σ 10 µl	1 h 37°C (sticky ends) 16°C or 4°C (blunt ends)

3.3.6. Polymerase chain reaction (PCR)

The polymerase chain reaction (PCR) is a powerful method for the amplification of very small amounts of DNA. The reaction is catalyzed by a thermostable DNA polymerase, usually *Pfu* polymerase (originally isolated from *Pyrococcus furiosus*). This enzyme exhibits a proofreading activity (3'→ 5' exonuclease activity). Sometimes when *Pfu* polymerase was not able to perform the PCR reaction, *Taq* polymerase (isolated from *Thermus aquaticus*) was used. This polymerase despite its very high processivity (incorporation of 1000 nt / min) has an error rate of 1/10,000 and produces adenine overhangs. Those PCR products can be directly used for TA-cloning (see 3.4.10.8.). As a template for PCR, single- or double-stranded DNA is required, as well as a forward and a reverse DNA primer and a buffer containing Mg^{2+} and dNTPs.

A PCR reaction usually consists of three temperature steps :

Denaturation at 95°C: double-stranded DNA is melted and becomes accessible to primers and polymerase.

Annealing of primers: within a certain temperature range (50-65°C); specific binding of starter DNA.

Elongation at 68-72°C: 5'→ 3' elongation of the annealed primer. Example of a PCR program and a reaction solution are shown below. The polymerase was always added as the last component after pre-heating the reaction mix to 95°C (hot start PCR). For PCR with overlapping DNA fragments, first 8 cycles were performed in the absence of primers for overlap extension; afterwards the primers were added and the PCR reaction was continued as usually. The elongation time varied depending on the size of the amplified DNA fragment.

After PCR, 5 to 10 µl of the reaction were checked on an agarose gel and depending on the downstream reactions different procedures were applied (precipitation, digestion, ligation etc.).

PCR program

Initial denaturation	95 °C	3 min	
denaturation	95 °C	1 min	
annealing	50- 65°C	1 min	
elongation	68 –72°C	30 s – 5 min	25-30 cycles
Final elongation	68 –72°C	5 min	

PCR reaction

template	x µl	single bacterial colony, 5 ng plasmid or 10 ng genomic DNA
10 x PCR buffer MBI(–$MgCl_2$, + KCl)	5 µl	
25 mM $MgCl_2$	5 µl	c_{End} = 2,5 mM
10 mM dNTPs	1 µl	
Primer forward 100 pmol / µl	0.5 µl	
Primer reverse 100 pmol / µl	0.5 µl	
H_2O	37,7-x µl	
Pfu/*Taq* DNA polymerase (10 U / µl)	+ 0.3 µl	added at 95°C during initial denaturation step
	Σ 50 µl	

3.4. RNA Techniques

3.4.1. Total RNA isolation

3.4.1.1. Trizol RNA isolation

Total cellular RNA from *Aquificales* was isolated by the TRIzol method (Invitrogen). 0.2 g of cell pellet was resuspended in 0.5 ml of TRIzol followed by 5 min incubation at room temperature. 0.1 ml of chlorophorm was added, and the mixture was vortexed and incubated another 2 min at room temperature. After 15 min centrifugation (13,000 rpm, 4°C, Biofuge fresco, Heraeus) the aqueous phase was transferred into a new 1.5 ml tube and precipitated with 0.8 vol/vol isopropanol for 10 min at room temperature. Then 1 hour centrifugation (13,000 rpm, 4°C) was applied. The RNA pellet was washed with 70% ethanol, centrifuged for another 15 min (13,000 rpm, 4°C), and air dryed. The RNA was dissolved in RNase free water (usally 200 µl) and remaining residual DNA was removed by DNase I digest (Turbo DNase, Ambion). An example of a DNase I digest protocol is given below.

DNase I digestion		
RNA 20 µg	50 µl	
10 x Turbo DNase buffer	6 µl	
Turbo DNase I (2 U / µl)	4 µl	
	Σ 60 µl	1 h 37°C

Often DNase I digestion was repeated once more to deprive RNA of any trace amounts of genomic DNA. After digestion the RNA was phenol/chlorophorm extracted and ethanol precipitated. Finally the RNA was dissolved in water and the concentration was again determined.

3.4.1.2. Column RNA isolation

Alternatively to TRIzol preparation, the RNeasy Kit from Qiagen was used. This method permits to enrich the pool of isolated RNAs in molecules that are bigger than 200 nucleotides. Details of the procedure are precisely described in the manual from the manufacturer. When using this method it was important not to take more than 60 mg of cell pellet because of the limited binding capacity of the matrix resin.

3.4.2. T7 Transcription of unmodified RNA

Transcription is the procces of synthesis of RNA on the basis of a DNA template. For efficient transcription *in vitro*, recombinantly expressed RNA polymerase from bacteriophage

T7 was used. This enzyme consisting of a single 100 kDa subunit specifically recognises the T7 phage promoter sequence 5'-TAA TAC GAC TCA CTA TA -3'. This recognition results in polymerisation starting immediately downstream of this sequence in 5'→ 3' direction. It is important for the reaction efficiency that the first nucleotide of the transript is guanine. In this work RNA run-off transcription (polymerisation is terminated when the polymerase reaches the end of the template) was used with linearized plasmids or PCR products as templates. If the transcribed RNA was used for 5'-end labelling with γ-^{32}P ATP, transcription was performed in the presence of guanosine in excess over GTP.

transcription reaction, 50 µl:		**final concentration**
RNase-free water	25.15 µl	
HEPES pH 8.0, 1 M	4 µl	80 mM
DTT 100 mM	7.5 µl	15 mM
$MgCl_2$ 3 M	0.55 µl	33 mM
spermidine 100 mM	0.5 µl	1 mM
NTP mix (25 mM each ATP, CTP, UTP, GTP)	7.5 µl	3.75 mM (each)
template (linearised plasmid) 1 µg / µl	4 µl	40 µg / ml
pyrophosphatase 200 U / ml	0.5 µl	2 U / ml
T7 RNA Pol. 200 U / µl	0.3 µl	In house preparation

The components of the reaction (see above) were mixed in a 1.5 ml reaction tube, T7 RNA polymerase was added at the end, and the reaction was incubated at 37°C for 2-4 h. 10 µl of the transcription mix. was checked by denaturing PAGE for efficiency of transcription. To obtain large amounts of RNA preparative scale (1-5) ml transcriptions were performed. These reactions were always performed in aliquots of 500 µl and T7 RNA polymerase was added in two steps: at the beginning and after two hours. After transcription RNA was purified according to following procedure:

First the whole transcription reaction was ethanol precipitated (3.2.6.). The pellet after precipitation was resuspended in RNase free water and an equal volume of PPF buffer. Then the sample was loaded on a preparative denaturing PAA gel (for example, a 2 ml sample was loaded into a pocket 10 cm wide, 2 cm deep and 1 mm thick). The gel was run so in such a way that extreme heating (usally not more than 30 mA) was avoided. For P RNAs to achieve good resolution, 7 % gels were run until xylene cyanol had migrated 12 cm from the slot. After UV shadowing (3.2.2.2.), bands of interest were cut out, transferred into an appropriate

volume of elution buffer (3.2.3.1.) and shaken at 4 °C overnight. The eluted RNA was then concentrated by ethanol precipitation (3.2.6.) and resuspended in double-distilled water. The RNA concentration was determined (3.2.4.) and the quality was checked by denaturing PAGE.

3.4.3. T7 Transcription of RNA carrying randomly distributed phosphorothioate analogues

Incorporation of *S*p-NTPaS analogues into RNA was performed during *in vitro* transcription. Many nucleotide analogues are poor substrates for the wild-type T7 RNA polymerase. In our lab the Y639F mutant T7 RNA polymerase was used. This enzyme shows a greater tolerance towards changes of functional groups in the minor groove (Sousa R. *at al.,* 1995*)* and therefore incorporates nucleotide analogues much more efficiently.

The reaction mix was prepared as shown below except for guanosine and T7 RNA polymerase. The mixture was then prewarmed to 37°C, the appropriate amount of the pre-heated guanosine solution (75°C) was quickly added, and the mixture was vortexed to avoid guanosine precipitation. The reaction was finally initiated by addition of enzyme (T7 RNA polymerase).

transcription reaction, 500 µl:		**final concentration**
RNase-free water	83.5 µl	
HEPES pH 8.0, 1 M	40 µl	80 mM
DTT 100 mM	75 µl	15 mM
$MgCl_2$ 3 M	5.5 µl	33 mM
spermidine 100 mM	5 µl	1 mM
NTP mix (25 mM each)	75 µl	3.75 mM (each)
ATPaS or UTPaS 4.33 mM	11 µl	0.095 mM
template (linearised plasmid) 0.5 µg / µl	40 µl	40 µg / ml
pyrophosphatase 200 U / ml	5 µl	2 U / ml
guanosine (30 mM, kept at 75 °C)	150 µl	9 mM
T7 RNA Pol. 200 U / µl	10 µl	4000 U / ml

The reaction mixture was incubated for 4 h at 37°C. The RNA transcript was purified as described for unmodified RNA with the following exceptions:

- all precipitation steps were performed in the presence of NH_4OAc, pH 7.0, to avoid degradation (hydrolysis) of RNA randomly modified with phosphorothioate analogues (acid-sensitive).
- for elution, the buffer 2 was chosen (3.2.3.1.)

3.4.4. 5'- end labelling of RNA with g-^{32}P ATP

5'- end labelling of RNA was performed with T4 polynucleotide kinase (T4 PNK) (3.3.4.). This enzyme requires 5'-OH ends, so RNA transcripts subjected to labelling must lack 5'-phosphates. Radioactive phosphate was transferred from γ-^{32}P ATP.

5'- end labelling reaction	
10 x T4 PNK buffer (forward reaction)	1.5 µl
25 mM DTT	1.5 µl
RNA	x µl (~20 pmol)
RNase-free water	ad 11 µl
γ-^{32}P ATP (3000 Ci/mmol, 10 µCi/µl, 3.3 µM)	3.0 µl
T4 PNK (10 U / µl)	1.0 µl
	Σ 15 µl

The reaction was started by addition of T4 PNK kinase and incubated for 1 h at 37°C. After this time samples were loaded on a thin (< 1 mm) denaturing polyacrylamide gel. After electrophoresis, the image plate was exposed to the gel for 1 min, with small radioactively marked stickers fixed on the foil covering the gel to allow localization of the RNA band. After scanning of the image plate (Bio-Imaging Analyzer, FLA 3000-2R, FUJIFILM), the band of interest was cut out, eluted by diffusion (3.2.3.1.), concentrated by ethanol precipitation (3.2.6.) and resuspended in 10-20 µl double-distilled water. Evaluation of efficiency of the labelling was determined by measuring 1 µl of labelled RNA with a scintillation counter (Packard 2000CA, Tricarb, liquid scintillation analyser) by Cerenkov measurement.

3.4.5. 3'- end labelling of RNA with [5'-^{32}P] pCp

3'- end labelling was achieved by ligation of 5'-^{32}P cytidine 3',5' bisphosphate (^{32}P-pCp) to the 3' hydroxyl group of RNA. The reaction was catalyzed by T4 RNA ligase (England & Uhlenbeck, 1978). The reaction mix was prepeard as shown below and incubated overnight at 4°C. The RNA was purified in the same way as for 5'end labelling (3.4.4.).

3'- end labelling reaction	
10 x T4 RNA ligase buffer	0.6 µl
1.5 mM ATP (use fresh dilution)	0.33 µl
RNA (purified by denaturing PAGE)	x µl (~20 pmol)
[5'-^{32}P] pCp (3000 Ci/mmol, 10 µCi/µl,)	3.0 µl
T4 RNA Ligase (NEB,10 U / µl)	1.0 µl
	Σ 6 µl

3.4.6. Folding analysis on non-denaturing gels

Folding assays were performed in the buffer KN including trace amounts of 3'-^{32}P-end labelled (<50 fmol) P RNAs which were either kept at 4°C (no preincubation) or preincubated for 55 min at 37°C, or 5 min at 55°C followed by 50 min at 37°C. In case of samples including the protein subunit, the *E. coli* or *B. subtilis* P proteins were added to a final concentration of 40 nM after the preincubation of the RNA (see below), followed by incubation for another 15 min at 37°C. For those RNAs kept at 4°C, protein was added at 4°C without further incubation. After mixing the samples with an equal volume of 2 x native loading buffer (3.2.1.3.2.1.), they were loaded onto the non-denaturing 11.25 % (v/v), thin (< 1 mm) polyacrylamide gel (3.2.1.3.2.1.). The gel and running buffer contained 66 mM Hepes, 33 mM Tris, pH 7.4 and 0.1 mM EDTA (1 x THE), supplemented with 100 mM NH_4OAc and 2 or 4.5 mM $MgCl_2$. Gels were run at 180-250 V until xylene cyanol had migrated 11.5 cm from the slot, controlling the temperature of the gel to not exceed 15°C. RNA bands were visualized with a Bio-Imaging Analyzer (FLA 3000-2R, FUJIFILM).

Buffer KN 4.5 (Dinos *et al.*, 2004) *

Hepes-NaOH, pH 7.4	20 mM
$Mg(OAc)_2$	4.5 mM
NH_4OAc	150 mM
Spermidine	2 mM
Spermine	0.05 mM
β-mercaptoethanol	4 mM

*pH of the buffer at 37°C was 7.4

Folding analysis		c_{End}
M1 RNA (50 fmol)	x µl	10 nM
5 x buffer KN	1 µl	1 x
RNase P protein	x µl	40 nM
H_2O	ad 5 µl	
	Σ 5 µl	
Preincubation:	a) No preincubation (4°C) b) 55 min 37°C, +/- protein 15 min 37°C c) 5 min 55°C, 50 min 37°C, +/- protein 15 min 37°C	
	+ 5 µl 2 x native loading buffer Analysis on 11.25 % PAA (1 x THE, 100 mM NH_4OAc, x mM $MgCl_2$)	

3.4.7. Partial hydrolysis of *T. thermophilus* P RNA by nuclease T1

Ribonuclease T1 (RNase T1) is an endoribonuclease that specifically degrades single-stranded RNAs at G residues. It cleaves the phosphodiester bond 3' of G residues leaving 5'-OH and 2', 3'-cyclic phosphates that are further hydrolyzed to 3'-phosphates. The ribonuclease T1 does not require metal ions for activity. T1 hydrolysis assays were performed under native and denaturing conditions after incubation at 37°C or 55°C to analyse folding of RNase P RNA.

The reaction mix (without T1 nuclease) was preincubated 10 min at 55°C or 37°C, then T1 nuclease was added and hydrolysis was performed at 37°C for another 10 min. The reaction was stopped by ethanol precipitation (3.2.6.). The pellet was suspended in 12 µl of PPF buffer and RNAs were resolved on 12% PAA urea gels (1 mm thick, 16 cm wide and 40 cm long). Gels were run at 6-10 mA until xylene cyanol had migrated 36 cm from the slot. The gel temperature was controlled to prevent heating.

2x native buffer *

Hepes-NaOH, pH 7.0	100 mM
$Mg(OAc)_2$	9 mM
NH_4OAc	200 mM

*- the pH of 1 x buffer at 37°C was 7.5

1.25 x denaturing buffer*

Na-citrate pH=5.0	25 mM
Urea	8.75 M
EDTA	1.25 mM

*- the pH of 1 x buffer at 37°C was 5.0

T1 hydrolysis (native) 50 µl:		**Final concentration**
2 x native buffer	25 µl	1 x
5' or 3'-endlabelled RNA	~0.5 µl (2 x 10^4 cpm)	400 cpm / µl
Carrier RNA (6 S RNA)	2 µl	60 ng / µl
T1 nuclease	0.8 µl	0.016 U / µl
RNase-free water	21.7 µl	

T1 hydrolysis (denaturing) 50 µl:		Final concentration
1.25 x denaturing buffer	40 µl	1 x
5' or 3'-endlabelled RNA	~0.5 µl (2 x 10^4 cpm)	400 cpm / µl
Carrier RNA (6 S RNA)	2 µl	60 ng / µl
T1 nuclease	0.8 µl	0.016 U / µl
RNase-free water	6.7 µl	

3.4.8. Lead-induced hydrolysis of *T. thermophilus* P RNA

Metal ions can induce RNA degradation. Especially Pb^{2+} induced cleavage can be well used to localize high-affinity metal binding sites as well as to probe the secondary structure of RNA molecules. The reaction mix (without Pb^{2+}) was preincubated for 10 min at 55°C or 37°C. Then Pb^{2+} was added and hydrolysis was performed at 37°C for another 20 min. The reaction was stopped by ethanol precipitation with the subsequent procedure as for T1 cleavage (3.4.7.).

2 x native Pb^{2+} probing buffer *	
Tris -HCl, pH 7.0	100 mM
$Mg(OAc)_2$	0.2 M
NH_4OAc	0.2 M

*- the pH of 1 x buffer at 37°C was 7.5

Pb^{2+} hydrolysis (native) 50 µl:		Final concentration
2 x buffer	25 µl	1 x
5' or 3'-endlabelled RNA	~0.5 µl (2 x 10^4 cpm)	400 cpm / µl
Carrier RNA (6 S RNA)	2 µl	60 ng / µl
$Pb(OAc)_2$ 100 mM (freshly prepared)	1-2,5 µl	2-5 mM
RNase-free water	21.5-20 µl	

3.4.9. Iodine-induced hydrolysis of phosphorothioate analogue-modified RNA

RNAs with nucleotide analogues carrying phosphorothioate modification (one non-bridging phosphate oxygen replaced with sulphur) incorporated during transcription (see 3.4.3.) are specifically sensitive for cleavage by iodine. Iodine treatment results in A-, C-, G- or U-specific cleavage (depending on the identity of the incorporated phosphorothioate nucleotide

analogue) that after denaturing PAGE is visible as a ladder. The preparation of iodine solution and the setup of the reaction are outlined below. The reaction mix was incubated for 20 min at 37°C followed by ethanol precipitation (3.2.6.) and further procedure as for T1 cleavage (3.4.7.).

I_2 solution, 50 µl:		**Final concentration**
10 mg / ml I_2 in ethanol	5 µl	1 mg / ml
ethanol abs.	5 µl	20 %
RNase-free water	40 µl	

Iodine-induced hydrolysis reaction, 50 µl:		**Final concentration**
5'- or 3' -endlabelled RNA	~1 µl (2 x 10^4 cpm)	400 cpm / µl
100 mM HEPES pH 7.5	5 µl	10 mM
1 mg / ml I_2 solution	5 µl	0.1 mg / ml
Carrier RNA (6 S RNA)	2 µl	60 ng / µl
RNase-free water	~37 µl	

3.4.10. Construction and analysis of a cDNA library from *Hydrogenobacter thermophilus* TK6

Construction and analysis of a cDNA library from *Hydrogenobacter thermophilus TK6* was a complex procedure that included several steps:

- Total RNA isolation, DNase I digestion and RNase P processing assay
- Gel fractionation and RNase P processing assay
- cDNA synthesis including C-tailing reaction, TAP treatment, 5' RNA/DNA adapter ligation, first strand synthesis by reverse transcriptase, second strand synthesis (PCR)
- TA cloning and blue white screening
- Colony PCR
- *In vitro* transcription and RNase P processing assay

3.4.10.1. Total RNA isolation, DNase I digestion and RNase P processing assay

The first step and the basis for construction of the cDNA library was to determine if total RNA exhibited any pre-tRNA processing activity. Initially total RNA isolation and DNase I digest was performed as described in (3.4.1.). Total RNA was then tested for the presence of RNase P RNA activity in KN buffer (3.6.1.) with 10 mM Mg^{2+}:

Total RNA activity mix (see below, without *B. subtilis* protein) was preincubated for 5 min at 55°C and for another 50 min at 37°C. Then the protein was added and incubation was continued for 5 more min at 37°C. The reaction was started by fast addition (and mixing) of 16 µl activity mix to 4 µl of substrate mix (preincubated for 5 min at 55°C and 25 min at 37°C). After 2 h of incubation at 37°C, 10 µl of sample was taken and mixed with an equal amount of PPF (see 3.2.1.3.1.) buffer and loaded on 20 % denaturing PAA gel (see 3.2.1.3.1.). The gel was run until xylene cyanol had migrated 10 cm from the slot and exposed overnight to a image plate (3.2.2.4.).

Total RNA activity mix		**Final concentration**
5 x KN buffer (no Mg^{2+})	3.2 µl	1 x
0.2 M $Mg(OAc)_2$ pH=7.4	0.8 µl	10 mM
Total RNA	5µl (~1 µg)	~50 ng / µl
B.subtilis P protein (0.4 µM)	2 µl	~40 nM
RNase-free water	5 µl	
	Σ 16 µl + 4 µl of substrate mix	

Substrate mix		**Final concentration**
5 x KN buffer (no Mg^{2+})	0.8 µl	1 x
0.1 M $Mg(OAc)_2$ pH=7.4	0.4 µl	10 mM
RNase-free water	~2.5 µl	
5' end labelled $ptRNA^{Gly}$ *T.th*	~0.3 µl (3×10^3 cpm)	750 cpm / µl
Σ 4 µl pre-incubated 5 min 55°C and 25 min 37°C		

3.4.10.2. Gel fractionation and RNase P processing assay

To narrow down the complexity of the RNA pool in the search for a potential RNase P RNA, a preparative 8% PAA denaturing gel was run with 100 µg of total RNA loaded into 15 cm wide pockets. The gel was run until xylene cyanol had migrated 13 cm from the slot. Then the gel was stained with ethidium bromide (3.2.2.1) and, with a sterile scalpel, the gel was

fractionated into small strips containing RNAs of different sizes. For reproducibility of the fractionation, a molecular marker was also loaded onto the gel. Gel strips were transferred into elution buffer (buffer 1, 3.2.3.1.) and eluted overnight at 4°C while shaking, concentrated by ethanol precipitation (see 3.2.6.) and resuspended in 100 µl RNase free water. Then RNase P processing assays were performed (3.4.10.1) using 5 µl (0.3-1 µg) of eluted RNA.

3.4.10.3. cDNA synthesis

3.4.10.3.1. C-tailing reaction

Poly(A) polymerase naturally catalyzes the addition of 5'-adenosine monophosphate to the 3'-hydroxyl end of single-stranded RNA using ATP as substrate. Poly(A) polymerase will add either single or multiple residues, depending upon the reaction conditions. The enzyme can also add poly C and poly U to RNA but it does so with reduced efficiency (<5 %). All classes of RNA can be used as primer. Longer RNA molecules are better primers than short oligomers.

C-tailing mix (see below) without poly (A) polymerase was prewarmed to 37°C and enzyme was added followed by 2 h incubation at 37°C. Then the RNA was phenol/chlorophorm extracted (see 3.2.7.), ethanol precipitated (see 3.2.6.) and the pellet was suspended in 20 µl of RNase-free water.

C-tailing mix, 50 µl:		**final concentration**
active fraction of RNA	25 µl (~5 µg)	~100 ng / µl
Tris-HCl 1 M pH 7.9	2.5 µl	50 mM
NaCl 5 M	2.5 µl	0.25 M
$MgCl_2$ 25 mM	4 µl	2 mM
BSA 20 µg / µl	1.25 µl	0.5 µg / µl
$MnCl_2$ 50 mM	2 µl	2 mM
CTP 10 mM	3 µl	0.6 mM
RNase inhibitor (40 U / µl, Fermentas)	1 µl	0.8 U / µl
Poly (A) polymerase (2.5 U / µl, Invitrogen)	1.5 µl	0.752 U / µl
RNase-free water	7.75 µl	
	Σ 50 µl 2h 37°C	

3.4.10.3.2. TAP treatment

TAP (Tobacco acid pyrophosphatase) is an enzyme that removes two phosphates from the 5'-triphosphate ends of RNA, enabling subsequent RNA ligation. This reaction permits to include in the library also primary unprocessed transcripts.

The TAP mix (see below) was incubated for 2 h at 37°C and subsequently the RNA was phenol/chlorophorm extracted and ethanol precipitated. After drying, the pellet was suspended in 14.5 µl of RNase-free water.

TAP mix, 30 µl:		**Final concentration**
10 x TAP buffer	3 µl	1 x
C-tailed RNA	20 µl	170 ng / µl
TAP (10 U / µl Epicentre)	1 µl	0.3 U / µl
RNase-free water	6 µl	

3.4.10.3.3. 5' RNA/DNA adapter ligation

T4 RNA ligase was used for RNA ligation of a RNA/DNA adapter oligonucleotide to the 5' end of C-tailed, TAP treated RNA. The last three positions of this oligonucleotide (5' GTC AGC AAT CCC TAA GGAG) were ribonucleotides (all others were standard deoxyribonucleotides).

For this reaction, the RNA obtained from the previous reaction and the adapter oligonucleotide were mixed, incubated for 5 min at 90°C, and chilled on ice for another 5 min. Then the rest of the components of the 5'RNA/DNA adapter ligation mix listed below were added and the mixture was incubated overnight at 4°C. This step was followed by phenol/chlorophorm extraction, ethanol precipitation and the dryied pellet was suspended in 36 µl of RNase-free water.

5' RNA/DNA adapter ligation mix, 40 µl:		**final concentration**
RNA	14.5 µl	~130 ng / µl
Adapter oligonucleotide (100 pmol / µl)	10 µl	25 pmol / µl
BSA 0.1 % (w/v)	4 µl	0.01 % (w/v)
10 x T4 RNA ligase buffer	4 µl	1 x
ATP 10 mM	4 µl	1 mM
RNase inhibitor (40 U / µl, Fermentas)	0.5 µl	0.5 U / µl
T4 RNA ligase (NEB)	3 µl	0.75 U / µl
	Σ 40 µl , 4°C overnight	

3.4.10.3.4. First strand synthesis by reverse transcriptase

A reverse transcriptase, also known as RNA-dependent DNA polymerase, is a DNA polymerase enzyme that transcribes single-stranded RNA into DNA. As primers a mix of three oligonucleotides containing a poly G tail (for annealing to the added poly C tail of the RNA), 3' terminated with different nucleotides and with an adapter sequence on the 5'end were used:

5´AGGAGCCATCGTATGTCGGGGGGGGGGGGGG**A**
5´AGGAGCCATCGTATGTCGGGGGGGGGGGGGG**T**
5´AGGAGCCATCGTATGTCGGGGGGGGGGGGGG**C**

The above oligonucleotides (each 100 pmol / µl stock) were mixed in a ratio 1: 1: 1 (the final concentration of each was 33 pmol / µl). C-tailed, TAP-treated and adapter-ligated RNA was mixed with the oligonucleotide mix and incubated for 5 min at 65°C and chilled on ice for another 3 min. Then all other components listed below were added (without reverse transcriptase) and prewarmed to 42°C for 2 min.

Reverse transcription mix, 20 µl:		**final concentration**
RNA (C-tailed, TAP-treated, adapter-ligated)	10.5 µl	~70 ng / µl
Oligonucleotide mix (33 pmol / µl each)	1 µl	1.65 pmol / µl of each
dNTPs mix (2.5 mM each dATP, dCTP, dGTP, dTTP)	1 µl	0.125 mM each
5 x RT buffer (Invitrogen)	4 µl	1 x
DTT 100 mM	2 µl	10 mM
RNase inhibitor (40 U / µl, Fermentas)	0.5 µl	1 U / µl
SS RT (200 U, Invitrogen SSII RNase H minus RT Kit)	1 µl	10 U / µl
	Σ 20 µl	

Finally reverse transcriptase was added and the reaction was performed in a thermocycler as follows:

RT program	
42°C	5 min
55°C	20 min
60°C	20 min
65°C	20 min
85°C	5 min

Products of this reaction were directly used for PCR.

3.4.10.3.5. Second strand synthesis (PCR)

For synthesis of the second strand, a standard PCR (3.3.6.) reaction was performed using 2 µl of the reverse transcription reaction as template. The primers used for this PCR were complementary to the adapter sequences within the template.

5´ PCR-Primer: 5´ GTCAGCAATCCCTAACGAG

3´ PCR-Primer: 5´AGGAGCCATCGTATGTCG

The PCR reaction was performed with *Taq* DNA polymerase with the following temperature cycles:

Steps of PCR program	
1: 95°C	5 min
2: 95°C	1 min
3: 52°C	0.5 min
4: 72°C	1 min, 30 cycles from step 2
5: 72°C	7 min

The PCR products were then run on a 1% agarose gel and bands of interest were excised (i.e. fragments corresponding to a size of 300-600 bp) and extracted from the gel using the QIAquick Gel Extraction Kit from Quigen (3.2.5.).

3.4.10.4. TA cloning and blue white screening

Gel-purified DNA was directly cloned into the pCR2.1-TOPO cloning vector (Invitrogen) by TA cloning. In this vector, inserts are ligated into the middle of the *lac Z* gene, the product of which is β- galactosidase, causing a blue colour of colonies with a functional *lac Z* gene when the artificial substrate X-galactose is added to the growth medium. Successful ligation of inserts into the vector disrupts the *lac Z* gene and results in white colonies.

Ligation was performed according to the manufacturer's protocol and chemical transformation was done using TOPO 10 *E. coli* cells (Invitrogen). Cells were plated on ampicillin LB agar plates supplemented with 0.005% X-galactose (stock 2 %) and grown at 37°C overnight.

3.4.10.5. Colony PCR

PCR was used as a quick method to screen the plasmid library, only white colonies were analysed. A single white colony was transferred into 50 µl of LB medium and vortexed. 5 µl of this resuspension was used as a template for PCR (3.3.6.) using the same program like in (3.4.10.7.). The 5' primers used in this PCR introduced a T7 promoter sequence (marked in gray):

5´ PCR-Primer: 5´ TAATACGACTCACTATAGGTCAGCAATCCCTAACGAG

3´ PCR-Primer: 5´AGGAGCCATCGTATGTCG

10 µl aliquots of PCR products were checked on an agarose gel for inserts in the size range of interest. The rest of the PCR reaction was ethanol precipitated and used later in run-off transcription.

3.4.10.6. *In vitro* transcription and RNase P processing assay

Selected templates from the previous step were transcribed with T7 RNA polymerase as described in (3.4.2.) in a volume of 50 µl. 8.2 µl of each transcription reaction were directly taken for RNase P processing assays (3.4.10.1.).

3.4.11. FPLC (Fast Performance Liquid Chromatography)

FPLC was used to partially purify RNA-protein complexes from species belonging to the *Aquificales*. A frozen (-80°C) cell pellet (~200 mg) was resuspended in about 6 ml of buffer A (FPLC), containing 60 mM NH_4Cl, and lysed by sonication (Branson Sonifier 250, output 20, duty cycle 30-40 %, 10 min on ice), followed by centrifugation for 45 min at 4°C and 10,000 g.

Buffer A (FPLC)	
NH_4Cl	0.06-0.55 M
$Mg(OAc)_2$	10 mM
DTT	6 mM
Tris-HCl, pH 7.2	50 mM

The pellet was discarded and the supernatant was loaded onto a DEAE fast flow sepharose column (column XK16, Amersham Biosciences). The flow rate of injection was 1 ml / min, the rate for washing and elution was 2 ml / min. DEAE sepharose is a weak anion exchanger, so molecules negatively charged at pH 7.2 can bind to the column matrix. We assumed RNase P holoenzymes to be negatively charged because of the RNA subunit probably making the major contribution to the net charge of the enzyme. During FPLC the first peak detected by UV (260) (flow through) always corresponded to unbound material, then absorbance again reached the basal level and an NH_4Cl gradient from 60 to 550 mM NH_4Cl was applied. Gradient fractions of 2 ml were collected and analysed for RNase P activity (3.4.11.1.). Active fractions were frozen in liquid nitrogen and stored at -80°C. Finally the column was washed with 1 M NaCl and then rinsed with double-distilled water followed by washing with 20 % ethanol.

3.4.11.1. RNase P processing assays with FPLC fractions

To test FPLC fractions for RNase P processing activity, buffer conditions were adjusted; the resulting FPLC activity mix (see below) was preincubated at 55°C for 5 min, followed by another 30 min at 37°C.

FPLC activity mix		**Final concentration**
5 x KN buffer (no Mg^{2+}, see 3.4.6.)	3.2 µl	1 x
0.1 M $Mg(OAc)_2$ pH=7.4	0.6 µl	10 mM
FPLC fraction	10 µl	
RNase-free water	2.2 µl	
	Σ 16 µl + 4 µl of substrate mix	

The pre-tRNA processing reaction was initiated by addition of 4 µl substrate mix containing 5' end ^{32}P labelled pre-tRNA (3.4.10.1.). Incubation time was 1 h at 37°C.

3.4.12. Micrococcal nuclease treatment

Micrococcal nuclease (S7 nuclease) is nonspecific endo-exonuclease that digests single stranded and double stranded nucleic acids. This enzyme is strictly dependent on Ca^{2+} ions and its activity can be modulated by titration of Ca^{2+} with EGTA (ethylene glycol tetraacetic acid). In my study this nuclease was used to deprive holoenzyme of RNase P of RNA subunit and investigate the role of protein subunit. For that purpase the micrococcal nuclease mix (see below) was incubated for 40 min at 37 C and then 5µl of 100 mM EGTA were added (final concentration 30 mM). 10 µl of this mix were then taken and tested in pre-tRNA processing assay (see 3.4.11.1.).

Micrococaccal nuclease mix (11.5 µl)		**Final concentration**
FPLC active fraction or 50 nM *E. coli* M1 in FPLC buffer A (3.4.11.)	10 µl	
0.1 M $CaCl_2$	0.5 µl	4.5 mM
Micrococcal nuclease 300 U / µl Fermentas	1 µl	26 U / µl
	Σ 11.5 µl incubate 40 min at 37 °C	

3.5. Protein methods

3.5.1. Laemmli SDS-PAGE

SDS-PAGE (Sodium dodecylsulphate polyacrylamide gel electrophoresis) is a powerful method used to separate proteins in polyacrylamide gel. SDS is an anionic detergent that denaturates proteins and introduces negative charges enabling to separate protein mixtures according to their molecular weight. The protocol is based on Laemmli *et al*. (1970). Gels were prepared using the Mini Protean 3 cell chamber system (Biorad). First, the separation gel was prepared (for *E. coli* P protein 17 %), poured between assembled glass plates and overlaid with isopropanol. After polymerization isopropanol was washed away and the solution of stacking gel (4 %) was poured on top. Pockets were created with a comb inserted into the top of the gel. The polymerized gel was fixed in the electrophoresis chamber and covered with 1 x gel running buffer. Protein samples in 1 x sample loading buffer were loaded into pockets and the gel was run at 180 V for 40 min.

4 x Separation gel buffer (Laemmli)	
Tris-HCl pH 8.8	1.5 M

8 x Stacking gel buffer (Laemmli)	
Tris-HCl pH 6.8	1 M

5 x Gel running buffer (Laemmli)	
Tris-HCl pH 8.3	20 mM
Glycine	0.25 M
SDS	0.1 % (w/v)

4 x Loading buffer (Laemmli)	
SDS	4 % (w/v)
Glycerol	20 % (w/v)
β-mercaptoethanol	5 % (w/v)
Tris-HCl pH 6.8	250 mM
Bromophenol blue	0.001 %

SDS-PAGE gels (Laemmli)

Separation gel (5 ml)	10 %	15 %	17 %
Acrylamide (48 %)/ bisacrylamide (2 %)	1 ml	1.5 ml	1.7 ml
4 x Separation gel buffer (Laemmli)	1.25 ml	1.25 ml	1.25 ml
20 % (w/v) SDS	25 µl	25 µl	25 µl
H_2O	2.73 ml	2.23 ml	2.03 ml
10 % (w/v) APS	50 µl	50 µl	50 µl
TEMED	5 µl	5 µl	5 µl

Stacking gel (5 ml)	4 %
Acrylamide (48 %)/ bisacrylamide (2 %)	400 µl
8 x Stacking gel buffer (Laemmli)	625 µl
20 % (w/v) SDS	25 µl
H_2O	3.95 ml
10 % (w/v) APS	50 µl
TEMED	5 µl

3.5.2. Coomassie staining

After electrophoresis the gel was tranferred into container with gel staining solution and soaked for 10 min at room temperature while shaking, followed by destaining with hot water.

Gel staining solution	
Methanol	40 % (v/v)
Acetic acid	10 % (v/v)
Coomassie Brilliant Blue R250	0.5 % (w/v)

Destaining solution
water

3.5.3. Preparation of recombinant RNase P proteins

For purification of *E. coli* and *B. subtilis* RNase P proteins with a N-terminal His-tag (His-tagged peptide leader: MRGSHHHHHHGS, encoded in plasmid pQE-30 in *E. coli* JM109) (Rivera-León *et al.*, 1995) cell cultures were grown to an OD_{578} of 0.6 and IPTG was added to a final concentration of 1 mM. Cells were harvested after 3 h of induction by centrifugation for 10 min at 5,000 rpm and 4°C. The subsequent steps were performed at 4°C or on ice, and all buffers were supplemented 40 µg / ml of the protease inhibitor phenylmethylsulfonyl fluoride (PMSF). The cell pellet was resuspended in 10 ml of sonication buffer SB (50 mM Tris-HCl, pH 8.0, 0. 3 M NaCl, 0.1 % triton X-100, 1 M NH_4Cl), and sonicated (Branson Sonifier 250, output 20, duty cycle 50 %, 15 min on ice). After centrifugation for 30 min (4°C, 14,500 g), the supernatant was mixed with Ni-NTA agarose (400 µl for 2 liters of cell culture) prewashed twice with 10 ml SB buffer. Under gentle mixing at 4°C for 2, proteins were bound to the matrix followed by three times washing (centrifugation-resuspension cycles; centrifugation at 4°C and 8,500 rpm in a desktop centrifuge) with 2 ml cold washing buffer (30 mM imidazol, 50 mM Tris-HCl, pH 8.0, 8 M urea, 0.1 % triton X-100). The

protein was then eluted with 500 µl elution buffer (50 mM Tris-HCl, pH 7.0, 10 % glycerol, 7 M urea, 20 mM EDTA, 0.3 M imidazol) for 45 min at 4°C under gentle shaking. The eluate was dialyzed twice for 1 h and overnight against volumes of 500 ml dialysis buffer (50 mM Tris-HCl, pH 7.0, 0.1 M NaCl, 10 % glycerol; dialysis bags: Roth, molecular weight cut off 12-14 kDa, were boiled for 10 min in distilled water before use). The content of the dialysis bags was transferred to a 2- ml Eppendorf tube and centrifuged for 20 min at 4°C and 12,000 rpm in a desktop centrifuge, the pellet was discarded and the supernatant with pure proteins was aliquoted, frozen in liquid nitrogen and stored at -80°C. All purification steps were checked by SDS-PAGE on 17 % gels to confirm the purity and concentration of the RNase P proteins.

3.6. Kinetic Analysis

3.6.1. Kinetic analysis of *in vitro* reconstituted RNase P holoenzymes

RNase P holoenzyme analyses were performed under *multiple turnover* conditions, where substrate is present in excess over enzyme; thus, one enzyme molecule can cleave more than one substrate molecule during the reaction. This approach makes it possible to calculate k_{obs} (µmol substrate per min and µmol enzyme). This rate can be limited by either substrate association (k_1), cleavage (k_2) or product release (k_3) or a conformational rearrangement of the substrate/enzyme or product/enzyme complex .

$$E + S \underset{k_{-1}}{\overset{k_1}{\rightleftarrows}} ES \overset{k_2}{?} EP \underset{k_{-3}}{\overset{k_3}{\rightleftarrows}} E + P \qquad (k_{obs})$$

where E = P RNA, S = ptRNA and P = tRNA, k_n: rate constants

Processing assays of reconstituted RNase P holoenzymes were performed basically as described in (3.4.10.1.). Always buffer KN (containing 2 or 4.5 mM Mg^{2+}) was used as reaction buffer. In this assay 10 nM of RNase P RNAs, 100 nM pre-$tRNA^{Gly}$ substrate (with trace amounts (< 1 nM) of 5'-^{32}P-endlabelled material and 40 nM protein were used. Preincubation of RNase P RNA was performed for 5 min at 55°C and 50 min at 37°C, after which RNase P protein was added, followed by another 5 min at 37°C. The substrate mix was preincubated under the same conditions for 5 min at 55°C and 25 min at 37°C. Processing reactions were started by combining 16 µl enzyme and 4 µl of substrate mixes to a total

volume of 20 µl, and assayed at 37°C. At different time points 4 µl aliquots were collected, mixed with an equal volume of PPF (3.2.1.3.1.) buffer and analyzed by denaturing PAGE on 20 % gels.

Buffer KN 2/4.5 (Dinos *et al.*, 2004) *****

Hepes-KOH, pH 7.4	20 mM
$Mg(OAc)_2$	2 or 4.5 mM
NH_4OAc	150 mM
Spermidine	2 mM
Spermine	0.05 mM
β-mercaptoethanol	4 mM

*- the pH of 1 x buffer at 37°C was 7.4

3.6.2. Kinetic analysis of RNase P RNA

RNase P RNA activity in the absence of the protein subunit (RNA alone reactions) were performed as *single turnover* kinetics. In this type of experiment the enzyme concentration is much higher than the concentration of substrate ([E]>>[S]). This experiment permits calculation of three different constants:

K_M = the enzyme concentration at which the half-maximum cleavage rate is observed.

k_{obs} = the rate constant observed in the *single turnover* reaction at a certain enzyme concentration.

k_{react} (V_{max}) = the highest possible reaction velocity in a *single turnover* reaction. This condition is observed when enzyme concentration is at saturation.

Before starting the reaction, enzyme and 5'-^{32}P-labelled substrate were preincubated separately in the same buffer (1 x reaction buffer) for 5 min at 55°C and 55 min at 37°C.

5 x reaction buffer *

MES pH=6.0	250 mM
NH_4OAc	0,5 M
EDTA	0,5 mM
$Mg(OAc)_2$	0,5 M

*- the pH of 1 x buffer at 37°C was 6.0

P RNA preincubation, 16 µl		**Final concentration**
x µM P RNA	x µl	0.1 - 3 µM
5 x reaction buffer	3.2 µl	1 x
RNase-free water	to 16 µl	

Substrate preincubation, 4 µl		Final concentration
5' -endlabelled substrate	x µl (2000 cpm)	< 1 nM
5 x reaction buffer	0.8 µl	1 x
RNase-free water	to 4 µl	

After preincubation, 4 µl of the substrate solution were mixed with the 16 µl of P RNA solution. The P RNA-substrate mix was further incubated at 37°C or 55°C and 4 µl aliquots were collected at different time points. Each aliquot including the zero control (without P RNA) was mixed with an equal volume of PPF buffer and analysed by denaturing PAGE. For data evaluation, see (3.6.3.).

3.6.3. Evaluation of kinetic analysis

Samples from kinetics were analysed on 20 % denaturing PAA gels, imaging plates were exposed to the gel overnight and scanned with the Bio-Imaging System (Raytest). Bands corresponding to (uncleaved) ptRNA or released 5'-flank (equals mature tRNA) were quantified using the software AIDA and all further evaluation was done using the software Grafit (3.0).

The processed amount of tRNA could be calculated as follows:

$$tRNA_{processed} = \frac{[5'-flank]}{[5'-flank] + ptRNA}$$

To calculate the k_{obs} values by fitting, a single order rate equation was applied:

$$A_t = A \cdot \left(1/e^{-kobs} \cdot t\right)$$

with A_t: amount of tRNA cleaved at timepoint t, A: maximum amount of pre-tRNA that could be cleaved (limit), k_{obs}: observed rate constant.

3.7. Cloning experiments

3.7.1. Plasmids for T7 transcriptions of diverse P RNAs

All P RNAs used in this work were produced by run-off transcription with T7 RNA polymerase. For this purpose, the desired *rnpB* gene was cloned into the multi copy plasmid pUC19 *via EcoRI* and *BamHI* restriction endonucleases. First, the *rnpB* gene was amplified with a primer pair where the sense primer contained a *BamHI* site and T7 promoter at its 5'-end and the reverse primer encoding an *EcoRI* site at its 5'-end. After PCR the product was

digested with *EcoRI* and *BamHI* and ligated into pUC19 cleaved with the same enzyme pair. This strategy was used for cloning the *rnpB* genes from *P. marina* (used primers # 1and 2, section 6.6) and *S. azorense* (used primers # 3 and 4, section 6.6). The template used for amplification of the inserts was genomic DNA (see PCR protocol 3.3.6.)

For generating loop L9 mutants of RNase P RNAs (*E. coli* and *P. haloplanktis*), plasmids with the wt version of the genes were taken as template, and PCR amplified the entire vector by use of two phosphorylated primers (3.3.4.) priming "5'-end to 5'-end" within the L9 region to introduce the desired mutation(s) (used primers for *P. hal* # 5 and 6, *E. coli* # 29 and 30). After PCR, the sample was digested with *DpnI* to selectively eliminate the (methylated) plasmid template, and PCR products were circularized with T4 DNA ligase.

A two-step cloning procedure was applied to generate *E. coli P1P9 Tth, E. coliP1P9 Mgen* and *E. coli P1P9 MgenA117C.* First, P9 elements were exchanged by the method described above for L9 mutants of *E. coli* and *P. haloplanktis*; in a second PCR, element P1 was exchanged and simultaneously restriction sites and a T7 promoter were introduced. Products of this reaction were digested with *EcoRI/BamHI* and ligated into pUC19. All clonings were confirmed by sequencing. Primers used in the first step were # 11 and 12 (for *E. coli P1P9 Tth*; see section 6.6), # 34 and 48 (for *E. coliP1P9 Mgen*), # 36 and 37 (for *E. coli P1P9 MgenA117C*). Primers for the second PCR step were # 9 and 10 (for *E. coli P1P9 Tth*; see section 6.6), # 34 and 35 (for *E. coliP1P9 Mgen* and *E. coli P1P9 MgenA117C*).

3.7.2. Construction of derivatives of the low copy plasmids pACYC177 for complementation studies in *E.coli rnpB* mutant strains

To analyze if engineered P RNAs can complement the *E. coli rnpB* mutant strain BW (Wegscheid and Hartmann, 2006), the *rnpB* gene of interest was cloned into the low copy plasmid pACYC177 under control of the native *E. coli rnpB* promoter (EP). First, to amplify the native promoter a PCR was done using as template a derivative of plasmid pSP64 (pSP64 *E. coli rnpB*wt; Wegscheid and Hartmann, 2006) that encodes the entire *E. coli rnpB* gene including the promoter and terminator regions. This PCR (primers #15, 16; section 6.6) introduced an *NheI* restriction site. To amplify the *rnpB* gene to be introduced, a reverse primer including a *HindIII* site (primers #18, 20 or 22 in section 6.6) and a forward primer encoding a 3'-terminal fragment of the *E. coli* native *rrnpB* promoter at the 5'-end (primer #17, 19 or 21) were used. The products of both PCR reactions were gel purified and combined in an overlap PCR using primers #15 and #18, 20 or 22. These products were digested with

NheI/HindIII and ligated into pACYC177 cut with the same enzymes. This strategy was used for cloning of all derivatives of *P. haloplanktis rnpB, E. coli P1P9 Tth, E. coli P1P9 Mgen* and *E. coli P1P9 MgenA117C.* The pACYC177 plasmid used for insertion of *rnpB* variants is shown below (picture adapted from Wegscheid, 2006); the shown original construct, containing the *E. coli wt rnpB* gene under the native *E. coli rnpB* promoter (EP), also served as the positive control in the complementation tests in *E. coli* strain BW.

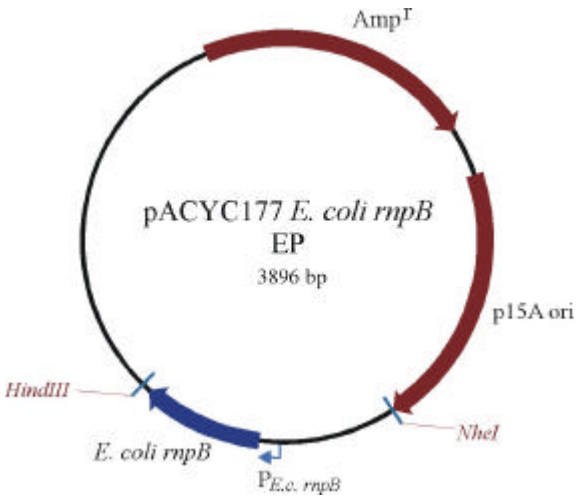

There was also another way for introduction of *rnpB* genes into pACYC177. First, from the original vector (pACYC177 *E. coli rnpB* EP; see above), the *E. coli rnpB* coding region was deleted and several restriction sites (*SmaI, KpnI, XhoI, EcoRI*) located exactly at the boundaries of *rnpB* promoter and terminator were introduced. We achieved this by PCR of the entire plasmid with phosphorylated primers matching sequences immediately upstream and downstream of the *E. coli rnpB* coding sequence within pACYC177 *E. coli rnpB* EP (primers #23 and 24). After PCR, and *DpnI* digestion, the PCR product was circularized with T4 DNA ligase. The resulting vector pACYC(res) permitted straightforward insertion of any *rnpB* gene. In this strategy, the *rnpB* gene of interest was first amplified with a phosphorylated primer containing half of a *SmaI* restriction site (primers #25 or 27) and a second primer with a *KpnI* site (primers #26 or 28); the PCR product was digested with *KpnI* and ligated into pACYC(res) also cut with *KpnI* and *SmaI*. This approach was used for cloning of *T. thermophilus* and *D. radiodurans.*

3.8. References

Birnboim, H.C., 1983. A rapid alkaline extraction method for the isolation of plasmid DNA. *Methods Enzymol*. **100:** 243-255.

Birnboim, H.C. and Doly, J., 1979. A rapid alkaline extraction procedure for screening recombinant plasmid DNA. *Nucleic Acids Res.* **7:** 1513-23.

Buck, A.H., Dalby, A.B., Poole, A.W., Kazantsev, A.V. and Pace, N.R. 2005. Protein activation of a ribozyme: the role of bacterial RNase P protein. *EMBO J.* **24:** 3360-3368.

Dinos, G., Wilson, D.N., Teraoka, Y., Szaflarski, W., Fucini, P., Kalpaxis, D. and Nierhaus, K.H. 2004. Dissecting the ribosomal inhibition mechanisms of edeine and pactamycin: the universally conserved residues G693 and C795 regulate P-site RNA binding. *Mol. Cell.* **13:** 113-24.

England, T.E. and Uhlenbeck, O.C. 1978. 3'-terminal labelling of RNA with T4 RNA ligase. *Nature*, **275:** 560-561.

Laemmli, U.K. 1970. Cleavage of structural proteins during the assembly of the head of bacteriophage T4. *Nature* **227(259):** 680-685.

Rivera-León, R., Green, C.J. and Vold, B.S. 1995. High-level expression of soluble recombinant RNase P protein from *Escherichia coli. J. Bacteriol.* **177:** 2564–2566.

Sousa R., Padilla R. 1995. Amutant T7 RNA polymerase as a DNA polymerase. *EMBO* **14(18):** 4609-4621

Schägger, H. and von Jagow, G. 1987. Tricine-sodium dodecyl sulfate-polyacrylamide gel electrophoresis for the separation of proteins in the range from 1 to 100 kDa. *Anal. Biochem*. **166(2):** 368-379.

4. Results and Discussion

4.1. RNase P in the *Aquificales*

The *Aquificales* is a group of thermophilic bacteria, with *Aquifex aeolicus* being the best-known representative. The phylogeny of this bacterium is unclear; according to analysis of 16S rRNA and elongation factors Tu and G, *Aquifex* represents the deepest branch of the bacterial phylogenetic tree (Burggraf *et al.*, 1992; Huber *et al.*, 1992; Bocchetta *et al.*, 2000). On the other hand, approaches analyzing conserved small insertions and deletions in a variety of proteins locate *Aquifex* close to the d/e division of proteobacteria. Intriguingly, neither a gene for the RNA nor the protein component of RNase P has been identified in the sequenced genome of *A.aeolicus*. Further, in *in vitro* activity tests using cell extracts or RNA alone no processing activity of pre-tRNA was observed (Willkomm *et al.*, 2002). Also an RNomics approach did not reveal any potential candidate of RNase P RNA (Willkomm *et al.*, 2005).
According to my unpublished data a slight change in the buffer composition compared to previous experiments (from 100 mM NH_4Cl, 50 mM glycine, 10 mM $MgCl_2$, pH 7.4, to 100 mM NH_4Cl, 50 mM Tris-HCl, pH 7.2, 10 mM MgOAc and 6 mM DDT, 3.4.11) resulted in detection of FPLC fractions (for details see 3.4.11) from *Aquifex aeolicus* total cell lysates, which displayed an RNase P-like pre-tRNA cleavage activity (Fig. 1).

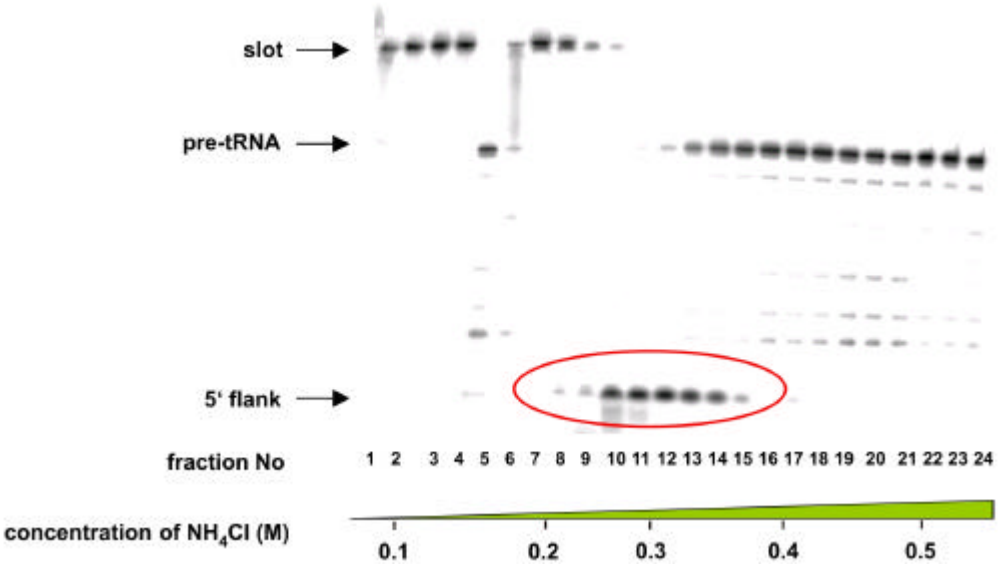

Fig. 1. pre-tRNA processing assay with FPLC fractions from *A. aeolicus*. Fractions containing RNase P activity are marked by a red oval. Numbering of the lanes indicates the number of the FPLC fraction. For details of the FPLC fractionation and the processing assay see 3.4.11.1. and 3.4.11.

Fractions containing the RNase P-like processing activity were collected in the range of 0.3-0.4 M NH_4Cl of the FPLC elution gradient, a similar range of concentrations as observed in parallel experiments for *E. coli* or *B. subtilis.* This finding, and the fact that the *A. aeolicus* activity required the presence of the divalent metal ions Mg^{2+} or Mn^{2+} (data not shown), suggest that this organism might have a typical bacterial-type RNase P. Also other relatives of *A. aeolicus* (*Aquifex pyrophilus* VF5, *Hydrogenobacter thermophilus* TK6 and *Thermocrinis ruber*) were analyzed using FPLC, with very similar results. All of them showed a specific cleavage pattern like that observed for *A. aeolicus*. To provide proof that these results were not an artifact caused by contamination with other bacteria and/or RNase P enzymes handled in our lab, cleavage assays were repeated at elevated temperature (65°C and 70°C, Fig. 2). In addition we checked if a protein subunit is essential for cleavage in *A. aeolicus* lysates and if so, whether activity can be restored using purified proteins from *E. coli* (C5) and *B. subtilis* (P). Towards that aim an aliquot of an active FPLC fraction from the *A. aeolicus* lysate was phenol/chloroform extracted (see 3.2.7.) and ethanol precipitated (see 3.2.6.).

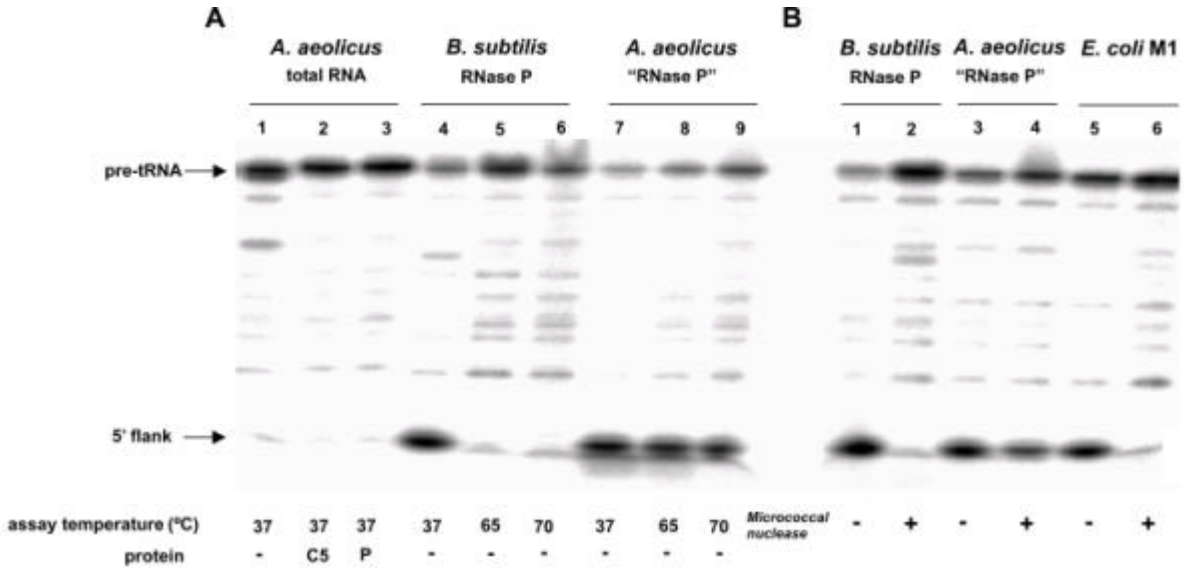

Fig. 2: Pre-tRNA processing assays. **(A)** An active *A. aeolicus* FPLC fraction after extraction and precipitation (lane 1) and after supplementation with the *E. coli* (lane 2) or *B. subtilis* (lane 3) RNase P proteins. Lanes 7-9 show activity of the untreated *A.aeolicus* FPLC fraction without addition of heterologous P proteins at different temperatures. An FPLC fraction with *B. subtilis* RNase P (lanes 4-6) served as reference. **(B)** Pre-tRNA processing by the *B. subtilis* (lanes 1-2) and *A. aeolicus* (lanes 3-4) fraction after or without micrococcal nuclease treatment. As a reference *E. coli* RNase P RNA (M1) was used (lanes 5 -6).

Only the *A. aeolicus* sample remained active at elevated temperatures, while *B. subtilis* ceased to show activity at 65°C (Fig. 2 A, lanes 4-9). This experiment proved that our FPLC

fractions were not contaminated with material from mesophilic bacteria and that the *A. aeolicus* enzyme is indeed thermostabile. Further, the active *A. aeolicus* FPLC fraction deprived of proteins by phenol extraction could not cleave pre-tRNA (Fig. 2 A, lane 1), indicating that the *A. aeolicus* enzyme at least partly consists of protein. Supplementation with *E. coli* and *B. subtilis* RNase P proteins (Fig. 2 A, lanes 2 and 3) did not restore activity. This finding makes *A. aeolicus* unique among all tested *Aquificales* which were all able to process pre-tRNA when reconstituted with *E. coli* or *B. subtilis* P proteins. Also the experiment with micrococcal nuclease revealed a unique features of *A. aeolicus*: in that the active FPLC fraction retained substantial activity after nuclease treatment (3.4.12.), in contrast to the *B. subtilis* fraction or pure M1 RNA from *E. coli* (Fig. 2 B). This might suggest that the RNase P-like activity of *A. aeolicus* consists of protein only.

In line with these experimental data suggesting a protein component in *A. aeolicus* RNase P that differs fundamentally from that of other bacteria, no *rnpA* gene (encoding the bacterial protein subunit) was found in the sequenced genome of *A. aeolicus.* However, total RNA from the closest relative of *A. aeolicus, A. phyrophilus*, showed pre-tRNA processing activity in the presence of *E. coli* or *B. subtilis* proteins (see Fig. 5). Therefore, we addressed the question whether this species also lacks an *rnpA* gene. In most bacteria, the *rnpA* gene is sandwiched between the *rmpH* gene, encoding ribosomal protein L34, and *YidD-YidC* genes (Fig. 3A); only in *A. aeolicus* the *rnpA* gene is missing from the otherwise preserved genomic context (see Fig. 3A).

Since no sequence information on this candidate region in the genome of *A. pyrophilus* was available, we performed genomic PCRs (see 3.3.6) from *A. pyrophilus* with degenerated primers (see 6.6.) designed on the basis of conserved regions within the *rmpH* and *Yid D/C* genes of *A. aeolicus.* The alignment of the sequence obtained from *A. pyrophilus* with the corresponding sequence from *A. aeolicus* is shown in Fig. 3 B. Sequencing analysis thus revealed that like *A. aeolicus, A. pyrophilus* is lacking an *rnpA* gene at the expected position (Fig. 3 A and B).

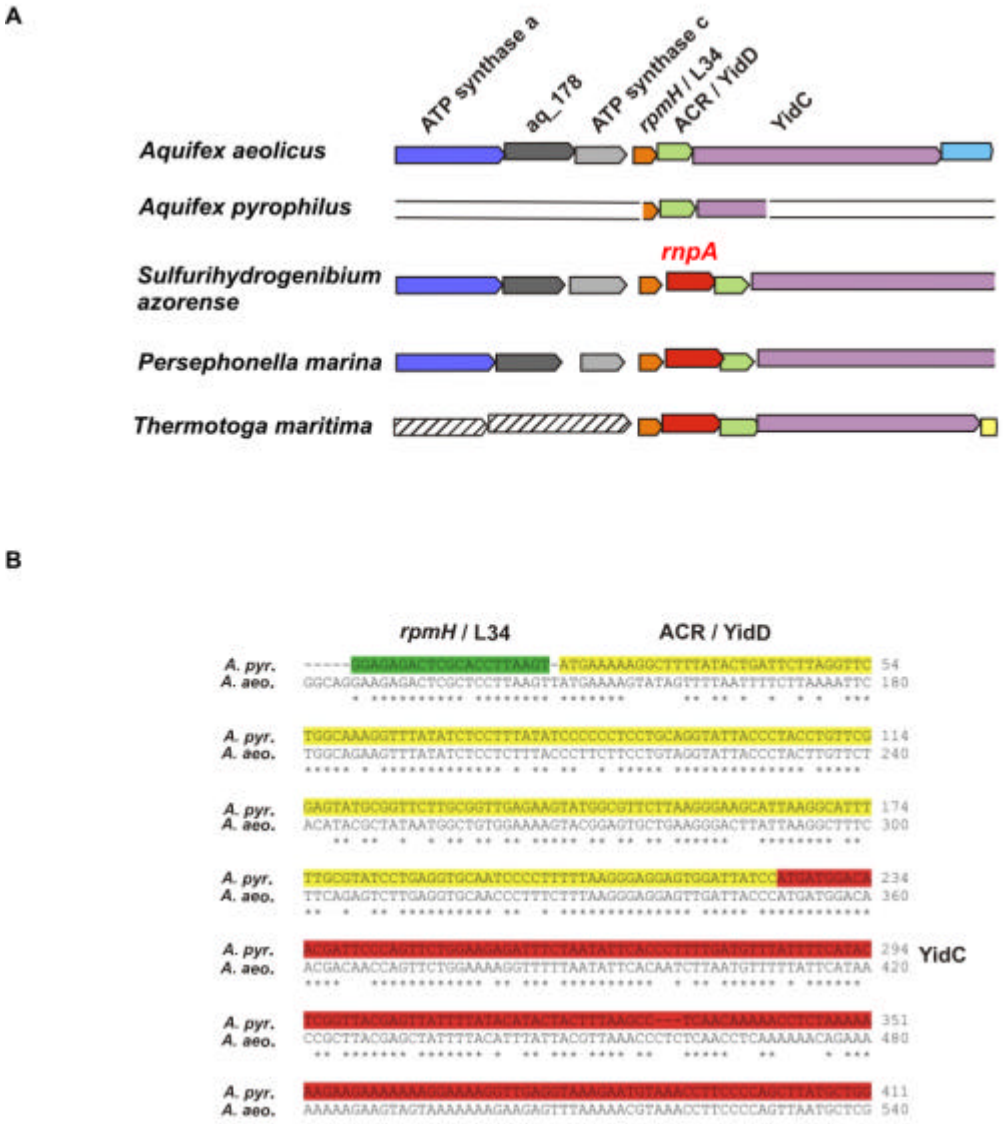

Fig. 3: (A) Schematic illustration of the *rmpH/rnpA* gene context in four *Aquificales* relative to *T. maritima* representing the mainstream of bacteria **(B)**. Clustal W alignment of *A. pyrophilus* and *A. aeolicus* sequences in the region of *rmpH-YidC* genes. Stars indicate nucleotide identity between sequences. No *rnpA* gene is present between *rmpH* and *YidC* in both *Aquificales*.

Based on the processing activity we had observed upon supplementation of phenol-extracted FPLC fractions from the cell lysates of *Aquificales* other than *A. aeolicus* with *E. coli* and *B. subtilis* P proteins we presumed that these organisms possess bacterial-like P RNA subunits. Accordingly, total RNA of these species could be activated to similar extents by the *E. coli* and *B. subtilis* proteins and indeed showed pre-tRNA cleavage at the canonical position specific for RNase P. We then decided to construct a cDNA library of *Hydrogenobacter thermophilus* TK6 that is a close relative of *A. aeolicus*. To identify respective RNase P RNAs, first total RNA was isolated (see 3.4.1.2.) and analysed for RNase P activity in

reconstituted holoenzyme assays (see 3.4.10.1.). Then a preparative PAA gel was run (see 3.4.10.2.), stained with ethidium bromide (see 3.2.2.1.), and the gel was cut into small stripes (Fig. 4 A) from which RNAs of different size ranges were eluted separately in elution buffer 1 (see 3.2.3.1.), followed by ethanol precipitation.. After precipitation each fraction was tested for RNase P activity. Fraction no. 3 (comprising RNA sizes of approximately 400 to 600 nt, see Fig. 4 B) then was the starting pool of RNA for the cDNA library construction (as described in detail in 3.4.10.).

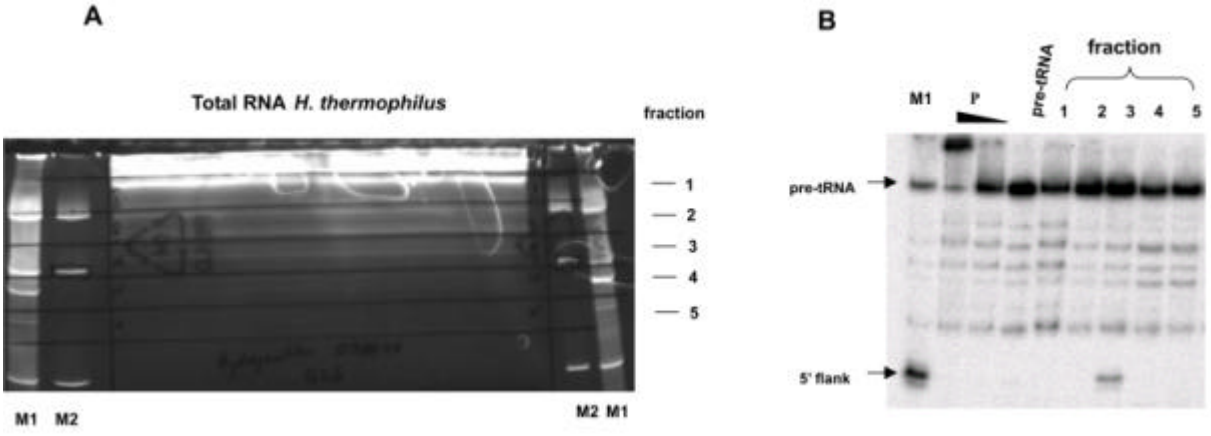

Fig. 4: (A) Preparative 8% PAA gel of total RNA from *H. thermophilus.* Gel fractions (1-5) are marked at the right of the gel. M1, M2: DNA ladders obtained by digestion of pCR2.1-TOPO with *PvuI/EcoRI* or *PvuII* restriction enzymes. Migration of those DNA fragments in the denaturing PAA gel could not be correlated with the precise size of RNA, but permitted to reproducibly fractionate the gel. **(B)** Pre-tRNA processing assay of eluted fractions performed with the *B. subtilis* P protein. 1-5, assay with eluted fractions; M1, positive control assay with *E. coli* RNase RNA (M1); P, assay with different amounts of P protein only with pre-tRNA; pre-tRNA, pre-tRNA alone incubated in processing buffer.

The RNomics approach involving the analysis of around 1500 clones from the *Hydrogenobacter* cDNA library did not yield a single clone with a potential RNase P RNA sequence. One of the reasons for failure might be the usually low expression levels of RNase P RNA that additionally vary depending on the growth phase.

We also fractionated total RNA from other *Aquificales* (*A. aeolicus, A. pyrophilus, T. ruber*) and tested the eluted RNA in pre-tRNA processing assays in the presence of the *B. subtilis* P protein (Fig. 5). Again *A. aeolicus* did not show any activity in contrast to its relatives.

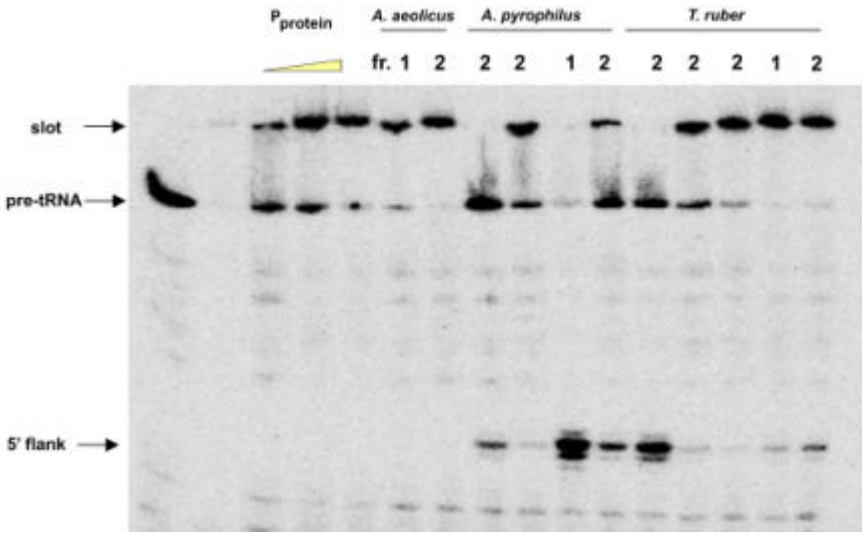

Fig. 5: Pre-tRNA processing assay with eluted *Aquificales* RNA after gel fractionation and in the presence of the *B. subtilis* P protein. Fr. 1 or 2 correspond to the excised fragments of the preparative PAA gel shown in Fig. 4 A. $P_{protein}$, assay with different amounts of P protein only with pre-tRNA; pre-tRNA, pre-tRNA alone incubated in processing buffer.

We next continued our search for RNase P in the *Aquificales* by analysis of the genomes of *Persephonella marina* and *Sulfurihydrogenobium azorense* which at that time had been fully sequenced. Surprisingly, these two organisms turned out to have bacterial-like RNase P enzymes with just minor idiosyncrasies (Marszalkowski *at al*., 2006, see publication in 4.2) and encode an *rnpA* gene within the context conserved among bacteria.

Thus, RNase P in *A. aeolicus* appears to be exceptional even among the *Aquificales*: though we observed activity in lysate fractions similar to the other *Aquificales*, activity was not restored upon reconstitution of RNA with bacterial P proteins. *A pyrophilus* accordingly represents an intermediate, with the *rnpA* gene missing in the preserved context as in *A. aeolicus*, but with successful reconstitution of the RNA to a functional holoenzyme upon addition of bacterial proteins. Further approaches towards identifying the exceptional RNase P from *A. aeolicus* will include bioinformatic studies as well as biochemical purification, both approaches currently being underway.

4.1.1. References

Burggraf S., Olsen G.J., Stetter K.O., Woese C.R., 1992. A phylogenetic analysis of *Aquifex pyrophilus. Syst. Appl. Mikribiol.* **15:** 352-356

Bocchetta M., Gribaldo S., Sanangelantoni A., Cammarano P., 2000. Phylogenetic depth of the bacterial genera Aquifex and Thermotoga inferred from analysis of ribosomal protein, elongation factor, and RNA polymerase subunit sequences. *J.Mol.Evol*. **50:** 366-388.

Huber, R., Wilharm T., Huber D., Trincone A., Burggraf, S., König H., Rachel R., Rockinger I., Fricke H., Stetter K.O., 1992. *Aquifex pyrophilus* gen. nov.sp. nov., represents a novel group of marine hyperthermophilic hydrogen-oxidizing bacteria. *Syst. Appl. Microbiol.* **15:** 340-351

Marszalkowski, M., Teune, J.H., Steger, G., Hartmann, R.K. and Willkomm, D. 2006. Thermostabile RNase P RNAs lacking P18 identified in the Aquificales. *RNA*, **12:**1-7.

Willkomm D.K., Feltens R., Hartmann R.K., 2002. tRNA maturation in *Aquifex aeolicus.* Biochemie **84:** 713-722

Willkomm, D.K., Minnerup, J., Hüttenhofer, A., Hartmann, R.K. 2005. xperimental RNomics in Aquifex aeolicus: identification of small non-coding RNAs and the putative 6S RNA homolog. *Nucleic Acids Res.* **33(6):** 1949-60.

4.2. Thermostabile RNase P RNAs lacking P18 identified in the Aquificales

RNA

Thermostable RNase P RNAs lacking P18 identified in the Aquificales

Michal Marszalkowski, Jan-Hendrik Teune, Gerhard Steger, Roland K. Hartmann and Dagmar K. Willkomm

RNA published online Sep 27, 2006;
Access the most recent version at doi:10.1261/rna.242806

JOBNAME: RNA 12#11 2006 PAGE: 1 OUTPUT: Wednesday September 27 16:21:46 2006
csh/RNA/125782/rna2428

REPORT

Thermostable RNase P RNAs lacking P18 identified in the Aquificales

MICHAL MARSZALKOWSKI,[1] JAN-HENDRIK TEUNE,[2] GERHARD STEGER,[2] ROLAND K. HARTMANN,[1] and DAGMAR K. WILLKOMM[1]

[1]Philipps-Universität Marburg, Institut für Pharmazeutische Chemie, D-35037 Marburg, Germany
[2]Heinrich-Heine-Universität Düsseldorf, Institut für Physikalische Biologie, D-40225 Düsseldorf, Germany

ABSTRACT

The RNase P RNA (rnpB) and protein (rnpA) genes were identified in the two Aquificales Sulfurihydrogenibium azorense and Persephonella marina. In contrast, neither of the two genes has been found in the sequenced genome of their close relative, Aquifex aeolicus. As in most bacteria, the rnpA genes of S. azorense and P. marina are preceded by the rpmH gene coding for ribosomal protein L34. This genetic region, including several genes up- and downstream of rpmH, is uniquely conserved among all three Aquificales strains, except that rnpA is missing in A. aeolicus. The RNase P RNAs (P RNAs) of S. azorense and P. marina are active catalysts that can be activated by heterologous bacterial P proteins at low salt. Although the two P RNAs lack helix P18 and thus one of the three major interdomain tertiary contacts, they are more thermostable than Escherichia coli P RNA and require higher temperatures for proper folding. Related to their thermostability, both RNAs include a subset of structural idiosyncrasies in their S domains, which were recently demonstrated to determine the folding properties of the thermostable S domain of Thermus thermophilus P RNA. Unlike 16S rRNA phylogeny that has placed the Aquificales as the deepest lineage of the bacterial phylogenetic tree, RNase P RNA-based phylogeny groups S. azorense and P. marina with the green sulfur, cyanobacterial, and d/e proteobacterial branches.

Keywords: Aquificales; Sulfurihydrogenibium azorense; Persephonella marina; RNase P; tRNA processing

INTRODUCTION

The Aquificales are a group of thermophilic bacteria, with Aquifex aeolicus being the best-known representative. 16S rRNA, as well as elongation factors Tu and G, phylogenies have suggested that Aquifex represents the deepest branch of the bacterial phylogenetic tree (Burggraf et al. 1992; Huber et al. 1992; Bocchetta et al. 2000). However, other phylogenetic approaches analyzing conserved small insertions and deletions in a variety of proteins (Gupta 2000; Griffiths and Gupta 2004) and those based on RNA polymerase b, b9, and s^{70} subunits (Gruber and Bryant 1998; Klenk et al. 1999) have favored a close affiliation of Aquifex with the d/e division of the proteobacteria and the Chlamydia-Cytophaga group.

Although RNase P is the ubiquitous tRNA 59-end maturation enzyme found in all kingdoms of life, neither a candidate gene for its RNA (rnpB) nor its protein subunit (rnpA) has been identified in the sequenced genome of A. aeolicus (Deckert et al. 1998; Swanson 2001). Likewise, no RNase P-like activity could be detected in cell lysates of the bacterium (Willkomm et al. 2002), and a recent RNomics approach also failed to reveal an RNase P RNA candidate (Willkomm et al. 2005).

To shed light on tRNA 59-end maturation in the Aquificales, we analyzed close relatives of A. aeolicus, namely Sulfurihydrogenibium azorense and Persephonella marina, for which genome sequences had been made accessible by The Institute for Genomic Research (TIGR). Our results demonstrate that the two bacteria harbor a bacterial type A RNase P RNA, although with deviations from the bacterial consensus, the major one is the lack of P18. Despite the absence of the L18–P8 interdomain contact, both RNase P RNAs are more active and stable than Escherichia coli RNase P at higher temperatures (55°C–65°C). The RNase P protein genes (rnpA) of S. azorense and P. marina were identified as well and co-localize with the rpmH gene encoding ribosomal protein L34 as in the majority of bacteria (Hartmann and Hartmann 2003).

Reprint requests to: Dagmar K. Willkomm, Philipps-Universität Marburg, Institut für Pharmazeutische Chemie, Marbacher Weg 6, D-35037 Marburg, Germany; e-mail: willkomm@staff.uni-marburg.de; fax: +6421-28-25854.

Article published online ahead of print. Article and publication date are athttp://www.rnajournal.org/cgi/doi/10.1261/rna.242806.

JOBNAME: RNA 12#11 2006 PAGE: 6 OUTPUT: Wednesday September 27 16:22:37 2006
csh/RNA/125782/rna2428

For calculation of phylogenetic trees, we structurally aligned the RNase P RNA sequences of P. marina and S. azorense and—as outgroups—Homo sapiens and Thermococcus litoralis or Sulfolobus acidocaldarius to the structural alignment of bacterial RNase P RNA sequences from Massire et al. (1998), using ConStruct (Luck et al. 1999) and making manual adjustments. After removal of all partial sequences (e.g., those lacking P1), phylogenetic trees were predicted using fastDNAml (Felsenstein 1981; Olsen et al. 1994).

The rnpA genes encoding the protein subunit of bacterial RNase P were identified by using a local version of tblastn, which is part of the BLAST package (Altschul et al. 1990). The RNase P protein sequence from E. coli (Acc. AAC76727) was used as a query to search for potential rnpA coding regions in the provided genomes. Finally, the resulting sequence(s) were used to query the NCBI BLAST servers for validation.

Secondary structure predictions were performed using Mfold (Zuker 2003). ClustalW (www.ebi.ac.uk/clustalw) was used for nucleic acid sequence alignments, and protein sequences were aligned with MultAlin (Corpet 1988).

Cloning of RNase P RNA candidates

For the construction of plasmids pUC19T7Pma_rnpB and pUC19T7Saz_rnpB, to be used as templates for in vitro transcription of the two P RNAs, respective DNA sequences were amplified by genomic PCR using primers 59-GCGGGATCCTAATACGACTCACTATAGGATATCTCTGCCGGTGGTTTCC-39 and 59-CGCCTTAAGACCGGTGGCCTCCAGTAA-39 for P. marina, and 59-GCGGGATCCTAATACGACTCACTATAGGTATAAGGCTACGGCTTTGAG-39 and 59-CGCCTTAAGTTTAAGGCTACGGCTTTGGAG-39 for S. azorense. PCR fragments were cloned into pUC19 via EcoRI and BamHI sites included in the primers (underlined); the sense primers additionally introduced a T7 promoter (in italics).

In vitro transcription and 59-end labeling

RNAs were produced by run-off transcription with T7 RNA polymerase and subsequent gel purification as described in Busch et al. (2000). The substrate, T. thermophilus ptRNA^{Gly}, was transcribed from plasmid pSBpt39HH (Busch et al. 2000), and E. coli P RNA from plasmid pDW98 (Smith et al. 1992) linearized with BsaAI. S. azorense and P. marina P RNAs were transcribed from plasmids pUC19T7Saz_rnpB and pUC19T7Pma_rnpB, both linearized with EcoRI, resulting in 20 and 17 extra nucleotides, respectively, beyond the 39-ends shown in Figure 1. Substrate 59-end labeling with [g-^{32}P]-ATP and T4 polynucleotide kinase was performed as detailed in Heide et al. (1999).

Sequencing of PCR products and recombinant plasmids

DNA sequencing was performed by MWG-BIOTECH AG (Ebersberg, Germany).

Preparation of recombinant RNase P proteins

E. coli and B. subtilis RNase P proteins carrying an N-terminal His-tag (His-tagged peptide leader: MRGSHHHHHHGS, encoded in plasmid pQE-30 in E. coli JM109) were expressed essentially as described (Rivera-León et al. 1995). Cell cultures were grown in LB broth containing 100 mg/mL ampicillin to an OD_{600} of 0.6, and IPTG was added to a final concentration of 1 mM. Cells were harvested at 4°C after another 3 h of growth (OD_{600} ≥ 2.5). The following steps were performed at 4°C or on ice, and all buffers contained 40 mg/mL of the protease inhibitor phenylmethylsulfonyl fluoride (PMSF). Cells were suspended in 10–15 mL sonication buffer SB (50 mM Tris-HCl, pH 8.0, 0.3 M NaCl, 0.1% triton X-100, 1 M NH_4Cl). After sonication (Branson Sonifier 250, output 20, duty cycle 50%, 15 min on ice), the sample was centrifuged for 30 min (4°C, 14,500*g*), and the supernatant was mixed with Ni-NTA agarose (400 mL for 2 L of cell culture), which had been prewashed twice with 10 mL SB buffer. The sample was then incubated for 1–2 h at 4°C under gentle mixing or rotating. The Ni-NTA agarose slurry was washed three times (centrifugation–resuspension cycles; centrifugation at 4°C and 8500 rpm in a desktop centrifuge) with ice-cold washing buffer (30 mM imidazol, 50 mM Tris-HCl, pH 8.0, 8 M urea, 0.1% triton X-100). Proteins were then eluted with 500 mL elution buffer (50 mM Tris-HCl, pH 7.0, 10% glycerol, 7 M urea, 20 mM EDTA, 0.3 M imidazol) for 45 min at 4°C under gentle shaking. Eluates were dialyzed twice for 1 h and subsequently overnight against volumes of 500 mL dialysis buffer (50 mM Tris-HCl, pH 7.0, 0.1 M NaCl, 10% glycerol, dialysis bags: Roth, molecular weight cut-off 12–14 kDa); during dialysis, a white precipitate formed. The contents of the dialysis tubes were transferred to a 2 mL Eppendorf tube and centrifuged for 20 min at 4°C and 12,000 rpm in a desktop centrifuge. The supernatant contained RNase P protein devoid of any P RNA contamination, whereas the pellet included traces of P RNA and was therefore discarded. All purification steps were monitored by 17% SDS-PAGE to assess the purity and concentration of RNase P proteins.

Kinetics

For single-turnover RNA-alone reactions, trace amounts (<1 nM) of 59-end labeled T. thermophilus ptRNA^{Gly} substrate were preincubated in reaction buffer (100 mM $Mg[OAc]_2$, 100 mM NH_4OAc, 0.1 mM EDTA, 50 mM MES pH 6.0 [37°]) for 5 min at 55°C and 25 min at 37°C. Likewise, P RNAs were preincubated in the same buffer for 5 min at 55°C and 55 min at 37°C. Processing reactions were started by combining enzyme and substrate solutions and assayed at 37°C. For processing assays at 55°C and 65°C, P RNA solutions were preincubated for 1 h at 55°C or 65°C.

For holoenzyme cleavage assays, buffer KN (20 mM Hepes-KOH, pH 7.4, 2 mM $Mg[OAc]_2$, 150 mM NH_4OAc, 2 mM spermidine, 0.05 mM spermine, and 4 mM b-mercaptoethanol) (Dinos et al. 2004) was used to closely mimic physiological conditions. In addition, these assays were performed in the identical buffer, but at pH 6.5 and 10 mM $Mg[OAc]_2$. In vitro reconstitution of RNase P holoenzymes was performed as follows: RNase P RNAs were incubated in buffer KN for 5 min at 55°C and 50 min at 37°C, after which RNase P protein was added, followed by another 5 min at 37°C before addition of substrate. Aliquots of the cleavage reactions were withdrawn at various time points and analyzed by electrophoresis on 20% polyacrylamide/8 M urea gels. Data analysis and calculations were performed essentially as previously described (Busch et al. 2000).

JOBNAME: RNA 12#11 2006 PAGE: 2 OUTPUT: Wednesday September 27 16:21:46 2006
csh/RNA/125782/ma2428

RESULTS AND DISCUSSION

Identification of rnpB genes in S. azorense and P. marina

RNase P RNA (P RNA) genes (rnpB) were identified in the completed but yet unpublished genome sequences of S. azorense and P. marina (available at TIGR, www.tigr.org) using the program PatScan as described under Materials and Methods.

P RNA structures and kinetics

The secondary structures of the P RNAs from P. marina and S. azorense are shown in Figure 1. The two P RNAs are highly similar (average pairwise sequence identity z 65% in a structure-based alignment). Besides a few 1- or 2-nucleotide (nt) insertions/deletions, P. marina differs from S. azorense by two major expansions, one in P12 and the other in P16/17 to create the P16.1 element in the P. marina structure. The hallmark of the two Aquificales P RNAs is the absence of helix P18, a structural feature originally identified in the genus Chlorobium (Haas et al. 1994). Deletion of P18 eliminates one of the three tetraloop-helix interactions (L8/P4, L9/P1 L18/P8) that bridge S- and C-domains (Fig. 1). In both RNAs, helices P1 (16 or 18 bp) and P9 (6 bp) are extended, helix P14 has 10 instead of the usual 9 bp, and S. azorense P RNA also lacks the bulged nucleotide close to the base of P14. The apical P12 structures are idiosyncratic, and P. marina P RNA has a small stem–loop (P16.1) inserted between helices P16 and P17.

We analyzed the kinetics of the two P RNAs next to E. coli P RNA under single turnover conditions (E>>S) at 0.1 M Mg^{2+}, 0.1 M NH_4^+, and pH 6.0. P RNAs were preincubated in assay buffer for 5 min at 55°C and 55 min at 37°C to resolve potential folding traps as observed for the thermostable P RNA of Thermus thermophilus (R.K. Hartmann, unpubl.). Indeed, this preincubation protocol eliminated compacted conformers of S. azorense and P. marina P RNAs, which appeared as fast-migrating bands on native PAA gels (data not shown). In contrast,

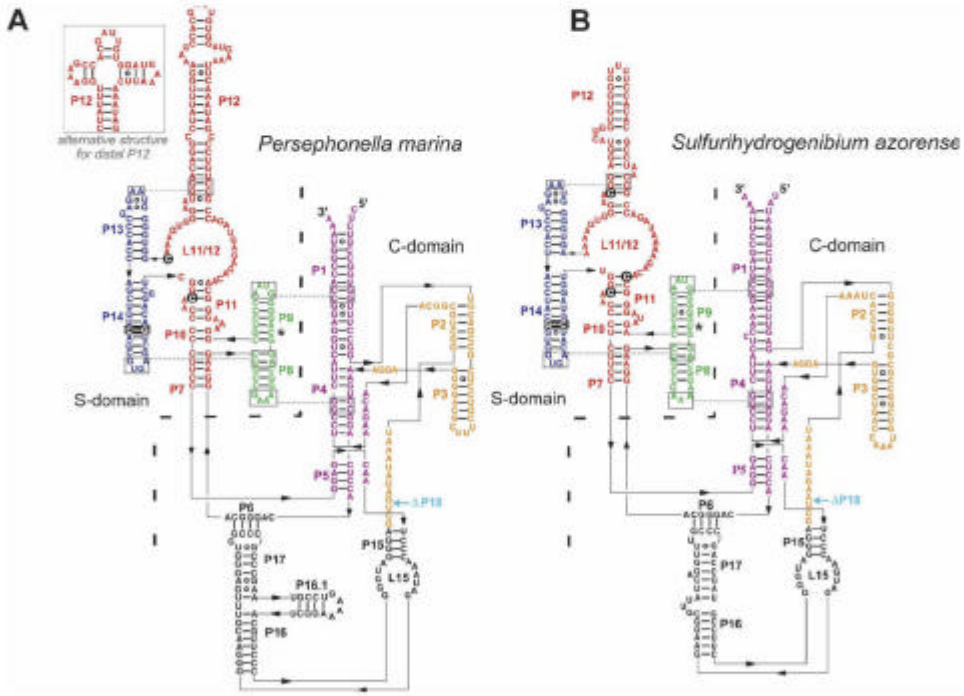

FIGURE 1. Secondary structure presentation of P RNAs from (A) P. marina (accession no. DQ529278) and (B) S. azorense (accession no. DQ529245), according to Tsai et al. (2003) and taking into account the data of Torres-Larios et al. (2005). The C-domain (catalytic domain) and the S-domain (specificity domain) are separated by the broken line. (P) Paired regions; (L) loop regions; (open boxes) tertiary contacts, connected by stippled lines. Highlighted nucleotides and asterisk next to helix P9 mark nucleotide identities and structural features also found in the thermostable S domain of T. thermophilus P RNA (Baird et al. 2006). For the distal part of P12 in the P. marina structure, an alternative cruciform structure is depicted. However, the long P12 stem–loop shown in the main structure contains an internal loop with a stabilizing sarcin-ricin motif in its bulge (59-AGUA- and 59-GAA-; Leontis and Westhof 1998; Zhong et al. 2006) and is energetically favored according to thermodynamic calculations (Hofacker 2003).

Fig. 1 live 4/C

JOBNAME: RNA 12#11 2006 PAGE: 3 OUTPUT: Wednesday September 27 16:22:12 2006
csh/RNA/125782/rna2428

preincubation only for 1 h at 37°C incompletely (S. azorense) or completely (P. marina) failed to resolve these conformers. The kinetic results are summarized in Table 1. At 37°C and in comparison with E. coli P RNA, the S. azorense ribozyme cleaved the precursor $tRNA^{Gly}$ ($ptRNA^{Gly}$) substrate with about the same single turnover $K_{m(sto)}$, but at a three- to fourfold reduced maximum cleavage rate (k_{react}). Catalytic performance of P. marina P RNA was lower, with approximately a sevenfold increase in $K_{m(sto)}$ and a 31-fold decrease in k_{react}. Since the two Aquificales are thermophilic bacteria (growth optima z 70°C; Götz et al. 2002; Aguilar et al. 2004), we tested processing activity at two additional temperatures (55°C and 65°C), using P RNA concentrations (0.27 mM for E. coli, 0.27 mM for S. azorense, and 2.0 mM for P. marina) around the respective $K_{m(sto)}$ value determined at 37°C (see Table 1). For this purpose, P RNAs were preincubated in assay buffer for 1 h at 55°C or 65°C before addition of substrate and incubation at the same temperature. Whereas the rate of cleavage (k_{obs}) by E. coli P RNA decreased from 4.7 min^{-1} at 37°C to 2.8 min^{-1} at 55°C to 1.3 min^{-1} at 65°C, the two Aquificales P RNAs showed a higher substrate turnover at 55°C versus 37°C (Table 1). In the case of S. azorense P RNA, the cleavage rate at 65°C was still equal to that at 37°C, although substrate affinity is expected to be lower at 65°C than 37°C. Inspection of experimental endpoints (EP, maximum fraction of substrate that could be converted to mature tRNA during extended incubation times) obtained in the individual processing reactions revealed that # 40% of substrate could be cleaved by E. coli P RNA at 65°C. In contrast, endpoints remained normal (>80%) for reactions catalyzed by the two Aquificales P RNAs (Table 1). These findings suggest that E. coli P RNA, but not P. marina and S. azorense P RNAs, traps a substantial fraction of the substrate in an inactive conformation at 65°C, which we interpret as an indication of partial un- or misfolding of E. coli P RNA at this temperature.

Holoenzyme activity assays

The two Aquificales P RNAs, and E. coli P RNA as a control, were reconstituted with the E. coli or Bacillus subtilis P protein and tested for processing activity in the presence of 2 mM Mg^{2+} under multiple turnover conditions at 37°C (Table 1). In general, bacterial P RNAs do not show RNA-alone activity under these conditions. Both Aquificales P RNAs could be activated by the two heterologous P proteins, S. azorense P RNA more efficiently than P. marina P RNA, and both much less efficiently than E. coli P RNA. Since the conformation of the P. marina P RNA was not uniform at 2 mM Mg^{2+}, as inferred from native PAGE (data not shown), we measured the activity of the reconstituted holoenzymes at 10 mM Mg^{2+}, with the pH lowered to 6.5 to suppress RNA-alone cleavage. Under these conditions, all P RNAs were homogeneously folded according to native PAGE analyses (data not shown), and RNA-alone

TABLE 1. Kinetic data for reactions catalyzed by P RNA alone and hybrid holoenzymes

	37°C			5	5°C		6 5°C	
P RNA	$K_{m(sto)}$ (mM)	k_{react} (min^{-1})	k_{obs} (min^{-1})	EP	k_{obs} (min^{-1})	EP	k_{obs} (min^{-1})	EP
E. coli	0.24 (6 0.03)	9.7 (6 0.6)	4.7 (6 0.3)	0.92	2.8 (6 0.25)	0.8	1.3 (6 0.4)	0.4
S. azorense	0.28 (6 0.05)	2.7 (6 0.2)	1.4 (6 0.1)	0.9	3.1 (6 0.4)	0.93	1.25 (6 0.2)	0.85
P. marina	1.97 (6 0.39)	0.32 (6 0.02)	0.15 (6 0.01)	0.76	0.6 (6 0.01)	0.92	0.06 (6 0.01)	0.9

Holoenzymes		k_{obs} (min^{-1})	
P RNA	+ Protein	2 mM Mg^{2+}	10 mM Mg^{2+}
E. coli	E. coli	3.5 (6 0.3)	4.8 (6 0.58)
	B. subtilis	4.2 (6 0.2)	4.8 (6 1.1)
S. azorense	E. coli	0.05 (6 0.003)	0.43 (6 0.05)
	B. subtilis	0.24 (6 0.06)	0.47 (6 0.04)
P. marina	E. coli	0.028 (6 0.003)	0.56 (6 0.16)
	B. subtilis	0.014 (6 0.001)	0.70 (6 0.12)

RNA-alone reactions were performed under single-turnover conditions (E≫S) using trace amounts (<1 nM) of 5′-end labeled T. thermophilus $ptRNA^{Gly}$ as substrate in a reaction buffer containing 100 mM $Mg(OAc)_2$, 100 mM NH_4OAc, 0.1 mM EDTA, 50 mM MES pH 6.0 at the indicated temperatures; processing reactions were started by combining enzyme and substrate solutions. $K_{m(sto)}$ and k_{react} are the single turnover K_m and v_{max} values, k_{obs} values designate the cleavage rate at a single P RNA concentration (0.27 mM for E. coli, 0.27 mM for S. azorense, and 2.0 mM for P. marina RNase P RNA), and EP is the experimental endpoint (maximum fraction of substrate that could be converted to mature tRNA during extended incubation times). Assay conditions for holoenzyme reactions, performed under multiple turnover conditions: 150 mM NH_4OAc, 2 mM spermidine, 0.05 mM spermine, 4 mM b-mercaptoethanol, 10 nM P RNA, 40 nM P protein, and 100 nM $ptRNA^{Gly}$, 2 or 10 mM $Mg(OAc)_2$, 20 mM Hepes pH 7.4 (37°C) with 2 mM Mg^{2+}, and pH 6.5 with 10 mM Mg^{2+}; under holoenzyme conditions, no RNA-alone activity was observed in the time window of the assay, except for E. coli RNA alone at 10 mM Mg^{2+} (k_{obs} = 0.14 min^{-1}). In the holoenzyme reactions, k_{obs} is given as nanomoles of substrate converted per nanomole of RNase P RNA per minute. All values are based on at least three independent experiments. For more details, see Materials and Methods.

JOBNAME: RNA 12#11 2006 PAGE: 4 OUTPUT: Wednesday September 27 16:22:13 2006
cshvRNA/125782/rna2428

activity was low for the E. coli and not detectable for the P. marina and S. azorense P RNAs. At 10 mM Mg^{2+}, the activity of holoenzymes containing the Aquificales P RNAs increased relative to those with E. coli P RNA, and activity profiles for the two Aquificales P RNAs were now reversed, the chimeric P. marina holoenzymes being more active than the S. azorense counterparts. Our results illustrate that the Mg^{2+} requirements for folding and catalysis of the three P RNAs differ markedly, being highest for P. marina and higher for the Aquificales than for E. coli P RNA. We additionally tested if the P. marina and S. azorense rnpB genes might be able to replace the native rnpB gene in the B. subtilis mutant strain SSB318 (Wegscheid et al. 2006), but the results were negative (data not shown). Altogether, these results support the notion that the two Aquificales strains encode a canonical bacterial type A RNase P holoenzyme, however, with idiosyncratic features.

Identification of rnpA genes

The rnpA genes encoding the protein subunit of RNase P in P. marina and S. azorense were identified (Fig. 2A) by using a local version of tblastn (see Materials and Methods). Both rnpA genes are sandwiched between the rpmH gene encoding ribosomal protein L34 and the downstream yidD-YidC genes (Fig. 2B), which represent the genetic context found in most bacteria (Hartmann and Hartmann 2003). In the case of S. azorense rnpA, the only candidate start codon is a CUG immediately upstream of the rpmH stop codon (data not shown); CUG has been described as a low-efficiency start codon (O'Donnell and Janssen 2001). We also considered the possibility of a sequencing error in an A_9 stretch at the beginning of S. azorense rnpA (nucleotides 19–27 of rnpA, accession no. DQ529246). We thus sequenced a PCR fragment derived from S. azorense genomic DNA. However, the sequence as provided by TIGR turned out to be correct. An alignment with other bacterial P proteins (Fig. 2A) supported our annotation of rnpA genes.

Thermostability of Aquificales P RNAs

Thermostability of P. marina and S. azorense P RNAs despite the absence of P18 is a surprising finding of this study. The apical loop of P18 docks to P8 as one of the three major tertiary interactions (L8/P4, L18/P8, L9/P1) that bridge S- and C-domains (Fig. 1) in bacterial type A RNAs. The only other known bacterial P RNAs lacking P18 are from mesophilic Chlorobia (Haas et al. 1994), where RNA stability is expected to be less crucial than in thermophiles. Deletion of P18 from E. coli P RNA caused a 60-fold increase in K_m under multiple turnover conditions at 25 mM Mg^{2+} and 1 M NH_4^+ (Haas et al. 1994). The absence of the L18/P8 contact in the two Aquificales P RNAs may be compensated by strengthening the L9/P1 contact. Evidence for this possibility stems from the observation that helices P1 can be extended to 16 and 18 bp, respectively (Fig. 1), and P9 to 6 bp in both RNAs. Mesophilic P RNAs usually have 11 bp in P1 and 4–5 bp in P9, including a bulged nucleotide near the base of the stem in P1 as well as P9, which interrupts helix continuity (Massire et al. 1998; Fig. 3). Helix P9 is also stabilized in other thermostable P RNAs (5 bp and deletion of the bulge in Thermotoga maritima, and 5 G-C bp in T. thermophilus), as is P1 (12–14 bp in T. thermophilus and T. aquaticus, absence of the nucleotide bulge in P1 of T. maritima) (Massire et al. 1998; Fig. 3). Furthermore, the two Aquificales and

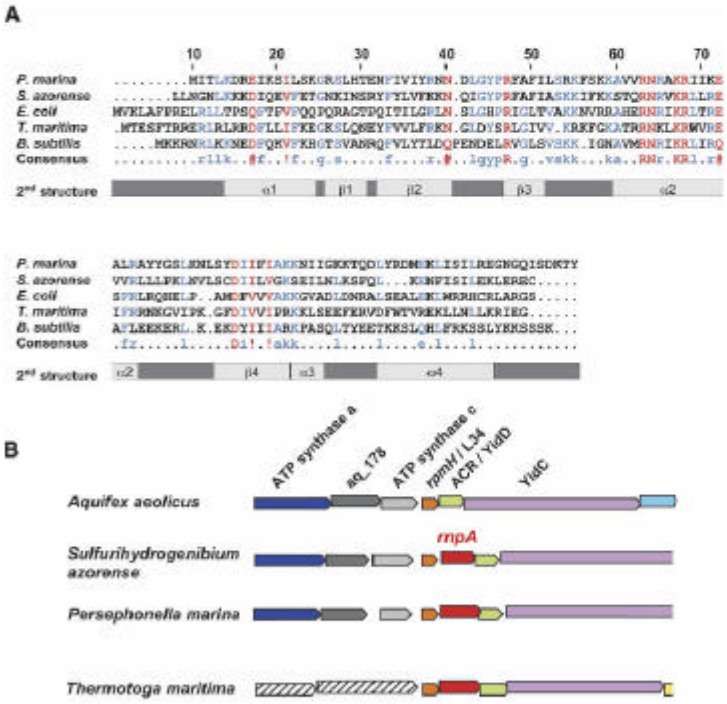

FIGURE 2. (A) Alignment of S. azorense and P. marina P protein sequences (accession nos. DQ529246 and DQ529279) with those of selected bacteria. (Red) Amino acid or type of amino acid conserved in all five sequences; (blue) conserved in at least three of the five sequences; (!)I or V; (#)D, E, N, or Q. Secondary structure elements are shown for the T. maritima P protein (Kazantsev et al. 2003). (B) Schematic illustration of the rpmH/rnpA gene context in the three Aquificales strains relative to T. maritima representing the mainstream of bacteria; accession nos. for the genomic regions of S. azorense and P. marina: DQ529246 and DQ529279.

JOBNAME: RNA 12#11 2006 PAGE: 5 OUTPUT: Wednesday September 27 16:22:32 2006
cshvRNA/125782/rna2428

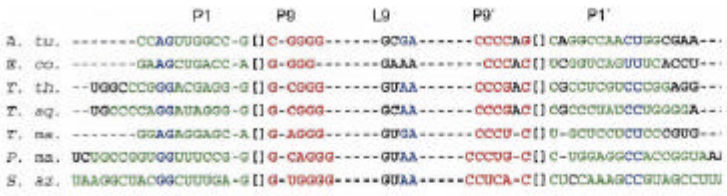

FIGURE 3. Partial alignment of P1, P9, and L9 sequences (P1 and P9 designate the 59halves and P19and P99the 39halves of the respective helix), according to Massire et al. (1998). (Blue) Nucleotides that take part in the tetraloop-helix interaction; (green) canonical pairings, including G-U pairs, within P1; (red) canonical pairings, including G-U pairs, within P9; (black) unpaired nucleotides, and all L9 nucleotides in E. coli RNase P RNA, as the geometry of this tertiary contact is unclear (Massire et al. 1998). RNase P RNAs from the two Thermus and the two Aquificales species are the only known examples of apical L9 59-GYAA tetraloops interacting with two consecutive G-C bp in P1. (A. tu.) Agrobacterium tumefaciens, (E. co.) E. coli, (T. th.) T. thermophilus, (T. aq.) T. aquaticus, (T. ma.) T. maritima, (P. ma.) P. marina, (S. az.) S. azorense.

Thermus P RNAs share the feature of a 59-GYAA L9 tetraloop and a P1 receptor site consisting of a G-C bp tandem, a combination not present in other bacteria (Massire et al. 1998; Fig. 3). Increased stiffness of P9 and its P1 receptor region in P. marina, S. azorense, and Thermus may stabilize the L9/P1 interaction, which in turn may partially compensate for the absence of the L18/P8 contact in the two Aquificales RNAs.

Tao Pan and coworkers have introduced 12 key base identities of the T. thermophilus S domain into that of E. coli (Baird et al. 2006). The E. coli S-domain mutant gained the same stability and Mg^{2+}-dependent folding cooperativity as the T. thermophilus S domain. Subsets of these T. thermophilus features are present in the two Aquificales P RNAs (Fig. 1, highlighted nucleotides, asterisk next to P9). This includes, for example, the stabilization of P9, P11, and P14 (for details, see Baird et al. 2006). These structural similarities to T. thermophilus P RNA may contribute as well to thermostability of the two Aquificales P RNAs.

Phylogenetic aspects

So far, no candidate genes for the RNA (rnpB) or the protein subunit (rnpA) have been identified in the sequenced genome of A. aeolicus (Deckert et al. 1998; Swanson 2001). However, in S. azorense and P. marina, rnpA is encoded with rpmH, as in the majority of bacteria. Surprisingly, the genetic context of rpmH genes in A. aeolicus, S. azorense, and P. marina is very similar except for the absence of rnpA in A. aeolicus. This not only holds for yidD and yidC downstream of rpmH/rnpA, a conserved trait in most bacteria, but also for the rpmH upstream region (Fig. 2B). Here, all three Aquificales encode a conserved hypothetical protein (aq_178 in A. aeolicus) and an ATP synthase subunit, a constellation not observed outside the Aquificales (Hartmann and Hartmann 2003). Thus, the apparent loss of genes for bacterial-like RNase P components is confined to the genus Aquifex or the Aquificaceae. We further inspected the genetic context of rnpB genes in S. azorense and P. marina, hoping that a conserved context may guide us to a so far unidentified rnpB gene in A. aeolicus. However, the context of rnpB already deviates entirely between S. azorense and P. marina (data not shown).

A number of phylogenies, in particular the one based on 16S rRNA, have positioned Aquifex and the Aquificales as the deepest branch of the bacterial phylogenetic tree (Burggraf et al. 1992; Huber et al. 1992; Bocchetta et al. 2000). Phylogenetic trees on the basis of RNase P RNA, which we constructed from a structure-based sequence alignment (Massire et al. 1998) using the program fastDNAml, unexpectedly did not corroborate an early origin of the Aquificales P RNAs (data not shown). With substantial variation in detail caused by small changes in the alignment, the P RNA trees all grouped the Aquificales with the green sulfur, cyanobacterial, and d or e proteobacterial branches, in general agreement with several protein-based phylogenies (Gruber and Bryant 1998; Klenk et al. 1999; Gupta 2000; Griffiths and Gupta 2004). The lack of P18 in the P. marina and S. azorense P RNAs, a feature they share with Archaea and Eukaryotes, thus seems to represent not an ancient, but a derived, trait.

MATERIALS AND METHODS

Bioinformatic analyses

Genes encoding RNase P RNA (rnpB) were identified in the completed but yet unpublished genome sequences of S. azorense and P. marina (available at TIGR, www.tigr.org) using PatScan (Dsouza et al. 1997). The pattern to describe the RNase P RNA-encoding genes consisted of several conserved sequence and structure-based pattern units. There are two main conserved sequence elements in the core structure: 59-GAGGAAN-NUCNNNNC (designated as CR I) (Chen and Pace 1997) and 59-AGNNNNAU...{2–67 nt}...ACANAA (designated as CR IV) (Chen and Pace 1997). These conserved sequence elements were surrounded by additional conserved structural elements to reduce the amount of false-positive hits. The pattern description was ("/" stands for line break):

%RNaseP Pattern description File

r1=f au; ua; gc; cg; gu; ugg=p2=6...7=ØGj3...4Þ=p3=1...6=3...72=r1z p3½;0;0 =GAGGA=p4=ANN=U=p6=CNNNN=C=p5=3...4=1...27=p7=3...7=50...300=r1z p7½;0;0 =r1z p5½;0;0 =NAA=p15=2...4=4...95=r1z p15=G=2...67=AGNNNNAU=r1z p2½;0;0 =2...60=ACANAA=r1z p6½;0;0 =r1z p4½;0;0 =A

JOBNAME: RNA 12#11 2006 PAGE: 6 OUTPUT: Wednesday September 27 16:22:37 2006
csh/RNA/125782/rna2428

For calculation of phylogenetic trees, we structurally aligned the RNase P RNA sequences of P. marina and S. azorense and—as outgroups—Homo sapiens and Thermococcus litoralis or Sulfolobus acidocaldarius to the structural alignment of bacterial RNase P RNA sequences from Massire et al. (1998), using ConStruct (Luck et al. 1999) and making manual adjustments. After removal of all partial sequences (e.g., those lacking P1), phylogenetic trees were predicted using fastDNAml (Felsenstein 1981; Olsen et al. 1994).

The rnpA genes encoding the protein subunit of bacterial RNase P were identified by using a local version of tblastn, which is part of the BLAST package (Altschul et al. 1990). The RNase P protein sequence from E. coli (Acc. AAC76727) was used as a query to search for potential rnpA coding regions in the provided genomes. Finally, the resulting sequence(s) were used to query the NCBI BLAST servers for validation.

Secondary structure predictions were performed using Mfold (Zuker 2003). ClustalW (www.ebi.ac.uk/clustalw) was used for nucleic acid sequence alignments, and protein sequences were aligned with MultAlin (Corpet 1988).

Cloning of RNase P RNA candidates

For the construction of plasmids pUC19T7Pma_rnpB and pUC19T7Saz_rnpB, to be used as templates for in vitro transcription of the two P RNAs, respective DNA sequences were amplified by genomic PCR using primers 59-GCGGGATCCTAATACGACTCACTATAGGATATCTCTGCCGGTGGTTTCC-39 and 59-CGCCTTAAGACCGGTGGCCTCCAGTAA-39 for P. marina, and 59-GCGGGATCCTAATACGACTCACTATAGGTATAAGGCTACGGCTTTGAG-39 and 59-CGCCTTAAGTTTAAGGCTACGGCTTTGGAG-39 for S. azorense. PCR fragments were cloned into pUC19 via EcoRI and BamHI sites included in the primers (underlined); the sense primers additionally introduced a T7 promoter (in italics).

In vitro transcription and 59-end labeling

RNAs were produced by run-off transcription with T7 RNA polymerase and subsequent gel purification as described in Busch et al. (2000). The substrate, T. thermophilus ptRNA^{Gly}, was transcribed from plasmid pSBpt39HH (Busch et al. 2000), and E. coli P RNA from plasmid pDW98 (Smith et al. 1992) linearized with BsaAI. S. azorense and P. marina P RNAs were transcribed from plasmids pUC19T7Saz_rnpB and pUC19T7Pma_rnpB, both linearized with EcoRI, resulting in 20 and 17 extra nucleotides, respectively, beyond the 39-ends shown in Figure 1. Substrate 59-end labeling with [g-^{32}P]-ATP and T4 polynucleotide kinase was performed as detailed in Heide et al. (1999).

Sequencing of PCR products and recombinant plasmids

DNA sequencing was performed by MWG-BIOTECH AG (Ebersberg, Germany).

Preparation of recombinant RNase P proteins

E. coli and B. subtilis RNase P proteins carrying an N-terminal His-tag (His-tagged peptide leader: MRGSHHHHHHGS, encoded in plasmid pQE-30 in E. coli JM109) were expressed essentially as described (Rivera-León et al. 1995). Cell cultures were grown in LB broth containing 100 mg/mL ampicillin to an OD_{600} of 0.6, and IPTG was added to a final concentration of 1 mM. Cells were harvested at 4°C after another 3 h of growth (OD_{600} ≥ 2.5). The following steps were performed at 4°C or on ice, and all buffers contained 40 mg/mL of the protease inhibitor phenylmethylsulfonyl fluoride (PMSF). Cells were suspended in 10–15 mL sonication buffer SB (50 mM Tris-HCl, pH 8.0, 0.3 M NaCl, 0.1% triton X-100, 1 M NH_4Cl). After sonication (Branson Sonifier 250, output 20, duty cycle 50%, 15 min on ice), the sample was centrifuged for 30 min (4°C, 14,500*g*), and the supernatant was mixed with Ni-NTA agarose (400 mL for 2 L of cell culture), which had been prewashed twice with 10 mL SB buffer. The sample was then incubated for 1–2 h at 4°C under gentle mixing or rotating. The Ni-NTA agarose slurry was washed three times (centrifugation–resuspension cycles; centrifugation at 4°C and 8500 rpm in a desktop centrifuge) with ice-cold washing buffer (30 mM imidazol, 50 mM Tris-HCl, pH 8.0, 8 M urea, 0.1% triton X-100). Proteins were then eluted with 500 mL elution buffer (50 mM Tris-HCl, pH 7.0, 10% glycerol, 7 M urea, 20 mM EDTA, 0.3 M imidazol) for 45 min at 4°C under gentle shaking. Eluates were dialyzed twice for 1 h and subsequently overnight against volumes of 500 mL dialysis buffer (50 mM Tris-HCl, pH 7.0, 0.1 M NaCl, 10% glycerol, dialysis bags: Roth, molecular weight cut-off 12–14 kDa); during dialysis, a white precipitate formed. The contents of the dialysis tubes were transferred to a 2 mL Eppendorf tube and centrifuged for 20 min at 4°C and 12,000 rpm in a desktop centrifuge. The supernatant contained RNase P protein devoid of any P RNA contamination, whereas the pellet included traces of P RNA and was therefore discarded. All purification steps were monitored by 17% SDS-PAGE to assess the purity and concentration of RNase P proteins.

Kinetics

For single-turnover RNA-alone reactions, trace amounts (<1 nM) of 59-end labeled T. thermophilus ptRNA^{Gly} substrate were preincubated in reaction buffer (100 mM $Mg[OAc]_2$, 100 mM NH_4OAc, 0.1 mM EDTA, 50 mM MES pH 6.0 [37°]) for 5 min at 55°C and 25 min at 37°C. Likewise, P RNAs were preincubated in the same buffer for 5 min at 55°C and 55 min at 37°C. Processing reactions were started by combining enzyme and substrate solutions and assayed at 37°C. For processing assays at 55°C and 65°C, P RNA solutions were preincubated for 1 h at 55°C or 65°C.

For holoenzyme cleavage assays, buffer KN (20 mM Hepes-KOH, pH 7.4, 2 mM $Mg[OAc]_2$, 150 mM NH_4OAc, 2 mM spermidine, 0.05 mM spermine, and 4 mM b-mercaptoethanol) (Dinos et al. 2004) was used to closely mimic physiological conditions. In addition, these assays were performed in the identical buffer, but at pH 6.5 and 10 mM $Mg[OAc]_2$. In vitro reconstitution of RNase P holoenzymes was performed as follows: RNase P RNAs were incubated in buffer KN for 5 min at 55°C and 50 min at 37°C, after which RNase P protein was added, followed by another 5 min at 37°C before addition of substrate. Aliquots of the cleavage reactions were withdrawn at various time points and analyzed by electrophoresis on 20% polyacrylamide/8 M urea gels. Data analysis and calculations were performed essentially as previously described (Busch et al. 2000).

JOBNAME: RNA 12#11 2006 PAGE: 7 OUTPUT: Wednesday September 27 16:22:39 2006
csh/RNA/125782/rna2428

ACKNOWLEDGMENTS

We thank the Deutsche Forschungsgemeinschaft for financial support (DFG HA1672/13-1) and the Wilhelm-Hahn-und-Erben-Stiftung for defraying publication charges. We also thank Anna-Louise Reysenbach (Portland, Oregon, USA) for the gift of S. azorense and P. marina genomic DNA, TIGR for making genomic sequences of the two organisms available before publication, and the reviewers for insightful comments.

Received July 28, 2006; accepted August 26, 2006.

REFERENCES

Aguiar, P., Beveridge, T.J., and Reysenbach, A.L. 2004. Sulfurihydrogenibium azorense, sp. nov., a thermophilic hydrogen-oxidizing microaerophile from terrestrial hot springs in the Azores. Int. J. Syst. Evol. Microbiol. 54: 33–39.

Altschul, S., Gish, W., Miller, W., Myers, E., and Lipman, D. 1990. A basic local alignment search tool. J. Mol. Biol. 215: 403–410.

Baird, N.J., Srividya, N., Krasilnikov, A.S., Mondragon, A., Sosnick, T.R., and Pan, T. 2006. Structural basis for altering the stability of homologous RNAs from a mesophilic and a thermophilic bacterium. RNA 12: 598–606.

Bocchetta, M., Gribaldo, S., Sanangelantoni, A., and Cammarano, P. 2000. Phylogenetic depth of the bacterial genera Aquifex and Thermotoga inferred from analysis of ribosomal protein, elongation factor, and RNA polymerase subunit sequences. J. Mol. Evol. 50: 366–380.

Burggraf, S., Olsen, G.J., Stetter, K.O., and Woese, C.R. 1992. A phylogenetic analysis of Aquifex pyrophilus. Syst. Appl. Microbiol. 15: 352–356.

Busch, S., Kirsebom, L.A., Notbohm, H., and Hartmann, R.K. 2000. Differential role of the intermolecular base-pairs G292-C(75) and G293-C(74) in the reaction catalyzed by Escherichia coli RNase P RNA. J. Mol. Biol. 299: 941–951.

Chen, J.L. and Pace, N.R. 1997. Identification of the universally conserved core of ribonuclease P RNA. RNA 3: 557–560.

Corpet, F. 1988. Multiple sequence alignment with hierarchical clustering. Nucleic Acids Res. 16: 10881–10890.

Deckert, G., Warren, P.V., Gaasterland, T., Young, W.G., Lenox, A.L., Graham, D.E., Overbeek, R., Snead, M.A., Keller, M., Aujay, M., et al. 1998. The complete genome of the hyperthermophilic bacterium Aquifex aeolicus. Nature 392: 353–358.

Dinos, G., Wilson, D.N., Teraoka, Y., Szaflarski, W., Fucini, P., Kalpaxis, D., and Nierhaus, K.H. 2004. Dissecting the ribosomal inhibition mechanisms of edeine and pactamycin: The universally conserved residues G693 and C795 regulate P-site RNA binding. Mol. Cell 13: 113–124.

Dsouza, M., Larsen, N., and Overbeek, R. 1997. Searching for patterns in genomic data. Trends Genet. 13: 497–498.

Felsenstein, J. 1981. Evolutionary trees from DNA sequences: A maximum likelihood approach. J. Mol. Evol. 17: 368–376.

Götz, D., Banta, A., Beveridge, T.J., Rushdi, A.I., Simoneit, B.R., and Reysenbach, A.L. 2002. Persephonella marina gen. nov., sp. nov. and Persephonella guaymasensis sp. nov., two novel, thermophilic, hydrogen-oxidizing microaerophiles from deep-sea hydrothermal vents. Int. J. Syst. Evol. Microbiol. 52: 1349–1359.

Griffiths, E. and Gupta, R.S. 2004. Signature sequences in diverse proteins provide evidence for the late divergence of the order Aquificales. Int. Microbiol. 7: 41–52.

Gruber, T.M. and Bryant, D.A. 1998. Characterization of the group 1 and group 2 s factors of the green sulfur bacterium Chlorobium tepidum and the green non-sulfur bacterium Chloroflexus aurantiacus. Arch. Microbiol. 170: 285–296.

Gupta, R.S. 2000. The phylogeny of proteobacteria: Relationships to other eubacterial phyla and eukaryotes. FEMS Microbiol. Rev. 24: 367–402.

Haas, E.S., Brown, J.W., Pitulle, C., and Pace, N.R. 1994. Further perspective on the catalytic core and secondary structure of ribonuclease P RNA. Proc. Natl. Acad. Sci. 29: 2527–2531.

Hartmann, E. and Hartmann, R.K. 2003. The enigma of Ribonuclease P evolution. Trends Genet. 19: 561–569.

Heide, C., Pfeiffer, T., Nolan, J.M., and Hartmann, R.K. 1999. Guanosine 2-NH2 groups of Escherichia coli RNase P RNA involved in intramolecular tertiary contacts and direct interactions with tRNA. RNA 5: 102–116.

Hofacker, I.L. 2003. Vienna RNA secondary structure server. Nucleic Acids Res. 31: 3429–3431.

Huber, R., Wilharm, T., Huber, D., Trincone, A., Burggraf, S., König, H., Rachel, R., Rockinger, I., Fricke, H., and Stetter, K.O. 1992. Aquifex pyrophilus gen. nov. sp. nov., represents a novel group of marine hyperthermophilic hydrogen-oxidizing bacteria. Syst. Appl. Microbiol. 15: 340–351.

Kazantsev, A.V., Krivenko, A.A., Harrington, D.J., Carter, R.J., Holbrook, S.R., Adams, P.D., and Pace, N.R. 2003. High-resolution structure of RNase P protein from Thermotoga maritima. Proc. Natl. Acad. Sci. 100: 7497–7502.

Klenk, H.P., Meier, T.D., Durovic, P., Schwass, V., Lottspeich, F., Dennis, P.P., and Zillig, W. 1999. RNA polymerase of Aquifex pyrophilus: Implications for the evolution of the bacterial rpoBC operon and extremely thermophilic bacteria. J. Mol. Evol 48: 528–541.

Leontis, N.B. and Westhof, E. 1998. A common motif organizes the structure of multi-helix loops in 16 S and 23 S ribosomal RNAs. J. Mol. Biol. 283: 571–583.

Lück, R., Gräf, S., and Steger, G. 1999. ConStruct: A tool for thermodynamic controlled prediction of conserved secondary structure. Nucleic Acids Res. 27: 4208–4217.

Massire, C., Jaeger, L., and Westhof, E. 1998. Derivation of the three-dimensional architecture of bacterial ribonuclease P RNAs from comparative sequence analysis. J. Mol. Biol. 279: 773–793.

O'Donnell, S.M. and Janssen, G.R. 2001. The initiation codon affects ribosome binding and translational efficiency in Escherichia coli of cI mRNA with or without the 59 untranslated leader. J. Bacteriol. 183: 1277–1283.

Olsen, G.J., Matsuda, H., Hagstrom, R., and Overbeek, R. 1994. fastDNAml: A tool for construction of phylogenetic trees of DNA sequences using maximum likelihood. Comput. Appl. Biosci. 10: 41–48.

Rivera-León, R., Green, C.J., and Vold, B.S. 1995. High-level expression of soluble recombinant RNase P protein from Escherichia coli. J. Bacteriol. 177: 2564–2566.

Smith, D., Burgin, A.B., Haas, E.S., and Pace, N.R. 1992. Influence of metal ions on the ribonuclease P reaction. Distinguishing substrate binding from catalysis. J. Biol. Chem. 267: 2429–2436.

Swanson, R.V. 2001. Genome of Aquifex aeolicus. Methods Enzymol. 330: 158–169.

Torres-Larios, A., Swinger, K.K., Krasilnikov, A.S., Pan, T., and Mondragon, A. 2005. Crystal structure of the RNA component of bacterial ribonuclease P. Nature 437: 584–587.

Tsai, H.Y., Masquida, B., Biswas, R., Westhof, E., and Gopalan, V. 2003. Molecular modeling of the three-dimensional structure of the bacterial RNase P holoenzyme. J. Mol. Biol. 325: 661–675.

Willkomm, D.K., Feltens, R., and Hartmann, R.K. 2002. tRNA maturation in Aquifex aeolicus. Biochimie 84: 713–722.

Willkomm, D.K., Minnerup, J., Hüttenhofer, A., and Hartmann, R.K. 2005. Experimental RNomics in Aquifex aeolicus: Identification of small non-coding RNAs and the putative 6S RNA homolog. Nucleic Acids Res. 33: 1949–1960.

Wegscheid, B., Condon, C., and Hartmann, R.K. 2006. Type A and B RNase P RNAs are interchangeable in vivo despite substantial biophysical differences. EMBO Rep. 7: 411–417.

Zhong, X., Leontis, N., Qian, S., Itaya, A., Qi, Y., Boris-Lawrie, K., and Ding, B. 2006. Tertiary structural and functional analyses of a viroid RNA motif by isostericity matrix and mutagenesis reveal its essential role in replication. J. Virol. 80: 8566–8581.

Zuker, M. 2003. Mfold web server for nucleic acid folding and hybridization prediction. Nucleic Acids Res. 31: 3406–3415.

4.3. Structural basis of a ribozyme's thermostability: P1-L9 interdomain interaction in RNase P RNA

Michal Marszalkowski, Dagmar K. Willkomm* and Roland K. Hartmann*

accepted RNA, September 2007

Structural basis of a ribozyme's thermostability: P1-L9 interdomain interaction in RNase P RNA

Michal Marszalkowski, Dagmar K. Willkomm* and Roland K. Hartmann*

Philipps-Universität Marburg, Institut für Pharmazeutische Chemie, Marbacher Weg 6, D-35037 Marburg, Germany

§ Corresponding authors: Dagmar K. Willkomm and Roland K. Hartmann, Institut für Pharmazeutische Chemie, Philipps-Universität Marburg, Marbacher Weg 6, D-35037 Marburg, Germany,

Tel. +49-6421-2825827; Fax +49-6421-2825854; e-mail: willkomm@staff.uni-marburg.de, roland.hartmann@staff.uni-marburg.de

Running title: P1-L9 interdomain interaction in RNase P RNA

keywords: bacterial RNase P RNA, P1-L9 interdomain contact, thermostability

ABSTRACT

For stability, many catalytic RNAs rely on long-range tertiary interactions, the precise role of each often being unclear. Here we demonstrate that one of the three interdomain architectural struts of RNase P RNA (P RNA) is the key to activity at higher temperatures: disrupting the P1-L9 helix-tetraloop interaction in P RNA of the thermophile *Thermus thermophilus* decreases activity at high temperatures in the RNA-alone reaction and at low Mg^{2+} concentrations in the holoenzyme reaction. Conversely, implanting the P1-P9 module of *T. thermophilus* in the P RNA from the mesophile *E. coli* converted the latter RNA into a thermostable one. Moreover, replacing the *E. coli* P1-P9 elements with a pseudoknot module that mediates the homologous interaction in *Mycoplasma* P RNAs not only conferred thermostability upon *E. coli* P RNA, but also increased its maximum turnover rate at 55°C to the highest yet described for a P RNA ribozyme.

INTRODUCTION

The ribonucleoprotein enzyme RNase P catalyzes tRNA 5'-end maturation in all organisms and organelles (Schön, 1999). In bacteria, the RNA subunit (P RNA), approx. 380 nt in size and encoded by the *rnpB* gene, forms a specific complex with a single protein cofactor of about 13 kDa. *In vitro*, bacterial P RNA has robust catalytic activity in the absence of the protein (Guerrier-Takada *et al.*, 1983), but the latter is essential for function *in vivo* (Schedl *et al.*, 1974; Gößringer *et al.*, 2006). P RNAs from bacteria are subdivided into two distinct structural groups, termed type A (for "ancestral") and type B (for "*Bacillus*"; Hall and Brown, 2001). P RNAs of both types consist of two independent folding domains, the specificity (S-) and the catalytic (C-) domain (Loria and Pan, 1996, 1997), which are oriented towards each other by three interdomain loop-helix contacts (L18-P8, L8-P4, P1-L9; Fig. 1 A) in P RNAs of type A architecture. These long-range interactions, considered as architectural struts that stabilize the RNA's overall conformation, were originally identified by phylogenetic covariation analyses (Brown *et al.*, 1996; Massire *et al.*, 1997 & 1998) and later confirmed in the crystal structure of P RNA from *Thermotoga maritima* (Torres-Larios *et al.*, 2005). The importance of the aforementioned as well as other (intradomain) long-range tertiary interactions for P RNA function was also demonstrated experimentally (e.g. Darr *et al.*, 1992; Pomeranz Krummel *et al.*, 1999). However, the specific functional contributions of the L18-P8, L8-P4 and P1-L9 contacts are poorly understood.

We recently reported that P RNAs from thermophilic bacteria share a 5'-GYAA L9 tetraloop and a P1 receptor site consisting of a G-C bp tandem, a combination not present in other bacteria (Marszalkowski, *et al.*, 2006). Also, helices P1 and P9 are stabilized in P RNAs from thermophiles by helix extension and/or deletion of nucleotide bulges. These observations prompted us to scrutinize the importance of the P1-L9 interaction in P RNA of the thermophile *Thermus thermophilus*, an A-type P RNA with robust *in vitro* activity at temperatures of up to 75°C (Hartmann and Erdmann, 1991), and to compare it to that of the mesophile *E. coli.*

RESULTS and DISCUSSION

Activity of *T. thermophilus* P RNA with a disrupted P1-L9 interaction

Initially, we disrupted the P1-L9 interaction in *T. thermophilus* P RNA by a sequence change of the L9 loop (5'-GUAA to 5'-UUCG, mL9 in Fig. 1 B).

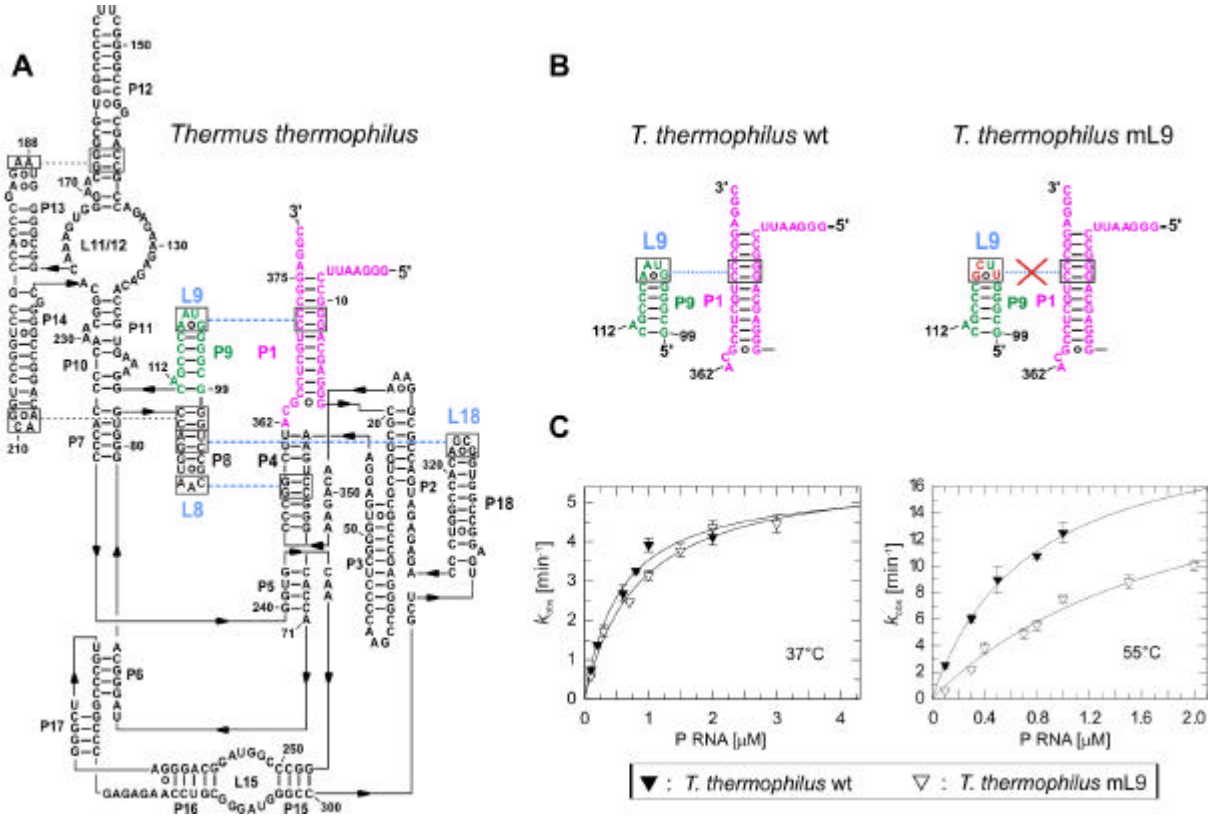

Fig. 1: (A) Secondary structure presentation of *T. thermophilus* RNase P RNA according to (Massire *et al*., 1998), with the three interdomain tetraloop-helix contacts L18-P8, L8-P4 and P1-L9 indicated by dashed blue lines. **(B)** P1-P9 region of the *T. thermophilus* wild-type P RNA (wt, left) and with the nucleotide exchanges (red) in loop L9 that disrupt the P1-L9 interaction (mL9, right). **(C)** Processing assays with the two *T. thermophilus* P RNA variants. Assay conditions: 0.1 to 3 µM P RNA, < 1 nM 5' endlabeled ptRNA, 100 mM $Mg(OAc)_2$, 100 mM NH_4OAc, 50 mM MES and 2 mM EDTA, pH 6.0, and 37°C or 55°C as indicated. Error bars indicate standard deviations.

At 100 mM Mg^{2+} in RNA-alone single turnover reactions, the mutant showed a defect at 55°C, but not at 37°C (Fig. 1 C). This was caused mainly by a 2- to 3-fold increase in $K_{m(sto)}$ (Table 1; $K_{m(sto)}$, the single turnover K_m, describes the enzyme concentration at which the half maximum rate under conditions of [E] >> [S] is achieved).An even more pronounced defect (up to 24-fold decrease in cleavage rate) was seen in activity assays with reconstituted RNase P holoenzymes at 37°C and 2.0 or 4.5 mM Mg^{2+} (Table 2).

Table 1: Summary of kinetic data of RNA-alone activity assays.

RNase P RNA	37ºC		55ºC	
	$K_{m(sto)}$ (µM)	k_{react} (min^{-1})	$K_{m(sto)}$ (µM)	k_{react} (min^{-1})
T. thermophilus wt	0.56 ±0.13	5.5 ±0.5	0.85 ±0.12	22.7 ±1.8
T. thermophilus mL9	0.83 ±0.12	5.8 ±0.3	2.1 ±0.5	20.9 ±3.2
E.coli wt	0.65 ±0.02	14.2 ±0.1	1.3 ±0.2	16.7 ±1.5
E. coli mL9	0.33 ±0.08	11.1 ±0.8	0.9 ±0.2	12.7 ±1.2
E.coli P1P9 *Tth*	0.44 ±0.09	11.4 ±0.7	0.6 ±0.1	25.2 ±2.0
E.coli P1P9 *Mgen*	0.54 ±0.15	10.9 ±1.1	1.8 ±0.2	35.1 ±1.9
E.coli P1P9 *MgenA117C*	0.30 ±0.08	10.4 ±0.7	3.3 ±0.7	58.6 ±8.3

RNase P RNA	$k_{react}/K_{m\ [37°]}$ ($min^{-1}µM^{-1}$)	$k_{react}/K_{m\ [55°]}$ ($min^{-1}µM^{-1}$)	$K_{react}/K_{m\ [55°]} : K_{react}/K_{m\ [37°]}$
T. thermophilus wt	9.82	26.71	2.72
T. thermophilus mL9	6.99	9.95	1.42
E. coli wt	21.85	12.85	0.59
E. coli mL9	33.64	14.11	0.42
E. coli P1P9 *Tth*	25.91	42.00	1.62
E. coli P1P9 *Mgen*	20.19	19.50	0.97
E. coli P1P9 *MgenA117C*	34.67	17.76	0.51

wt: wild-type, $K_{m(sto)}$: single turnover K_m (describes the enzyme concentration at which the half maximum rate under conditions of [E] >> [S] is achieved), k_{react}: single turnover V_{max}. All quantifications are based on at least three independent experiments; errors are standard errors of the curve fit; for reaction conditions see Methods.

Table 2: k_{obs} [min^{-1}] in RNase P holoenzyme assays of *T. thermophilus* and *E. coli* wild-type (wt) and mutant P RNAs.

RNase P RNA	*E. coli* P protein		*B. subtilis* P protein	
	2 mM Mg^{2+}	4.5 mM Mg^{2+}	2 mM Mg^{2+}	4.5 mM Mg^{2+}
T. thermophilus wt	1.3 ±.0.2	4.0 ± 0. 4	1.1 ±0.1	3.5 ±0.4
T. thermophilus mL9	0.054 ±0. 008	0.2 ±0.02	0.28 ±0. 03	0.55 ±0.02
E.coli wt	3.8 ±0.4	3.8 ±0.4	3.0 ±0.3	4.0 ±0.3
E. coli mL9	3.7 ±0.5	4.2 ±0.4	3.7 ±0.4	4.1 ±0.4
E.coli P1P9 *Mgen*	6.5 ±0.5	8.4 ±1.0		
E.coli P1P9 *MgenA117C*	3.2 ±0.3	3.2 ±0.3		

Reactions were performed as multiple turnover kinetics with recombinant P protein at 37°C in a buffer containing 20 mM Hepes, 150 mM NH_4OAc, 2 mM spermidine, 0.05 mM spermine, 4 mM β-mercaptoethanol, pH 7.4 at 37°C, and 2 or 4.5 mM $Mg(OAc)_2$ as indicated, at concentrations of 10 nM P RNA, 100 nM substrate and 40 nM P protein; k_{obs} is given as nmoles substrate converted per nmole of RNase P RNA per min. For further details see Methods.

Role of the P1-L9 interaction in folding of *T. thermophilus* P RNA

Effects of the L9 mutation on P RNA folding were analyzed by native PAGE (Buck *et al.*, 2005). While two main conformers were observed for *T. thermophilus* wt P RNA (bands 1 and 2 in Fig. 2 A), the L9 mutation indeed impeded formation of the faster migrating conformer 2, regardless of the presence or absence of P protein. To further characterize the two conformers of *T. thermophilus* wt P RNA, we eluted them separately from a native polyacrylamide gel at 4°C, and reloaded aliquots of each eluate onto another native gel. Under these conditions, with the temperature not exceeding 15°C during elution and re-electrophoresis, both conformers did not re-equilibrate to a substantial extent (Fig. 2 B). In parallel, equal amounts of the two eluted conformers were tested in the holoenzyme reaction, performed at 22°C to mimize conformational re-equilibration while maintaining high rates of substrate conversion. Approx. 15-fold higher activity (data not shown) was observed with the eluted conformer 2 (Fig. 2 B, lane b) relative to eluted conformer 1 (lane a).

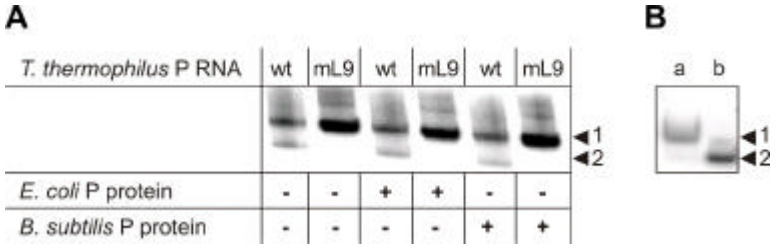

Fig. 2 (A) Native PAGE analysis of *T. thermophilus* P RNA and its L9 mutant in the presence (+) or absence (-) of P protein. Trace amounts (= 50 fmol) of 3' endlabeled P RNA were incubated in buffer KN4.5 for 5 min at 55°C followed by 50 min at 37°C, and either with our without addition of 40 nM RNase P protein for another 15 min at 37°C. Samples were loaded and run on 11.25% polyacrylamide gels in 1 x THE buffer supplemented with 100 mM NH_4OAc and 4.5 mM $MgCl_2$ (for further details, see Methods). **(B)** Stability of *T. thermophilus* wt P RNA conformers studied by re-electrophoresis after elution. *T. thermophilus* wt P RNA (10 nmol including 3'-endlabeled P RNA) was preincubated (see Methods) and then loaded on a native 11.25 % polyacrylamide gel as in panel A. The two conformers (bands 1 and 2) were then eluted separately at 4°C, and aliquots of each band were loaded onto another native 11.25 % polyacrylamide gel. Electrophoreses were performed at = 15°C. Under these conditions, with the temperature not exceeding 15°C during elution and re-electrophoresis, both conformers did not re-equilibrate to a substantial extent.

The catalytic deficits of the L9 mutant RNA observed at low metal ion concentration in the holoenzyme reaction thus appear to be directly correlated to a folding defect. Accordingly, the L9-P1 interaction is crucial for folding into a conformation that either stabilizes the catalytic core of the enzyme and its metal ion binding sites, or has increased affinity for the P protein and/or the substrate.

Role of the P1-L9 interaction in *E. coli* P RNA

We then investigated the role of the P1-L9 interaction in P RNA from the mesophile *E. coli* (Fig. 3 A) by disrupting the P1-L9 interaction (5'-GAAA to 5'-UCCG mutation, *E. coli* mL9, Fig. 3 B) as done previously (Pomeranz Krummel *et al.*, 1999). However, this neither substantially impaired the RNA-alone reaction at 37°C (in accordance with Pomeranz Krummel *et al.*, 1999) or 55°C nor the holoenzyme reaction (Fig. 3 C, Table 1 and 2), thus contrasting our results for *T. thermophilus* P RNA. The mutation was further neutral to viability (Table 3): the *E. coli* L9 mutant *rnpB* gene provided on a low copy plasmid fully rescued growth of the *E. coli* P RNA mutant strain BW (Wegscheid and Hartmann, 2006). Our data thus indicate that the P1-L9 interaction does not make a significant contribution to

overall stabilization of *E. coli* P RNA. We like to note that an *E. coli rnpB* gene with the same L9 mutation failed to rescue the phenotype of *E. coli* strain NHY322 *rnpA49*, for which the temperature sensitivity of a mutant P protein at 43°C is compensated by P RNA overexpression (Pomeranz Krummel *et al.*, 1999). We do not know the reasons for this discrepancy, but the different nature of the test strains precludes a direct comparison.

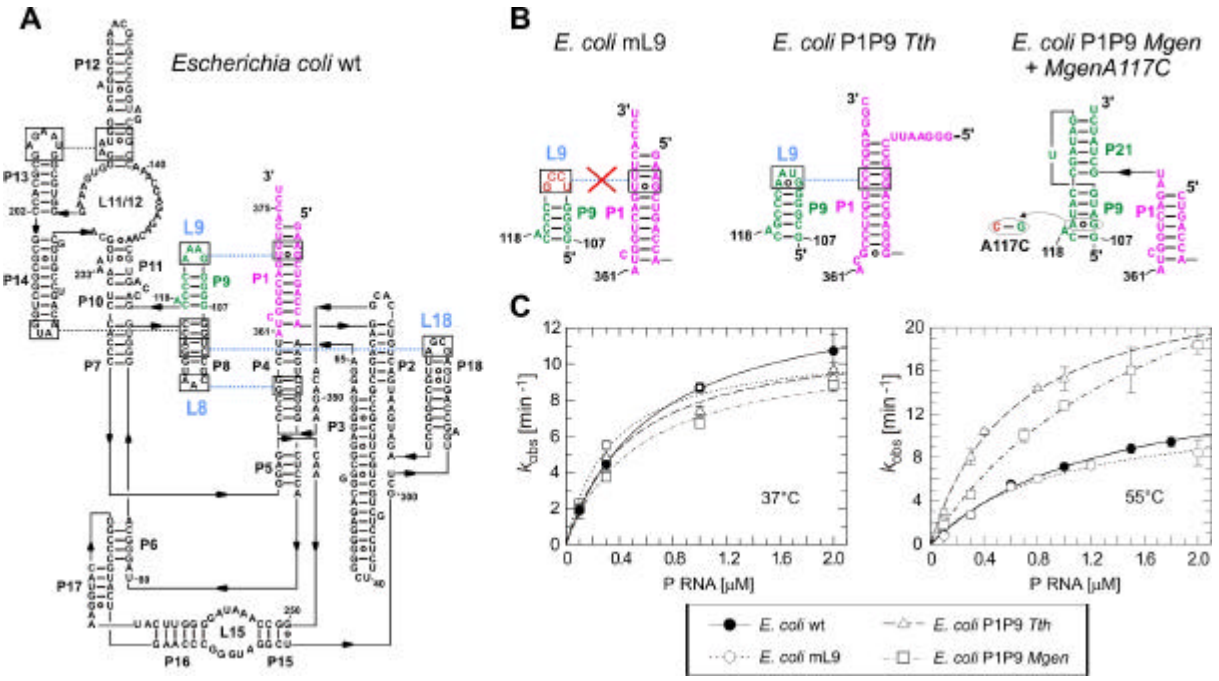

Fig. 3: Secondary structure presentation of **(A)** *E. coli* wild-type (wt) P RNA and **(B)** alterations in the P1-P9 mutants thereof. mL9: nucleotide changes (red) in loop L9 that disrupt the P1-L9 interaction; P1P9 *Tth*: *E. coli* P1P9 replaced with the corresponding elements of *T. thermophilus* P RNA; P1P9 *Mgen*: *E. coli* P1P9 replaced with the pseudoknot from *M. genitalium*; P1P9 *MgenA117C*: variant of P1P9 *Mgen*, with a single nucleotide (A117C) exchanged. **(C)** Processing assays with the *E. coli* P RNA variants performed as described in the legend to Fig. 1 C.

Table 3: *In vivo* complementation screen in *E. coli rnpB* mutant strain BW.

rnpB	**Complementation**	
	37°	**43°**
none	-	-
E. coli wt	++	++
E. coli C293 or C292	-	-
E. coli mL9	++	++
E. coli P1P9 *Tth*	++	++
E. coli P1P9 *Mgen*	++	++
E. coli P1P9 *MgenA117C*	+	++
T. thermophilus wt	-	-
T. thermophilus mL9	n.d.	n.d.

Growth of cells was monitored in the presence of 0.5% (w/v) glucose (without arabinose), conditions under which the chromosomal *rnpB* gene of the *E. coli* mutant strain BW is not expressed (at 37° as well as 43°C); cells were transformed with derivatives of the low copy plasmid pACYC177 that contained *rnpB* genes coding for P RNAs and mutants thereof under control of the native *rnpB* promoter. *E. coli rnpB* genes with G293C or G292C point mutations were previously shown to be lethal (Wegscheid and Hartmann, RNA 2006); - : no cell growth; ++ : growth with equal numbers of colonies on arabinose and glucose plates; + : somewhat decreased complementation efficiency according to number and size of colonies; n.d.: not determined because the *T. thermophilus* wild-type (wt) *rnpB* gene already does not complement, likely because of folding traps (unpublished results) at the growth temperatures of the *E. coli* strain.

Introduction of *T. thermophilus* and *Mycoplasma genitalium* P1-P9 elements into *E. coli* P RNA

We next replaced the P1-P9 elements of *E. coli* with those of *T. thermophilus* P RNA (*E. coli* P1P9 *Tth* in Fig. 3 B). Compared to the *E. coli* wt, ribozyme activity of this hybrid P RNA at 37°C was also essentially unchanged, but relatively increased to a substantial extent at 55° (Fig. 3 C and Table 1). Again the mutant P RNA was functional *in vivo* (Table 3). Finally, an exceptional kind of P1-P9 interaction exists in some P RNAs of the genus *Mycoplasma*,

which possess a P RNA of type B and where P9 and P1 juxtapose via a pseudoknot instead of the tetraloop-helix contact apparent in many type A P RNAs (Massire *et al.*, 1997). Built into *E. coli* P RNA as an interaction module expected to be of particularly high stability (*E. coli* P1P9 *Mgen*, Fig. 3 B), the pseudoknot of *M. genitalium* had little effect on the RNA-alone reaction at 37°C, but substantially increased the cleavage rate at 55°C (Fig. 3 C), the maximum cleavage rate obtained with this variant even exceeding that of *E. coli* P1P9 *Tth* (Table 1). In the holoenzyme reaction, cleavage rates were roughly twice that of *E. coli* wt P RNA (Table 2), and again, the hybrid P RNA was fully functional *in vivo* (Table 3). Lastly, we intended to stabilize the interacting module even further by an A117 to C mutation in *Mgen* P9 to introduce an additional Watson-Crick base pair (Fig. 3 B). This mutation generated a variant with the highest maximum turnover rate at 55°C yet described for a P RNA ribozyme (Table 1).

The fast substrate turnover catalyzed by the chimeric RNAs *E. coli* P1P9 *Mgen* and *MgenA117C* in the RNA-alone reaction at 55°C was associated with an increase in the single turnover $K_{m(sto)}$ compared with cleavage at 37°C, in particular for variant *E. coli* P1P9 *MgenA117C* (Table 1). This effect may be due to a loss in substrate binding affinity or to a reduction in the fraction of P RNAs that are competent to bind the substrate at 55°C. While this K_m effect may have various reasons, the stronger K_m effect for variant *E. coli* P1P9 *MgenA117C* (Fig. 3 B) may be explained by the mutant C117-G108 bp constraining the orientation of A118, such that stacking of A118 on another bulged A residue in P11 (A233, Fig. 3 A; Lescoute and Westhof, 2006) is weakened and becomes unstable at the higher temperature of 55°C.

Conclusions

From the presented data we conclude that the P1-L9 tertiary contact is crucial for folding and activity of P RNA from the thermophile *T. thermophilus* at high temperatures and low magnesium ion concentrations, conditions that require high intrinsic stability of the RNA. Our native PAGE analysis suggests that this interacting module represents one of the key anchoring points towards folding into the most active RNA conformer. These results extend present knowledge on the thermostability of P RNA from *T. thermophilus*: while Pan and coworkers identified 12 key base identities in the *T. thermophilus* S-domain that explain its stability increase over the corresponding *E. coli* domain (Baird *et al.*, 2006), we were able to pinpoint an interdomain strut crucial for function of the entire RNA.

In contrast, the P1-L9 interaction appears degenerate in *E. coli*-like mesophilic P RNAs and could be completely disrupted without compromising function *in vitro* as well as *in vivo*. Yet, though not made use of in *E. coli*, in this P RNA the location of the P1-L9 interaction module has nonetheless remained a key position for placing an architecturally highly effective interdomain strut: if building in a strongly interacting P1-L9 module, *E. coli* P RNA gains substantially in activity at high temperatures. The architectural framework governing P RNA overall statics has thus been preserved between the thermophilic and mesophilic P RNA.

Finally, our findings identify the P1-L9 receptor/tetraloop of *T. thermophilus* and the corresponding pseudoknot from *M. genitalium* as (thermo)stabilization modules for complex RNAs which comply with the concept of modular "plug and play" interchangeability (Costa and Michel, 1995, 1997; Qin *et al.*, 2001). They may thus expand the spectrum of modules that can be exploited to stabilize larger RNAs for structural analysis (Ferré-D'Amaré *et al.*, 1998).

MATERIALS and METHODS

Cloning of transcription templates and complementation plasmids

All plasmids were constructed by standard PCR and cloning techniques.

Preparation and labeling of substrate and P RNA

ptRNA substrate and P RNAs were obtained by run-off transcription with recombinant bacteriophage T7 RNA polymerase and 5' and 3' endlabeling essentially as described (Busch *et al.*, 2000, Heide *et al.*, 1999). The *T. thermophilus* ptRNA^{Gly} substrate was transcribed from plasmid pSBpt39HH linearized with BamHI (Busch *et al.*, 2000); *E. coli* wild-type P RNA was transcribed from plasmid pJA2' linearized with FokI (Vioque *et al.*, 1988; Busch *et al.*, 2000), *T. thermophilus* P RNA variants from plasmid pUC19*TthrnpB*wt and pUC19*TthrnpB*mL9 linearized with EheI; all *E. coli* mutant P RNAs were transcribed from respective pUC19-derivatives linearized with EcoRI (*E. coli* mL9, *E. coli* P1P9 *Tth*, *E. coli* P1P9 *Mgen*, and *E. coli* P1P9 *Mgen* A117C). The gift of pUC19*TthrnpB*wt from Andreas Werner, group of Eric Westhof, IBMC Strasbourg, is gratefully acknowledged.

RNase P RNA and holoenzyme activity assays

RNase P RNA-alone activity assays were performed in 100 mM $Mg(OAc)_2$, 100 mM NH_4OAc, 50 mM MES and 2 mM EDTA, pH 6.0, with trace amounts of 5' endlabeled substrate and P RNA concentrations in the range of 0.1 to 3 µM. Before starting the reaction, substrate and P RNA were preincubated separately in the assay buffer ($ptRNA^{Gly}$ substrate for 5 min at 55° and 20 min at 37°, P RNAs for 5 min at 55° and 55 min at 37°). Reactions were run for 5 to 30 min at 37° or 55°C as indicated. Activity of RNase P holoenzymes was measured in buffer KN (20 mM Hepes, 150 mM NH_4OAc, 2 mM spermidine, 0.05 mM spermine, 4 mM β-mercaptoethanol, pH 7.4 at 37°C) containing 2 or 4.5 mM $Mg(OAc)_2$ (buffer KN2 and KN4.5, [Wegscheid and Hartmann, RNA 2006]), at concentrations of 10 nM P RNA, 100 nM substrate and 40 nM P protein (recombinantly expressed and purified exactly as in [Marszalkowski *et al.*, RNA 2006]). Prior to the reaction, substrate and P RNA were preincubated in the reaction buffer (substrate as above, P RNA for 5 min at 55° and 50 min at 37°); P protein was then added to the P RNA and preincubation continued for another 5 min at 37°C, after which substrate was added. Analysis of cleavage reactions and data evaluation were carried out as described (Busch *et al.*, 2000).

Folding analysis by native PAGE

Folding analyses were performed essentially as described (Wegscheid & Hartmann, RNA 2006). In Fig. 2 A, trace amounts (= 50 fmol) of 3' endlabeled P RNA were incubated in buffer KN4.5 (see above) for 5 min at 55°C followed by 50 min at 37°C, and either with our without addition of 40 nM RNase P protein for another 15 min at 37°C. After addition of an equal volume of loading buffer (10% [v/v] glycerol, 4.5 mM $MgCl_2$, 0.025 % [w/v] each bromophenol blue and xylene cyanol), samples were run on an 11.25 %[v/v] polyacrylamide gel containing 66 mM Hepes, 33 mM Tris, 0.1 mM EDTA, 100 mM NH_4OAc and 4.5 mM $Mg(OAc)_2$, pH 7.4 (buffer system adapted from [Buck *et al.*, 2005]), with the gel temperature not exceeding 15°C. RNA bands were visualized with a Bio-Imaging Analyzer (FLA 3000-2R, FUJIFILM). For re-electrophoresis and activity testing of *T. thermophilus* wt P RNA conformers (Fig. 2 B), 20 nM of unlabeled P RNA plus 20 x 10^3 Cerenkov cpm of 3'-endlabeled P RNA per gel lane were preincubated in buffer KN4.5 for 10 min at 55°C in a volume of 7 µl; after addition of 7 µl loading buffer (see above), sample were subjected to native PAGE as described above. After electrophoresis and 1 h of phosphoimager plate exposition, the two conformers were excised separately from the gel and eluted in 50 µl of buffer KN4.5 (see above) without Mg^{2+} by shaking overnight at 4°C. To analyze stability of the conformers, eluted material from each band was subsequently supplemented with loading buffer and run on a second native polyacrylamide gel

(Fig. 2 B). To compare the conformers for differences in catalytic activity, ~ 3.5 nM of each eluted conformer were used in holoenzyme cleavage assays performed under multiple turnover conditions (reaction buffer KN4.5, 100 nM ptRNA, 40 nM *B. subtilis* RNase P protein). Assays were carried out at 22°C without any preincubation steps to eliminate potential heat-induced conformational changes.

***In vivo* complementation assays in *E. coli* strain BW**

In vivo complementation assays were performed in the E. coli rnpB mutant strain BW with derivatives of the low copy plasmid pACYC177 precisely as described (Wegscheid and Hartmann, RNA 2006).

ACKNOWLEDGEMENTS

This work was supported by the Deutsche Forschungsgemeinschaft and the Fonds der Chemischen Industrie.

REFERENCES

Baird, N.J., Srividya, N., Krasilnikov, A.S., Mondragon, A., Sosnick, T.R., and Pan, T. 2006. Structural basis for altering the stability of homologous RNAs from a mesophilic and a thermophilic bacterium. *RNA* **12**: 598-606.

Brown, J.W., Nolan, J.M., Haas, E.S., Rubio, M.A., Major, F., and Pace, N.R. 1996. Comparative analysis of ribonuclease P RNA using gene sequences from natural microbial populations reveals tertiary structural elements. *Proc. Natl. Acad. Sci. USA* **93**: 3001-3006.

Buck, A.H., Dalby, A.B., Poole, A.W., Kazantsev, A.V., and Pace, N.R. 2005. Protein activation of a ribozyme: the role of bacterial RNase P protein. *EMBO J.* **24**: 3360-3368.

Busch, S., Kirsebom, L.A., Notbohm, H., and Hartmann, R.K. 2000. Differential role of the intermolecular base-pairs G292-C75 and G293-C74 in the reaction catalyzed by *Escherichia coli* RNase P RNA. *J. Mol. Biol.* **299**: 941-951.

Costa, M., and Michel, F. 1995. Frequent use of the same tertiary motif by self-folding RNAs. *EMBO J.* **14**: 1276-1285.

Costa, M., Michel, F. 1997. Rules for RNA recognition of GNRA tetraloops deduced by *in vitro* selection: comparison with *in vivo* evolution. *EMBO J.* **16**: 3289-3302.

Darr, S.C., Zito, K., Smith, D., and Pace, N.R. 1992. Contributions of phylogenetically variable structural elements to the function of the ribozyme ribonuclease P. *Biochemistry* **31**: 328-333.

Ferré-D'Amaré, A.R., Zhou, K., and Doudna, J.A. 1998. A general module for RNA crystallization. *J. Mol. Biol.* **279**: 621-631.

Gössringer, M., Kretschmer-Kazemi Far, R., and Hartmann, R.K. 2006. Analysis of RNase P protein (rnpA) expression in *Bacillus subtilis* utilizing strains with suppressible rnpA expression. *J. Bacteriol.* **188**: 6816-6823.

Guerrier-Takada, C., Gardiner, K., Marsh, T., Pace, N., and Altman, S. 1983. The RNA moiety of ribonuclease P is the catalytic subunit of the enzyme. *Cell* **35**: 849-857.

Hall, T.A., and Brown, J.W. 2001. The ribonuclease P family. *Methods Enzymol.* **341**: 56-77.

Hartmann, R.K., and Erdmann, V.A. 1991. Analysis of the gene encoding the RNA subunit of ribonuclease P from *T. thermophilus* HB8. *Nucleic Acids Res.* **19**: 5957-5964.

Heide, C., Pfeiffer, T., Nolan, J.M., and Hartmann, R.K. 1999. Guanosine 2-NH_2 groups of *Escherichia coli* RNase P RNA involved in intramolecular tertiary contacts and direct interactions with tRNA. *RNA* **5**: 102-116.

Lescoute, A., and Westhof, E. 2006. The interaction networks of structured RNAs. *Nucleic Acids Res.* **34**: 6587-6604.

Loria, A., and Pan, T. 1996. Domain structure of the ribozyme from eubacterial ribonuclease P. *RNA* **2**: 551-563.

Loria, A., and Pan, T. 1997. Recognition of the T stem-loop of a pre-tRNA substrate by the ribozyme from Bacillus subtilis ribonuclease P. *Biochemistry* **36**: 6317-6325.

Marszalkowski, M., Teune, J.H., Steger, G., Hartmann, R.K., and Willkomm, D.K. 2006. Thermostable RNase P RNAs lacking P18 identified in the *Aquificales*. *RNA* **12**: 1915-1921.

Massire, C., Jaeger, L., and Westhof, E. 1997 Phylogenetic evidence for a new tertiary interaction in bacterial RNase P RNAs. *RNA* **3**: 553-556.

Massire, C., Jaeger, L., and Westhof, E. 1998. Derivation of the three-dimensional architecture of bacterial ribonuclease P RNAs from comparative sequence analysis. *J. Mol. Biol.* **279**: 773-793.

Pomeranz Krummel, D.A., and Altman, S. 1999. Verification of phylogenetic predictions *in vivo* and the importance of the tetraloop motif in a catalytic RNA. *Proc. Natl. Acad. Sci. USA* **96**: 11200-11205.

Qin, H., Sosnick, T.R., and Pan, T. 2001. Modular construction of a tertiary RNA structure: the specificity domain of the *Bacillus subtilis* RNase P RNA. *Biochemistry* **40**: 11202-11210.

Schedl, P., Primakoff, P., and Roberts, J. 1974. Processing of *E. coli* tRNA precursors. *Brookhaven Symp. Biol.* **26**: 53–76.

Schön, A. 1999. Ribonuclease P: the diversity of a ubiquitous RNA processing enzyme. *FEMS Microbiol. Rev.* **23**: 391-406.

Torres-Larios, A., Swinger, K.K., Krasilnikov, A.S., Pan, T., and Mondragon, A. 2005. Crystal structure of the RNA component of bacterial ribonuclease P. *Nature* **437**: 584-587.

Vioque, A., Arnez, J., and Altman, S. 1988. Protein-RNA interactions in the RNase P holoenzyme from *Escherichia coli. J. Mol. Biol.* **202**: 835-848.

Wegscheid, B., and Hartmann, R.K. 2006. The precursor tRNA 3'-CCA interaction with *Escherichia coli* RNase P RNA is essential for catalysis by RNase P *in vivo. RNA* **12**: 2135-214

4.4. *In vitro* and *in vivo* role of interdomain contacts in RNase P RNAs from psychrophilic, mesophilic and thermophilic bacteria

Michal Marszalkowski[1], Dagmar K. Willkomm[1], Ralph Feltens[2] and Roland K. Hartmann[1]*

submitted, 2007

Collaboration with the group of Eric Westhof, Institut de biologie moléculaire et cellulaire du CNRS, UPR9002, Architecture et Réactivité de l'ARN, Université Louis Pasteur 15 rue René Descartes, F-67084 Strasbourg Cedex, France

INTRODUCTION

In P RNAs of type A architecture, S- and C-domains are oriented towards each other by three interdomain loop-helix contacts (L18-P8, L8-P4, P1-L9; Fig. 1). These long-range interactions, considered as architectural struts that stabilize the RNA's overall conformation, were originally identified by phylogenetic covariation analyses (Brown *et al.*, 1996; Massire *et al.*, 1997 & 1998) and later confirmed in the crystal structure of P RNA from *Thermotoga maritima* (Torres-Larios *et al.*, 2005). Yet little is known about the individual contributions of these long-range interactions to P RNA function. Andreas Werner, during his Ph.D. work in the group of Eric Westhof, disrupted the L8-P4 and/or L18-P8 interaction by mutation in three model P RNAs: the one from *Thermus thermophilus* (thermophile) *Pseudoalteromonas haloplanktis* (psychrophile) and *Deinococcus radiodurans* (radiation-resistant bacterium); the latter shows some deviation from the canonical bacterial P RNA architecture, such as extension of the P9 stem and a pseudoknot contact between elements L9c and L12 in the S-domain (Fig. 1). In UV-melting experiments, A. Werner observed that simultaneous disruption of the L8-P4 and L18-P8 interaction results in stabilization of S-domain folding: the S-domains devoid of contacts to the C-domain tend to melt at higher temperature and with a single rather than multiple transitions (A. Wener, unpublished). In a collaboration with the Westhof group, we analyzed in parallel the processing activities of the various P RNA mutant constructs. In addition, folding of *T. thermophilus* P RNA, which requires a temperature step at 55°C to surpass a folding trap, was investigated in detail by probing and native PAGE experiments. The results described below will be part of a joint publication (in preparation) with the Westhof group.

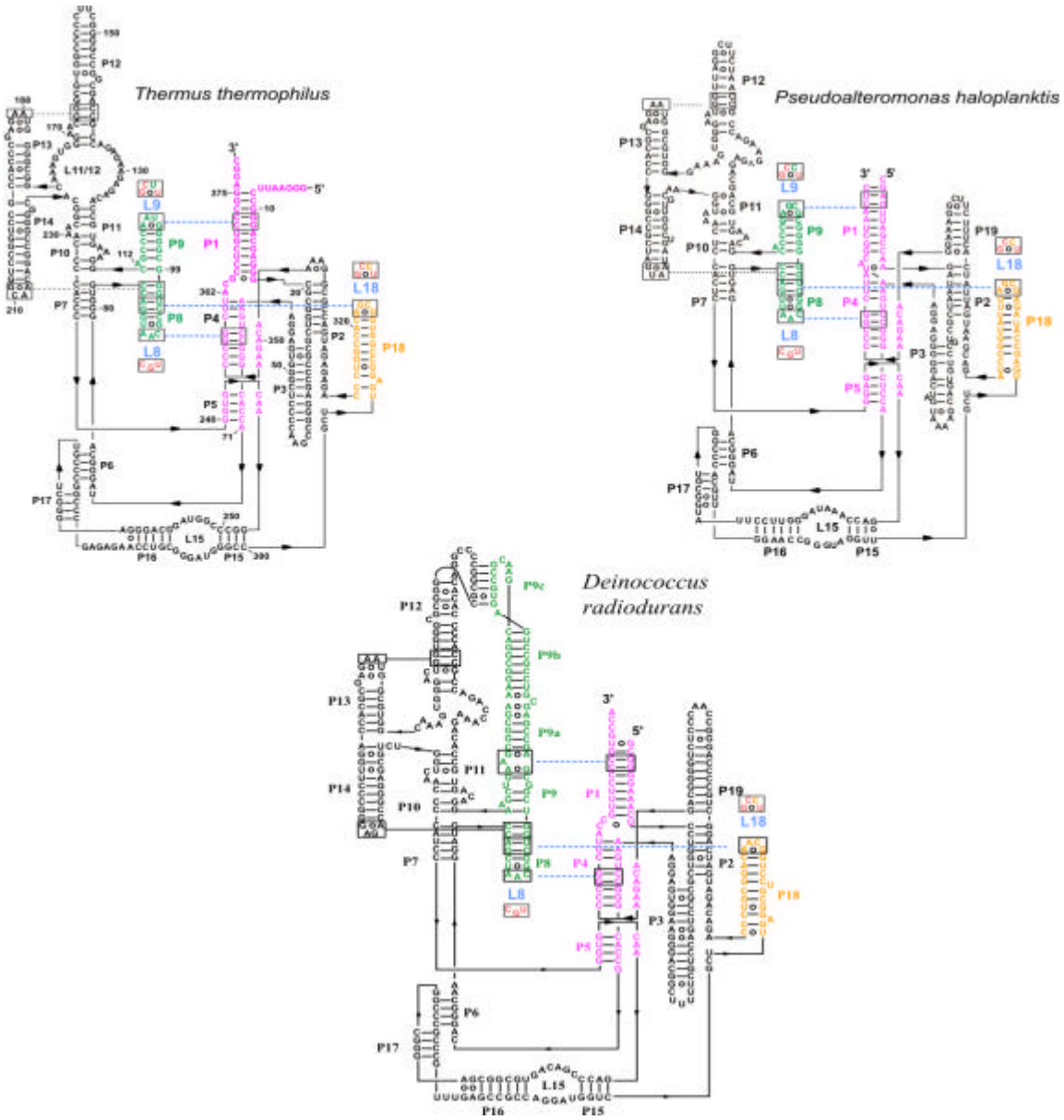

Fig. 1: Secondary structure presentation of *T. thermophilus*, *P. haloplanktis and D. radiodurans* RNase P RNAs according to (Massire *et al*., 1998), with the three interdomain tetraloop-helix contacts L18-P8, L8-P4 and P1-L9 indicated by dashed blue lines and the involved structural elements in colour. Nucleotide exchanges in L8, L9 and L18 (mL8, mL9 and mL18) that disrupt these tertiary interactions are highlighted in red.

RESULTS

Kinetic effects of L8, L9 and L18 mutations

To investigate the role of interdomain contacts in *T. thermophilus*, *P. haloplanktis* and *D. radiodurans* P RNAs, we tested the wt RNAs in comparison to variants thereof with disrupted interdomain contacts for their activity in RNA-alone reactions (Table 1). We refrained from disrupting the L9-P1 interaction in *D. radiodurans* P RNA because of its

distinct architecture: here an internal loop is predicted to form the contact with helix P1; in addition, helix P9 is largely extended and the apical ends of P9 (P9c) and P12 likely basepair (Fig. 1).

Table 1: Summary of kinetic data of RNA-alone activity assays.

	$K_{m(sto)}$ [μM]	k_{react} [min^{-1}]	$k_{react}/K_{m(sto)}$ [$M^{-1}s^{-1}$]	decrease $k_{react}/K_{m(sto)}$ relative to wt
T. thermophilus wt	0.56 (±0.13)	5.5 (±0.5)	1.6×10^5	-
T. thermophilus mL8	0.4 (±0.1)	3.0 (±0.2)	1.2×10^5	1.3
T. thermophilus mL18	1.7 (±0.26)	3.5 (±0.25)	3.4×10^4	4.7
T. thermophilus mL8/L18	2 (±0.2)	1.0 (±0.05)	8.3×10^3	19.2
T. thermophilus mL9	0.83 (±0.12)	5.8 (±0.3)	1.16×10^5	1.4
P. haloplanktis wt	0.4 (±0.1)	10.4 (±1)	4.3×10^5	-
P. haloplanktis mL8	0.34 (±0.05)	0.23 (±0.01)	1.1×10^4	39
P. haloplanktis mL18	0.28 (±0.02)	0.2 (±0.055)	1.2×10^4	36
P. haloplanktis mL8/L18	0.4 (±0.09)	0.023 (±0.001)	9.6×10^2	448
P. haloplanktis mL9	0.38 (±0.06)	10.08 (±0.6)	4.4×10^5	1
D. radiodurans wt	1.5 (±0.16)	2.35 (±0.09)	2.6×10^4	-
D. radiodurans mL8	5.6 (±1.6)	0.33 (±0.04)	9.8×10^2	26.5
D. radiodurans mL18	1.93 (±0.2)	0.34 (±0.02)	2.9×10^3	9
D. radiodurans mL8/L18	4.2 (±1.8)	0.017 (±0.002)	6.7×10^1	388

wt: wild-type, $K_{m(sto)}$: single turnover K_m, k_{react}: single turnover V_{max}. All quantifications are based on at least three independent experiments; errors are standard errors of the curve fit; assay conditions: 100 mM $Mg(OAc)_2$, 100 mM NH_4OAc, 0.1 mM EDTA, 50 mM MES, pH 6.0, trace amounts (< 1 nM) of *T. thermophilus* $ptRNA^{Gly}$, excess amounts of P RNA (E>>S); preincubations: P RNA, 5 min at 55°C and 55 min at 37°C; substrate: 5 min at 55°C and 25 min at 37°C.

Under the assay conditions applied in Table 1 (single turnover, 37°, in the presence of 0.1 M Mg^{2+}), disruption of the L8-P4 contact had little effect on *T. thermophilus* P RNA (1.3-fold decrease in $k_{react}/K_{m(sto)}$ relative to the wt RNA), but affected the two other P RNAs more seriously (39- and 26.5-fold decrease in $k_{react}/K_{m(sto)}$;Table 1). A similar trend was observed for P RNA variants with a disrupted L18-P8 interaction, although the *D. radiodurans* mL18 mutant P RNA was much less affected than the corresponding *P. haloplanktis* P RNA variant (9-versus 36-fold decrease in $k_{react}/K_{m(sto)}$). Mutation of L9 had a minor effect on *T. thermophilus* P RNA under these assay conditions, but remained without consequences in the reaction catalyzed by *P. haloplanktis* P RNA (Table 1). Simultaneous disruption of the L8-P4 and L18-P8 contacts (variants mL8/L18) impaired activity most severely. Again, the *T. thermophilus* mL8/L18 variant performed substantially better than the two other counterparts (19.2-fold versus 448-/388-fold decrease in $k_{react}/K_{m(sto)}$;Table 1).

From these findings we conclude that the *T. thermophilus* P RNA structure is more robust than that of the P RNAs from *P. haloplanktis* and *D. radiodurans*, as inferred from the lower sensitivity of the former RNA toward loss of individual interdomain contacts under the conditions tested.

***In vivo* complementation analysis**

The heterologous wt and mutant P RNAs were tested for their capacity to rescue the lethal phenotype of the *E. coli* P RNA (*rnpB*) mutant strain BW (Wegscheid and Hartmann, 2006). Among the heterologous wt *rnpB* genes, only that of *P. haloplanktis* was able to rescue growth of the mutant strain when provided on a low copy plasmid (Table 2). The failure of *T. thermophilus rnpB* genes to functionally replace *E. coli rnpB* can be explained by the fact that this RNA requires a temperature step of 55°C for proper folding (see below), suggesting insufficient folding in the *E. coli* host at 37° to 43°C. For *D. radiodurans* P RNA, the failure may be related to its unique architecture in the P9 and P12 regions (Fig. 1).

Table 2: *In vivo* complementation screen in *E. coli rnpB* mutant strain BW

rnpB	37°C	43°C
E. coli wt	++	++
P. haloplanktis wt	++	++
P. haloplanktis mL8	-	-
P. haloplanktis mL18	+	+
P. haloplanktis mL8/L18	-	-
P. haloplanktis mL9	++	++
T. thermophilus wt	-	-
D. radiodurans wt	-	-

Growth of cells was monitored in the presence of 0.5% (w/v) glucose (without arabinose), conditions under which the chromosomal *rnpB* gene of the *E. coli* mutant strain BW is not expressed (at 37° as well as 43°C); cells were transformed with derivatives of the low copy plasmid pACYC177 that contained *rnpB* genes coding for P RNAs and mutants thereof under control of the native *rnpB* promoter; - : no cell growth; ++ : growth with equal numbers of colonies on arabinose and glucose plates; + : somewhat decreased complementation efficiency according to number and size of colonies; wt, wild-type.

Based on the above findings we could only test the *P. haloplanktis* mutant P RNAs for complementation in strain BW. Whereas the mL8 and mL8/L18 variants were non-functional, a partial rescue of the growth phenotype was seen for the mL18 variant (Table 2). This indicates that the L8-P4 contact is more crucial for P RNA function than the L18-P8 contact, which might explain the observation that the P18 element has been lost in P

RNAs of some bacterial clades, such as in the *Aquificales* and the genus *Chlorobium* (Marszalkowski et al., 2006; Haas *et al*. 1994).

The *P. haloplanktis* mL9 mutant P RNA fully rescued growth of *E. coli* strain BW (Table 2), as did a corresponding *E. coli* mutant P RNA in our previous study (Marszalkowski *et al.*, 2007). We discussed this as evidence for the L9-P1 contact being degenerated in *E. coli*-like P RNAs from non-thermophilic bacteria (Marszalkowski *et al.*, 2007).

Activity assays at 15° versus 37°C

Since *P. haloplanktis* grows remarkably fast at temperatures between 0° and 15°C, we addressed the question if adaptation to low temperature might be observable on the level of P RNA function. For this purpose, the P RNAs from the psychrophile *P. haloplanktis*, the stress-resistant *D. radiodurans*, the thermophile *T. thermophilus* and the mesophile *E. coli* were analyzed for processing activity in the RNA-alone as well as holoenzyme reaction at 15°C versus 37°C. In the RNA-alone reaction, the maximum single turnover rate (k_{react}) was higher at 37° versus 15°C for all tested P RNAs (Table 4). The least difference was seen for *D. radiodurans* P RNA, but here it has to be considered that this RNA had the lowest k_{react} value at 37°C among all four P RNAs tested. *P. haloplanktis* P RNA showed the highest k_{react} value at 15°C and the second lowest ratio for k_{react}(37°C)/k_{react}(15°C) (9.2, Table 3).

Table 3: Summary of kinetic data of RNA-alone activity assays performed at 15°C or 37°C.

P RNA	k_{react} (min^{-1})		$K_{m(sto)}$ (µM)		$k_{react}/K_{m(sto)}$ (min^{-1} $µM^{-1}$) 15°C	$k_{react}/K_{m(sto)}$ (min^{-1} $µM^{-1}$) 37°C	relative decrease 37°/ 15°C
	15°C	37°C	15°C	37°C			
P. h.	1.13 (±0.08)	10.4 (±1)	0.3 ±0.07	0.4 ±0.1	3.8	26	6.8
D. r.	0.7 (±0.04)	2.35 (±0.09)	0.6 ±0.1	1.5 ±0.16	1.2	1.6	1.3
T. t.	0.3 (±0.006)	5.5 (±0.5)	0.06 ±0.008	0.56 ±0.13	5.0	9.8	2.0
E. c.	0.46 (±0.015)	14.2 ±0.1	0.06 ±0.01	0.65 ±0.02	7.7	21.8	2.8

	k_{react}(37°)/k_{react}(15°C)	$K_{m(sto)}$(37°C)/ $K_{m(sto)}$(15°C)
P. h.	9.2	1.3
D. r.	3.4	2.5
T. t.	18.3	9.3
E. c.	30.9	10.8

For experimental details, see Table 1.; *P. h. = P. haloplanktis*; *D. r. = Deinococcus radiodurans; T. t. = T. thermophilus; E. c. = E. coli.*

Table 4: Holoenzyme kinetics for the different wt P RNAs reconstituted with the *E. coli* P protein and assayed at 37°C versus 15°C

P RNA	k_{obs}(min $^{-1}$) at 37°C	k_{obs}(min $^{-1}$) at 15°C	k_{obs}(37°C)/ k_{obs}(15°C)
E. c.	3.8 (±0.2)	0.12 (±0.05)	31.7
T. t	3.8 (±0.2)	0.12 (±0.03)	31.7
D. r.	6.2 (±0.4)	0.89 (±0.1)	7.0
P. h.	3.0 (±0.1)	0.043 (±0.004)	69.8

For abbreviations, see Table 3. Reactions were performed as multiple turnover kinetics with recombinant E. coli P protein at 37°C in a buffer KN4.5 containing 20 mM Hepes, 150 mM NH_4OAc, 2 mM spermidine, 0.05 mM spermine, 4 mM β-mercaptoethanol, pH 7.4, 4.5 mM $Mg(OAc)_2$ at 37°C, at concentrations of 10 nM P RNA, 100 nM substrate and 40 nM P protein; k_{obs} is given as nmoles substrate converted per nmole of P RNA per min.

Also, *P. haloplanktis* P RNA had the lowest difference in the single turnover K_m at the two assay temperatures. These observations would be consistent with the notion that the P RNA of the psychrophile *P. haloplanktis* has been adapted to activity at low temperatures. We also tested the four P RNAs in the holoenzyme reaction at low Mg^{2+} (4.5 mM) with the *E. coli* P protein (Table 4). Here, the *D. radiodurans* P RNA performed best at 37° and 15°C, and the *P. haloplanktis* P RNA showed the most pronounced activity reduction from 37° to 15°C [k_{obs}(37°C)/k_{obs}(15°C) = 70, versus 7.0 for *D. radiodurans* and 32 for *E. coli* and *T. thermophilus* P RNAs; Table 4]. These results counteract the trend seen in the RNA-alone reaction (Table 3). A possible reason may be that the P protein of *P. haloplanktis* has adapted to function in the cold, but the heterologous *E. coli* P protein cannot optimally cooperate with the *P. haloplanktis* P RNA at 15°C.

L9-P1 interaction

We previously reported that disruption of the P1-L9 helix-tetraloop interaction in P RNA of the thermophile *Thermus thermophilus* decreases activity at high temperatures (55°C) in the RNA-alone reaction and at low Mg^{2+} concentrations in the holoenzyme reaction. This activity decrease has not been evident in RNA-alone processing assays performed at 37°C (Table 1; Marszalkowski *et al.*, 2007). Mutation of loop L9 in *E. coli* P RNA neither substantially impaired the RNA-alone reaction at 37°C or 55°C nor the holoenzyme reaction, in contrast to *T. thermophilus* P RNA; likewise, the *E. coli* L9 mutant *rnpB* gene provided on a low copy plasmid fully rescued growth of the *E. coli* P RNA mutant strain

BW (Marszalkowski *et al*., 2007). The lack of an *in vivo* phenotype caused by L9 mutation in *E. coli* RNA deviated from results of a previous study: an *E. coli rnpB* gene with the same L9 mutation failed to rescue the phenotype of *E. coli* strain NHY322 *rnpA49*, for which the temperature sensitivity of a mutant P protein at 43°C is compensated by P RNA overexpression (Pomeranz Krummel *et al.*, 1999). To shed more light on this discrepancy, we therefore tested the effect of L9 mutation for another P RNA, the one from *P. haloplanktis.* However, as for *E. coli* P RNA, we neither saw a defect in the RNA-alone reaction at 37°C (Table 1) and in the holoenzyme reaction with the *E. coli* or *B. subtilis* P protein, nor in the *in vivo* complementation assay (Table 2). These findings support the notion that the P1-L9 interaction does not make a significant contribution to overall stabilization of type A RNase P RNAs from mesophilic or psychrophilic bacteria, such as *E. coli* and *P. haloplanktis*.

Folding trap of *T. thermophilus* P RNA

In vitro transcribed *T. thermophilus* P RNA requires a 55°C preincubation step for efficient processing activity. This was found to be independent of the Mg^{2+} concentration in the range of 10 to 100 mM Mg^{2+} (data not shown). In contrast, preincubation of *E. coli* P RNA at 55°C versus 37°C had no or at most a twofold effect, depending on the Mg^{2+} concentration (data not shown).

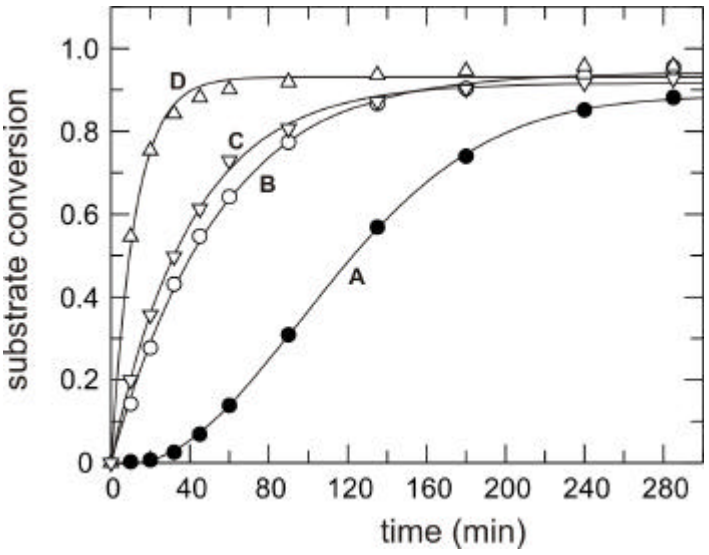

Fig. 2: Multiple turnover kinetics of ptRNAGly (200 nM) cleavage by *T. thermophilus* P RNA (20 nM) at 20 mM Mg^{2+}, 100 mM NH_4^+, 50 mM Hepes, pH 7.0. **(A)** preincubation of P RNA for 15 min at 37°C; after addition of substrate, the reaction was monitored for 285 min; **(B)** as in panel A, but addition of fresh substrate after 285 min of processing reaction; **(C)** as in panel B, but preincubation of P RNA for 300 min at 37°C; **(D)** as in panel A, but preincubation of P RNA for 15 min at 55°C;

The folding problem was investigated in processing reaction performed under multiple turnover conditions (20 nM P RNA, 200 nM ptRNA, 20 mM Mg^{2+}, 100 mM NH_4^+, 50 mM Hepes, pH 7.0). Preincubation for 15 min at 37°C instead of 55°C resulted in slow substrate turnover and sigmoidal kinetics (Fig. 2, curve A versus D). When the P RNA was preincubated for 300 min at 37°C before ptRNA addition, the rate of substrate cleavage increased, but still did not reach that obtained after preincubation for 15 min at 55°C (Fig. 2, curve C versus D). We also analyzed if the presence of the substrate may assist *T. thermophilus* P RNA folding into an active conformation: after preincubation at 37°C for 15 min substrate was added and the reaction was allowed to proceed for 285 min, after which 200 nM of fresh ptRNA substrate were added and processing monitored for another 285 min. The resulting curve B (Fig. 2) was almost identical to curve C (P RNA preincubation for 300 min at 37°C), suggesting that the presence of substrate had no significant effect on the slow refolding kinetics at 37°C. The sigmoidal curve A could be fit to equation 1, with k_{obs} describing the pseudo-first order rate when all P RNAs are folded (as achieved after preincubation at 55°C), k_1 the first order rate for a slow refolding step at 37°C), c the concentration of substrate at any time point, and c_0 the concentration of substrate at the start of the reaction.

equation 1:

$$\frac{C}{C_0} = \text{Limit} \cdot \left(1 - e^{-k_{obs} \times t} \cdot e^{\frac{k_{obs} \times e^{-k_1 \times t_0}}{k_1} (1 - e^{-k_1 \times t})} \right)$$

If the rate of cleavage after preincubation at 55°C (Fig. 2, curve D, k_{obs} = 0.083 min^{-1}) is taken as k_{obs} in equation 1, a k_1 value of 0.0016 min^{-1} for the folding step at 37°C is calculated.

Analysis of *T. thermophilus* P RNA refolding by probing

The structure of *T. thermophilus* P RNA was probed by Pb2+-induced hydrolysis and RNase T1 digestion under non-denaturing conditions (Fig. 3). For this purpose, 5'- or 3'-endlabeled P RNA was preincubated at 37°C or 55°C, followed by probing at 37°C. Differences in the hydrolysis pattern as a function of preincubation temperature were more pronounced with RNase T1 than Pb^{2+} ions (Fig. 3). We attribute this to the higher sensitivity of the bulky RNase T1 towards changes of accessibility compared with the small metal ion probe.

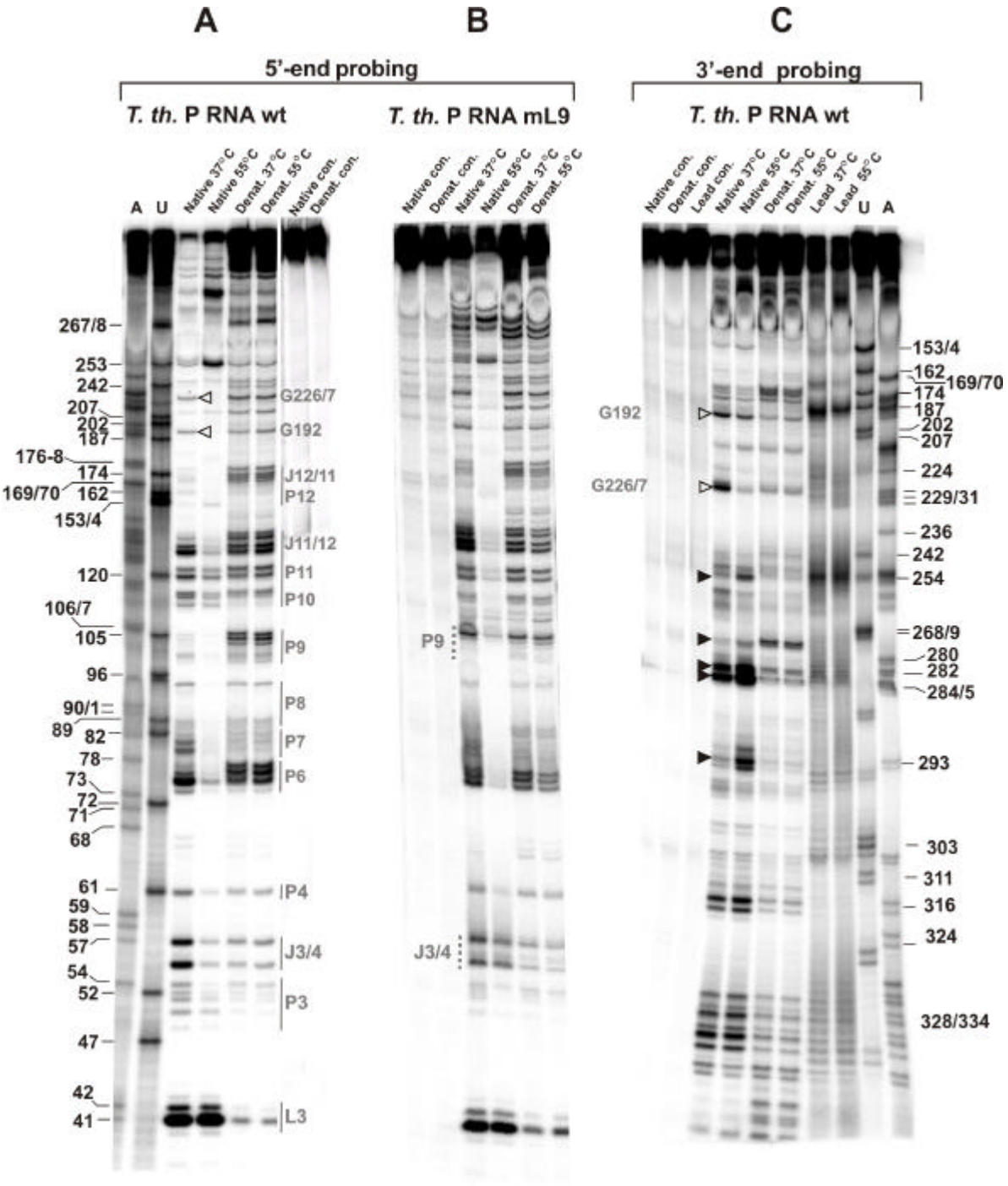

Fig. 3: RNase T1 probing of 5'-endlabeled *T. thermophilus* wt **(A)**, mL9 mutant **(B)**, and 3'-endlabeled wt P RNA **(C)**. Lanes A and U: AMPαS- or UMPαS-substituted *T. thermophilus* wt P RNA used to generate A- and U-specific ladders by iodine hydrolysis; lanes "Native 37°C" and "Native 55°C": P RNA preincubated for 10 min at 37°C or 55°C in the non-denaturing buffer B before addition of RNase T1 and limited hydrolysis for 10 min at 37°C; lanes "Denat. 37°C" and "Denat. 55°C": P RNA preincubated for 10 min at 37°C or 55°C in the denaturing buffer A before addition of RNase T1 and limited hydrolysis for 10 min at 37°C; lanes "Native con." and "Denat. Con.": P RNA preincubated for 10 min at 55°C in buffer B or buffer A, followed by incubation 10 min at 37°C without RNase T1; lanes "lead 37°C" and "lead 55°C": P RNA preincubated for 10 min at 37°C or 55°C in lead cleavage buffer before addition of lead ions and limited hydrolysis for 20 min at 37°C; lane "lead con.": P RNA preincubated for 10 min at 55°C in lead cleavage buffer, followed by

incubation 10 min at 37°C without lead ions. Cleavage fragments generated by iodine hydrolysis (lanes A and U) are assigned at the left (panel A) and right (panel C) margins according to the *T. thermophilus* P RNA numbering system shown in Fig. 1; note that shorter fragments of A and U ladders in panel C show double bands, which may have been due to end heterogeneity of the 3'-enlabeled P RNA. In panels A and C, regions of *T. thermophilus* P RNA that show reduced RNase T1 accessibility upon preincubation at 55°C are marked by open triangles or gray vertical lines, and those with enhanced accessibility are indicated by filled triangles. Differences in the RNase T1 protection pattern between *T. thermophilus* wt and mL9 P RNA are marked by vertical gray-dotted lines in panel B.

The following regions became more protected upon preincubation of 5'-endlabeled *T. thermophilus* P RNA at 55°C versus 37°C (marked in red in Fig. 3 A): P11 (G226;119/121), L13 (G192), P10 (G114/5), J11/12, 3'-side of P12, P6-8 (G75-G88), P9 (G101-104), P3 (G49-G53), J3/4 (G55/56) and P4 (G60); 3'-endlabeled *T. thermophilus* P RNA provided overlapping information, such as protection at G226, but also identified sites at which cleavage intensity increased upon preincubation at 55°C (marked with purple dots in Fig. 3 C); such sites were already seen with the 5'-endlabeled P RNA (Fig. 3 A), yet could not be assigned unambiguously due to low resolution: L15 (G256, G292/3), J6/17 (G274) and J17/16 (G283). These findings suggest that substantial compaction of the S-domain occurs during preincubation at 55°C, particularly in the P10 to J11/12 and the P6-8 regions, and including docking of L13 to helix P12. Protection in P6 can be explained by formation of this tertiary helix which entails changes in the P15-17 region, the hallmark being increased accessibility of loop L15 which pairs with tRNA 3'-CCA termini (Kirsebom and Svärd, 1994; Wegscheid and Hartmann, 2006). Another area of compaction is the 3'-side of P3, J3/4 and helix P4 near its U bulge in the catalytic core.

To identify regions affected by disruption of the L9-P1 interaction in *T. thermophilus* P RNA, we probed the 5'-endlabeled mL9 mutant RNA (Fig. 3 B). Protection from RNase T1 hydrolysis upon preincubation at 55°C was very similar to the pattern obtained with wt P RNA, suggesting overall compaction as for the wt RNA. The only exception was a reduced protection in J3/4 indicating that formation of the L9-P1 contact adjusts local conformation in the catalytic core. This finding is consistent with the activity decrease of the mL9 variant in the RNA-alone reaction at high temperatures (55°C) and at low Mg^{2+} concentrations in the holoenzyme reaction (Marszalkowski *et al.,* 2007).

Folding analysis by native PAGE

The results presented in Fig. 3 suggest considerable structure formation and compaction of *T. thermophilus* P RNA during the 55°C preincubation step. An independent though less

specific method to analyze folding is native PAGE. We recently demonstrated that *T. thermophilus* wt P RNA, but not the mL9 mutant thereof, is able to form a gel-resolvable compacted conformer (Fig. 4, band 2), whereas the mL9 mutant exclusively populates the slower migrating conformer (Fig. 4, band 1; Marszalkowski *et al*., 2007).

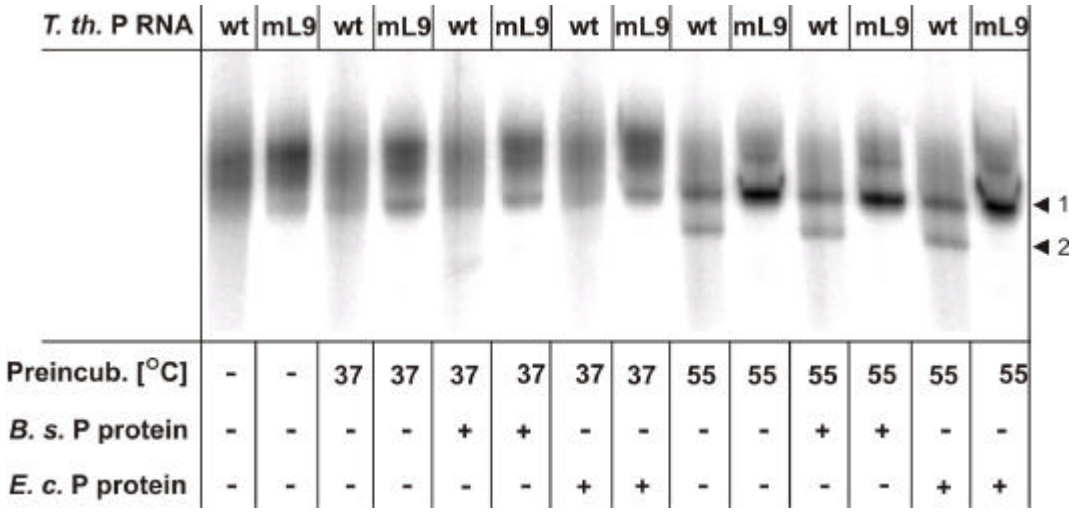

Fig. 4: Native PAGE analysis of *T. thermophilus* P RNA and its L9 mutant in the presence (+) or absence (-) of P protein from either *E. coli* or *B. subtilis*. Trace amounts (= 50 fmol) of 3' -endlabeled P RNA were incubated in buffer B (4.5 mM Mg^{2+}) for 5 min at 37°C or 55°C, followed by 50 min at 37°C, and either with our without addition of 40 nM RNase P protein for another 15 min at 37°C. Samples were loaded and run on 11.25% polyacrylamide gels in 1 x THE buffer supplemented with 100 mM NH_4OAc and 4.5 mM $MgCl_2$ (for further details, see Methods). Electrophoreses were performed at = 15°C.

The conformational equilibria were unaffected by the presence of the bacterial P protein during preincubation before gel loading, but required P RNA preincubation at 55°C (Fig. 4). When P RNAs were preincubated at 37°C instead of 55°C, gel mobility was more diffuse, with the bulk of RNA molecules migrating more slowly, and conformer 2 did not form at all in the case of the wt RNA. These results are in line with RNase T1 probing data (Fig. 3) and confirm that substantial structure formation and compaction of *T. thermophilus* occurs during the 55°C temperature step. These findings also provide an explanation why *T. thermophilus* P RNA was unable to replace its *E. coli* counterpart in the *E. coli* host (Table 3).

REFERENCES

Busch, S., Kirsebom, L. A., Notbohm, H., and Hartmann, R. K. (2000). Differential role of the intermolecular base-pairs G292-C(75) and G293-C(74) in the reaction catalyzed by *Escherichia coli* RNase P RNA. *J Mol Biol* .**299:** 941-951.

Dinos, G., Wilson, D.N., Teraoka, Y., Szaflarski, W., Fucini, P., Kalpaxis, D. and Nierhaus, K.H. 2004. Dissecting the ribosomal inhibition mechanisms of edeine and pactamycin: the universally conserved residues G693 and C795 regulate P-site RNA binding. *Mol. Cell.* **13:** 113-24.

Heide, C., Pfeiffer, T., Nolan, J. M., and Hartmann, R. K. (1999). Guanosine 2-NH2 groups of *Escherichia coli* RNase P RNA involved in intramolecular tertiary contacts and direct interactions with tRNA. *RNA* ***5*:** 102-116.

Marszalkowski, M., Teune, J. H., Steger, G., Hartmann, R. K., and Willkomm, D. K. (2006). Thermostable RNase P RNAs lacking P18 identified in the *Aquificales*. *RNA* **12:** 1915-1921.

Rivera-Leon, R., Green, C. J., and Vold, B. S. (1995). High-level expression of soluble recombinant RNase P protein from *Escherichia coli. J Bacteriol* **177:** 2564-2566.

Sousa R., Padilla R. 1995. A mutant T7 RNA polymerase as a DNA polymerase. *EMBO* **14(18):** 4609-4621

Vioque, A., Arnez, J., and Altman, S. (1988). Protein-RNA interactions in the RNase P holoenzyme from *Escherichia coli. J Mol Biol* **202:** 835-848.

Wegscheid, B., and Hartmann, R. K. (2006). The precursor tRNA 3'-CCA interaction with *Escherichia coli* RNase P RNA is essential for catalysis by RNase P in vivo. *RNA* **12:** 2135-2148.

Wolf-Dietrich Hardt and Roland K. Hartmann. Mutational analysis of the joining regions flanking helix P18 in *E. coli* RNase P RNA. *J Mol Biol.* 1996. **259(3):** 422-3

5. Summary

The ribonucleoprotein RNase P is an essential enzyme, which catalyses the 5'- end maturation of precursor tRNAs in all organisms and organelles. Bacterial RNase P consists of one catalytic RNA subunit of approx. 380 nt. in size and a 13 kDa protein subunit, encoded by *rnpB* and *rnpA* genes respectively. Both components are required for substrate cleavage under physiological conditions (*in vivo*). *In vitro* the RNA subunit is catalytically active only at elevated salt concentrations. *Aquifex aeolicus* seems to be until now the only known bacterium for which neither an *rnpB* nor an *rnpA* gene could be found in its sequenced genome.

Identification of *rnpB* and *rnpA* in the *Aquificales.*

Since the *Aquificales* (the close relatives of *A. aeolicus*) represent a group of bacteria for which not much information about RNase P RNA is available, we wanted to scrutinize if other members of this subphylum beside *A. aeolicus* also display idiosyncrasies regarding this essential enzyme. In cooperation with a bioinformatic research group (Gerhard Steger, Düsseldorf) we identified the P RNA (*rnpB*) and protein (*rnpA*) genes in the two *Aquificales Sulfurihydrogenibium azorense* and *Persephonella marina.* Their P RNAs adhere to the bacterial P RNA consensus and proved to be active catalysts at high metal ion concentrations *in vitro* and could be activated by heterologous bacterial P proteins at low salt. Both RNAs lack helix P18 and thus one of the three tetraloop-helix interactions that bridge S-and C-domains. *S. azorense* and *P. marina* P RNA are more thermostable than *E. coli* P RNA and require higher temperatures for proper folding. The P protein genes (*rnpA*) of *S. azorense* and *P. marina* were identified as well and co-localize with the *rmpH* gene encoding ribosomal protein L34 as in the majority of bacteria. We also identified RNase P activity in other *Aquificales* (*Aquifex pyrophilus*, *Hydrogenobacter thermophilus* TK 6 and *Thermocrinis ruber*) and demonstrated that active RNase P holoenzymes can be reconstituted from their total RNA upon addition of the *E. coli* or *B.subtilis* P protein. We were further able to demonstrate that a close relative of *A. aeolicus, A. pyrophilus*, is also lacks the *rnpA* gene in the canonical bacterial genomic context. Finally, we succeeded in detecting RNase P activity in fractions of *A. aeolicus* cell lysates and demonstrated that the enzyme possesses an essential protein component that, unlike in other bacterial RNase P enzymes, cannot be substituted for by *E. coli* or *B. subtilis* P proteins.

Strucural basis of a ribozyme's thermostability: P1-L9 interdomain interaction in RNase P RNA.

The two independent folding domains of type A bacterial P RNAs are interconnected by three long-range tertiary interaction: P1-L9, L8-P4 and P8-L18. Though predicted by phylogenetic analyses and confirmed by X-ray crystallography, the precise structural and functional role of these interactions is largely unclear.
Our analysis of the P RNAs from the thermophilic *Aqificales S. azorense* and *P. marina* (see above) revealed that these P RNAs and the one from the thermophile *Thermus thermophilus* share a 5'-GYAA L9 tetraloop and a P1 receptor site consisting of a G-C bp tandem, a combination not present in other bacteria. Also, helices P1 and P9 were observed to be stabilized in P RNAs from thermophiles by helix extension and/or deletion of nucleotide bulges. These observations prompted us to scrutinize the importance of the P1-L9 interaction in P RNA of the thermophile *Thermus thermophilus* and to compare it to that of the mesophile *E. coli.* The P1-L9 contact indeed turned out to be crucial for folding and activity of *T. thermophilus* P RNA at high temperatures and low magnesium ion concentrations as present in holoenzyme reactions. I showed by native PAGE that the P1-L9 interaction module represents the key anchoring points towards folding into the most active RNA conformer of *T. thermophilus* P RNA. In contrast, disruption of this interaction in the P RNA from the mesophile *E. coli* did not abrogate functionality *in vivo* or *in vitro*. However, exchanging the P1-L9 module in *E. coli* P RNA for that of *T. thermophilus* generated a thermostable *E. coli* variant. I also replaced the P1-L9 interaction module in *E. coli* P RNA with an alternative pseudoknot interaction module present in some *Mycoplasma* P RNAs, which again resulted in thermostabilization of the chimeric P RNA.
This work for the first time demonstrates that the module P1-L9 is directly linked to thermostabilization of P RNAs. This finding is an important step towards understanding structure-function relationships of catalytic RNAs.

***In vitro* and *in vivo* role of interdomain contacts in P RNAs from a psychrophilic, a mesophilic and a thermophilic bacterium.**

To further address the functional role of the interdomain interactions in RNase P RNA I investigated how disruption of the three main tertiary contacts affects activity of P RNAs

from bacteria growing at different temperatures (a psychrophile, a mesophile and a thermophile).

At 37°C and high Mg^{2+} concentrations (0.1 M), P RNA of the thermophile *Thermus thermophilus* was found to be most robust and rather insensitive toward L8 or L18 mutation; in contrast, activities of P RNAs from the psychrophile *Pseudoalternomonas haloplanktis* and mesophile *Deinococcus radiodurans* were strongly reduced upon disruption of the L8-P4 or L18-P8 contact. *In vitro* activity assays were further correlated with *in vivo* complementation of the mutant P RNAs in an *E. coli rnpB* mutant strain. For *P. haloplanktis* P RNA, such experiments revealed that disruption of the P1-L9 interaction is neutral to function *in vivo*, whereas the L8-P4 interaction is crucial for cellular function and more important than the L18-P8 contact. Finally, I found some evidence that the P RNA from *P. haloplanktis* is better adapted to the cold than P RNAs from *E. coli, D. radiodurans* or *T. thermophilus*, as the RNA was the only one for which the K_m of ptRNA processing remained unchanged upon lowering the temperature of the processing assay from 37° to 15°C.

P RNA from *Thermus* requires a preincubation step at 55ºC for folding and activation. By RNase T1 probing I could show that this step permits compaction of the S-domain and the catalytic core in the vicinity of helix P4. To identify regions affected by disruption of the L9-P1 interaction in *T. thermophilus* P RNA, I also probed the L9 mutant RNA. Protection from RNase T1 hydrolysis upon preincubation at 55°C was very similar to the pattern obtained with wild-type P RNA, suggesting overall compaction as for the wt RNA. The only exception was a reduced protection in J3/4 indicating that formation of the L9-P1 contact adjusts local conformation in the catalytic core.

In this part of my thesis I demonstrated that the interdomain tertiary interactions are of key importance for the function of bacterial P RNAs; however the individual contribution of the each of the three interactions differs markedly between the different P RNA species, which correlates with the growth optima of the respective host.

6. Appendix

6.1. Chemicals

Acrylamide M-Bis (50 % stock solution 24:1)	Gerbu
Agar Agar	Serva
Agarose	Roth
Ampicillin	Gerbu
Ammonium acetate	Fluka
Boric acid	Roth
Bovine serum albumin (BSA)	Sigma
Bromophenol blue (BPB)	Merck
Chloramphenicol	Sigma
Chloroform	Merck
Crystal violet	Fluka
Deoxynucleosidtriphosphates (dNTPs)	Boehringer
Disodiumhydrogenphosphate	Merck
Dithiothreitol (DTT)	Gerbu
Ethanol p.a. 99.8 %	Roth
Ethidiumbromide	Roth
Glycerol	Gerbu
Glycogen	Roche
Iod (I_2)	Merc
Isopropanol	Roth
Lead acetate	Roth
β-Mercaptoethanol	Serva
Nucleosidtriphosphates (NTPs)	Roche
Nucleosidtriphosphates phosphorothioates (ITPaS)	Boehringer
Peptone	Roth
Phenol	Roth
Potassiumdihydrogenphosphate	Fluka
Sodiumacetate	Merck
Sodiumcitrate	Roth
N,N,N‘,N‘-Tetraethylmethylenediamin (TEMED)	Serva
Tris-(hydroxymethyl)aminomethane	Gerbu
Urea	Gerbu
Xylenecyanol blue (XCB)	Serva
Yeast extract	Gerbu

All other chemicals (not listed above) were purchased from Sigma, Gerbu or Life Technologies and had a purity grade “pro analysis”.

6.2. Radioisotopes

[γ-^{32}P] ATP	Hartmann Analytic ICN Radiochemicals
[5’-^{32}P] pCp	Hartmann Analytic ICN Radiochemicals

6.3. Size markers

1 kb DNA ladder	New England Biolabs
10 bp DNA ladder	Invitrogen
2 Log DNA ladder	New England Biolabs
PageRuler™ Prestained Protein Ladder	MBI Fermentas

6.4. Enzymes

DNase I	Promega, Ambion
Pfu-Polymerase	Promega and our lab
Pyrophosphatase	Roche
Restriction endonucleases	MBI Fermentas and New England Biolabs
Taq polymerase	MBI Fermentas and our lab
Thermoscript	Invitrogen
T1 nuclease	Gibco BRL
T4 DNA ligase	Gibco BRL and MBI Fermentas
T4 Polynucleotide kinase	New England Biolabs
T7 RNA polymerase (Y639F)	our lab
Turbo DNase	Ambion

6.5. Equipment

Agarose gel chamber	Biorad, Mini Sub Cell
Autoclave	Systec V95
Electroporator	Biorad, Gene Pulser Xcell, PC- and CE- module
Gel documentation system	Cybertech, CS1 with Mitsubishi Video Copy Processor; Biostep, GelSystem MINI
Hand-monitor	Berthold, LB 1210 B
Heating blocks	Techne, Dri-Block DB-3D; Biometra, TB1
Incubator	Memmert BE400
Imager cassettes	Fuji Film, Bas cassette 4043, Rego, 35,6x43,2cm
Magnetic stirrers	Heidolph, MR 2002
Power supply	Pharmacia, EPS 3500; Bio Rad, Power Supply160/1.6 (Power Pac 3000); Apelex, PS 9009T
PAA-gel chamber	Custom-made, University of Lübeck
PCR cycler	Biometra, TGradient Thermocycler
pH-Meter	WTW, pH Level 1
Phosphoimager	Raytest, Bio-Imaging Analyser BAS 1000 (Fujifilm); FLA 3000, (Fujifilm)
Pipettes	Gilson-Pipetman, P20, P200, P1000 Abimed 0.
Protein Gel chamber	Mini Protean 3 cell, Biorad
Quartz cuvette	Hellma 104-QS, 105.202, 115B-QS, 105
Mixer	IKA, Vibrax-VXR; Eppendorf, Thermomixer 5436, Thermomixer comfort
Shaking incubator	GFL 3033
Spectrophotometer	Hewlett Packard, Photometer 8453; Varian, Cary 50 Conc; Thermo Spectronic, Biomate 3
Software	PCBas/Aida Image Analyser v.3.45,

	Corel Graphics Suite; GraFit 3.0; Microsoft Office; Pymol, Delano, W.L. 2002 Vector NTI®, Invitrogen
Speedvac	Heto vacuum centrifuge
Scintillation counters	Perkin Elmer, Wallac WINSPECTRAL a/b 1414 Liquid Scintillation Counter; Packard, Tricarb 2000CA
Centrifuges	Heraeus, Biofuge pico, biofuge fresco; Sigma, Typ 112; Eppendorf, centrifuge 5810R, minispin plus Stratagene, PicoFuge

6.6. Synthetic DNA Oligonucleotides

DNA oligonucleotides were obtained from Invitrogen or Metabion. The sequence of DNA oligonucleotides is given in the 5' to 3' direction. mutati.Underlined sequences indicate restriction enzyme recognition sites, and marked with gray the T7 promoter sequence.

Primer Nº	Name	Used for	5'→ 3' sequence
1	*P.marina5'*	T7 teplate for *P. marina* P RNA	GCGGGATCCTAATACGACT CACTATAGGATATCTCTGC CGGTGGTTTCC
2	*P.marina3'*	T7 teplate for *P. marina* P RNA	CGCCTTAAGACCGGTGGCC TCCAGTAA
3	*S.azorense5'*	T7 teplate for *S. azorense* P RNA	GCGGGATCCTAATACGACT CACTATAGGTATAAGGCTA CGGCTTTGAG
4	*S.azorense3'*	T7 teplate for *S. azorense* P RNA	CGCCTTAAGTTTAAGGCTAC GGCTTTGGAG
5	L9 PH mutation 5'	T7 teplate for l9 mut of *P. haloplanktis* P RNA	TCCGGCCCACGACAAGTGC AGC
6	L9PH mutation 3'	T7 teplate for l9 mut of *P.haloplanktis* P RNA	GCCCCCCAGCCGTTAAC
7	L9TT mutation 5'	T7 teplate for l9 mut of *T. thermophilus* P RNA	TTCGCCCGACGGAAAGTG CCACA
8	L9TT mutation 3'	T7 teplate for l9 mut of *T. thermophilus* P RNA	CCCGCCCAGGCGTTACC

9	ExchangeP1*E.coli* with TT T7 *BamHI* 5':	Insertion of P1 *T. th rnpB* into *E. coli rnpB*	GCGGGATCCTAATACGACTCACTATAGGGAATTCCGGGACGAGGGGACAGTCGCCGCTTCGT
10	ExchangeP1*E.coli* with TT P1*EcoRI* 3'	Insertion of P1 *T. th rnpB* into *E. coli rnpB*	CGCGAATTCGCCTCCGGGACGAGGCGTAAGCCGGGTTCTGTCGTGG
11	ExchangeP9 *E.coli* with TTP9 5'	Insertion of P9 *T. th rnpB* into *E. coli rnpB*	ACCCGACGACCAGTGCAACAGAGAG
12	Exchange P9*E.coli* with TTP9 3'	Insertion of P9 *T.th rnpB* into *E. coli rnpB*	TACCCCCGCCCAGGCGTTACCTGGCA
13	*EheI*P1th in *E.coli5'*	Exchange *EcoRI* into *EheI* of pUC19 *E .coli rnpB* P1P9 *T. th*	GGCGCCTCCGGGACGAGGC
14	pUC19for thP1in *Ecoli* 3'	Exchange *EcoRI* into *EheI* of pUC19 *E. coli rnpB* P1P9 *T. th*	TTCACTGGCCGTCGTTTTACAA
15	5'*Ecoli* promoter from pSP64 iccluding *NheI*	Amplification of native *E. coli* promoter frompSP64	GTAGAGGATCTGGCTAGCTTGC
16	3'*Ecoli* promoter from pSP64	Amplification of native *E. coli* promoter frompSP64	GGCGCAGTATAGAGGGTTTG
17	5'promoter over Ph	Amlification of *P. hal rnpB* with fragment of *E. coli* promoter	GCAAACCCTCTATACTGCGCGCCCGAGTTAGCCAAGATAATCG
18	3'Ph with *HindIII*	Amlification of *P. hal rnpB* with fragment of *E. coli* promoter	GCATAAGCTTGAGTTAGCCGTATAAGCCGG
19	5'Ecpromoter over Ecp1p9*thth*	Amlification of *E .coli* P1P9 *T. th rnpB* with fragment of *E. coli* promoter	GCAAACCCTCTATACTGCGCGCCGGGAATTCCGGGACGAGGG
20	3' Ecp1p9*thth* with HindIII	Amlification of *E. coli* P1P9 *T. th rnpB* with fragment of *E. coli* promoter	GCATAAGCTTGCCTCCGGGACGAGGCGTA
21	5'mycoplasmaEc promoter over	Amlification of *E. coli* P1P9 *Myc.genwt rnpB* with *E. coli* promoter	GCAAACCCTCTATACTGCGCGCCGGCTGACCAGACAGTCGCCG

22	3'*HindIII* mycoplasma pACYC	Amlification of *E .coli* P1P9 *Myc.genwt rnpB* with fragment of *E. coli* promoter	GCATAAGCTTAATTCAGAT AGCATCTGACC
23	5'*SmaI* over *E.coli* promoter	Construction of empty pACYC with *E .coli* native promoter	GAGCCCGGGCGCGCAGTA TAGAGGGTTTG
24	3'*KpnI, EcoRI* over *Ecoli* promoter	Construction of empty pACYC with *E. coli* native promoter	GAGGTACCGAATTCGGATC CTCTAGAGTCGACCTGC
25	5'thth5'blunt pACYC	Ampilfication of *T. th* wt *rnpB* for blunt ligation	GGGAATTCCGGGACGAGG GC
26	3'thth3'KpnIpACYC	Ampilfication of *T. th* wt *rnpB* for blunt ligation	GATCGGTACCGCCTCCGG GACGAGGCGTAAGC
27	5'DR5'bluntpACYC	Ampilfication of *D. radiodurans* wt *rnpB* for blunt ligation	GCGGGGAAACTCCTGGTCG CG
28	3'DR3'*KpnI* pACYC	Ampilfication of *D. radiodurans* wt *rnpB* for blunt ligation	GATCGGTACCTGGCACGGG GAAACGGTAAGC
29	5'L9EcpAYCYC	Introduction of l9 mutation in *E.coli* wt *rnpB*	GCCCACGACCAGTGCAACA GAGAG
30	3'l9EcpACYC	Introduction of l9 mutation into *E. coli* wt *rnpB*	GGACCCCCCAGGCGTTACC TGGC
31	5'Ecl9*EcoRI* for pUC19	T7 template for *E. coli* l9mutant	CGCGAATTCAGGTGAAAC TGACCGATAAGC
32	3'Ecl9*BamHI*T7	T7 template for *E. coli* l9mutant	CGCGGATCCTAATACGAC TCACTATAGAAGCTGACC AGACAGTCGC
33	PACYC sequencing	Sequencing of PACYC	TGAGAAATCACCATGAGTG AC
34	EcoP1P9Mgen1	Exchange of P1 *E. coli rnpB* with P1 from *M. genitalium*	TAGGATCCTAATACGACTC ACTATAGGCTGACCAGACA GTCGCCGC
35	EcoP1P9Mgen3	Exchange of P1 *E. coli rnpB* with P1 from *M. genitalium*	AGCGAATTCAGATAGCATC TGACCGATAAGCCGGGTTC

36	EcoP1P9Mgen mut2	Exchange P9 *E. coli rnpB* with P9 from *M. genitalium*	GTTGCACTGGTCGTGATGG CTATCACATC
37	EcoP1P9Mgen mut1	Exchange P9 *E. coli rnpB* with P9 from *M. genitalium*	GATGTGATAGCCATCACGA CCAGTGCAAC
38	5'RnpA A.pyr1	Genomic PCR for amplifying *rnpA* from *A. pyrophilus*	AGAACTAAGTCTGGAAGAA AGAT
39	5'RnpA A.pyr2	Genomic PCR for amplifying *rnpA* from *A. pyrophilus*	AGAACGAAGTCTGGAAGAA AGAT
40	5'RnpA Apyr3	Genomic PCR for amplifying *rnpA* from *A. pyrophilus*	AGAACGAAGTCTGGAAGGA AGAT
41	5'RnpA A.pyr4	Genomic PCR for amplifying *rnpA* from *A. pyrophilus*	AGAACTAAGTCTGGAAGGA AGAT
42	3'RnpA A.pyr1	Genomic PCR for amplifying *rnpA* from *A. pyrophilus*	GTAGGGTAATACCTACAGG
43	3'RnpA A.pyr2	Genomic PCR for amplifying *rnpA* from *A. pyrophilus*	GTAGGGTAAAAACCTACAG
44	3'RnpA A.pyr3	Genomic PCR for amplifying *rnpA* from *A. pyrophilus*	GTAGGGTAGTACCTACGGG
45	3'RnpA A.pyr4	Genomic PCR for amplifying *rnpA* from *A. pyrophilus*	GTAGGGTAGAACCTACAGG
46	3'RnpA A.pyr 5L1	Genomic PCR for amplifying *rnpA* from *A. pyrophilus*	TTCATCATCTCTTCCTGCA
47	3'RnpA A.pyr 5L2	Genomic PCR for amplifying *rnpA* from *A. pyrophilus*	TTCATTATCTCTTCCTGCA

48	EcoP1P9Mgen2	Exchange P9 from E. coli rnpB to M.genitalium P9	CTCTCTGTTGCACTGGTCGT TATGGCTATCACATCCCCA GGCGTTACCTGGCA

6.7. Bacterial strains

Strain	Relevant Genotype	Reference
E. coli BW	pBAD:*rnpB*, Cam^r	Wegscheid and Hartmann, 2006
E. coli DH5α	*supE*44 delta*lacU*169 (phi80 *lacZ* deltaM15) *hsdR*17 *recA*1 *endA*1 *gyrA*96 *thi*-1 *relA*1	Sambrook *et al.*, 1989
E. coli XL-2 Blue	*recA1 endA1 gyrA96 thi-1 hsdR17 supE44 relA1 lac* [F´ *proAB lacI*q*Z.M15* Tn*10* (Tet^r) Amy Cam^r]	Stratagene

6.8. Plasmid vectors

Vector	Relevant Genotype	Reference
pSP64	ori pMB1 Amp^r	Promega
pACYC177	p15A Amp^r Kan^r	Chang et al., 1978
PUC19	ori pMB1 Amp^r lacZlacI	Yanisch-Peron et al 1985
PQE30	Ori pBR322 Amp^r	Qiagen

6.9. Plasmid vectors for T7 transcriptions

Vector	Genotype	Reference	Linearised with
PDW98	E.coli P RNA	Busch et al, 2000	BsaAI
pSBpt3'HH	ptRNA^{Gly} *from Thermus thermophilus* with 14mer flank	Busch et al., 2000	Bam HI
pJA2'	*E. coli* P RNA, (wt)	Vioque et al., 1988	Fok I

6.10. Abbreviations and Units

A_{260}	absorption at 260 nm
A	Adenosine
aa	amino acid(s)
Amp	Ampicillin

APS	Ammonium peroxodisulfat
Bp	base pair(s)
BPB	Bromophenol blue
BSA	Bovine serum albumine
C	cytosine
C5	protein subunit of *E. coli* RNase P
cam	Chloramphenicol
c_{End}	end concentration
c_{Stock}	stock concentration
cpm	counts per minute
Da	dalton
DNA	deoxyribonucleic acid
DNase	deoxyribonuclease
dNTP	deoxynucleoside triphosphates
DTT	dithiothreitol
E	extinction
ε	molar extinction coefficient
EDTA	Ethylenediamine tetraacedic acid
EGTA	Ethylene glycol tetraacetic acid
EP	native *E. coli rnpB* promoter
Fig.	Figure
g	gram
G	guanosine
h	hour(s)
HEPES	N-2-Hydroxyethylpiperazin-N'-2-ethane sulfonic acid
IPTG	Isopropyl-β-D-thiogalactopyranosid
kb	kilo bases
l	liter
LB	Luria-Bertani
M	molar [mol/l]
mA	milliampere
MBq	Megabecquerel
min	Minute
MOPS	3-Morpholinopropanesulfonic acid
MW	Molecular weight
nt(s)	Nucleotide(s)
NTP	Ribonucleosidtriphosphate
p.a.	pro analysis
PAA	Polyacrylamide
PAGE	Polyacrylamid gel elektrophoresis
PCR	Polymerase chain reaction
pmol	Picomol

P Protein	Protein subunit of RNase P
P RNA	RNA subunit of RNase P
RNA	ribonucleic acid
RNase	ribonuclease
rpm	rounds per minute
SDS	natriumdodecylsulfat
s	second
T	thymine
TBE	Tris-Borat-EDTA Buffer
TEMED	N,N,N,N,-Tetramethylethylendiamin
T_m	melting temperature
Tris	Tris-hydroxymethylaminomethan
(p)tRNA	(precursor) transfer RNA
U	Unit(s) (unit for enzyme activity)
U	Uridine
wt	wild-type
XCB	Xylene cyanol blue

6.11. Index of Buffers and Solutions

1.25 xT1 denaturing buffer	43
TFB1	25
TFB3	25
10 x THE buffer	30
2 x Pb^{2+} buffer	44

6.12. References

Busch, S., Kirsebom, L. A., Notbohm, H., & Hartmann, R. K. 2000. Differential role of the intermolecular base-pairs G292-C(75) and G293-C(74) in the reaction catalysed by *Escherichia coli* RNase P RNA. *J Mol Biol*, **299:** 941-951.

Chang, A.C.Y. and Cohen, S.N. 1978. Construction and characterization of amplifiable multicopy DNA cloning vehicles derived from the P15A cryptic miniplasmid. *J. Bacteriol.*, **134:** 1141-1156.

Sambrook, J., Fritsch, E.F. and Maniatis, T.E. 1989. Molecular cloning. A laboratory manual. Cold spring Harbor Laboratory, Cold Spring Harbor, N.Y.

Vioque, A., Arnez, J. and Altman, S. 1988. Protein-RNA interactions in the RNase P holoenzyme from *Escherichia coli. J. Mol. Biol.* **202:** 835-848.

Wegscheid, B. and Hartmann, R.K. 2006. The precursor tRNA 3'-CCA interaction with *Escherichia coli* RNase P RNA is essential for catalysis by RNase P *in vivo. RNA.* **10/1261:**188306.

Yanisch-Perron C, Vieira J, Messing J. 1985. Improved M13 phage cloning vectors and host strains: nucleotide sequences of the M13mp18 and pUC19 vectors. *Gene*. **33(1):**103-19

7. Acknowledgements

I would like to thank…

…. Prof. Dr. Roland K. Hartmann for the scientific supervision and guidance during my Ph.D study. For being open for discussions and helpful in solving scientific problems.

…. Dr. K. Willkomm for priceless help, good advices, support and proofreading of my dissertation.

…. PD Dr. Klaus Reuter for being my second referee.

…. Prof. Dr. Maike Petersen, Prof. Dr. med. Klaus Kuschinsky and Prof. Dr. M. Schlitzer for participation in the examination commission.

…. Dr. Barbara Wegscheid, Dr. Heike Wünenberg, Dr. Simona Cuzic-Feltens and Dr. Marcus Gößringer for introducing me into the RNA world. For their friendship in and outside the lab.

…. Katja Hütte for fighting with all types of surrounding me bureaucracy.

…. all members of Hartmann group for their cooperativenes and helpfulness and nice atmosphere in the lab. Especially BB (Bloody Bastarsds) committee for perfect confusion and party climate in C102 during last six months of my Ph.D.

Finally but not least

…. to my family for their support and love

…. to my love Kamila Kitowaska for being allways with me in bad and good moments. For her permanent support and patience during my entire Ph.D and for making possible my residence in Germany.

8. Publications arising from this work

Marszalkowski M, Teune J.H., Steger G., Hartmann R.K. and Willkomm D. 2006.

Thermostabile RNase P RNAs lacking P18 identified in the *Aquificales*. *RNA*, **12**:1-7.

Marszalkowski M, Hartmann R.K. and Willkomm D. 2007 (RNA accepted)

Structural basics af a ribozyme's thermostability: P1-L9 interdomain interaction in RnaseP RNA. *RNA* accepted Sep. 2007.

Marszalkowski M, Hartmann R.K. and Willkomm D. 2007 (submitted)

In vitro and *in vivo* role of interdomain contacts in RNAs from apsychrophilc, amesophilic and athermophilic bacterium. Submitted Sep. 2007.

Oral presentations

Marszalkowski, M., Willkomm, D.K., Hüttenhofer, A., Hartmann, R.K.(2004)

News from Aquifex

NorFa Network on Molecular biology of RNA; Meeting in Bergen, Norwegen

9. Curriculum vitae

Michal Marszalkowski

Date of birth	25.07.1979
Place of birth	Gdynia, Poland
Nationality	polish

1986-1994	Primary School, Gdynia
1994-1998	Secondary School No VI , Gdynia
1998	High School diploma
1998-2003	Intercollegiate Faculty of Biotechnology University of Gdansk and Medical University of Gdansk
2003	Master degree of Biotechnology
2004-2007	PhD work. Group of Prof.Dr.R.K Hartmann, Institute of Pharmacutical Chemistry University of Marburg

10. Selbstständigkeitserklärung

Ich versichere, dass ich meine Dissertation

Structure-function relationships, tertiary interactions and thermostabilty of RNase P

selbstständig, ohne unerlaubte Hilfe angefertigt und mich dabei keiner anderen als der von mir ausdrücklich bezeichneten Quellen und Hilfen bedient habe.

Die Dissertation wurde in der jetzigen oder einer ähnlichen Form noch an keiner anderen Hochschule eingereicht und hat noch keinen sonstigen Prüfungszwecken gedient.

(Ort/Datum) (Unterschrift mit Vor- und Zuname)